CHARACTERIZATION OF STRESS RESPONSIVE MICRORNAS AND THEIR ROLES IN T CELL DEVELOPMENT

APPROVED BY SUPERVISORY COMMITTEE

Nicolai S. C. van Oers, Ph.D.

Lora Hooper, Ph.D.

Zhijian J. Chen, Ph.D.

Felix Yarovinsky, M.D.

Jen Liou, Ph.D.

DEDICATION

To my father, my mother, and my brother

ACKNOWLEDGEMENTS

I would first like to thank my thesis supervisor, Dr. Nicolai S. C. van Oers, for his endless patience and constant encouragement, and for helping me grow in many aspects. I would like to express my appreciation to the members of my thesis committee, Dr. Lora Hooper, Dr. Zhijian Chen, Dr. Felix Yarovinsky, and Dr. Jen Liou, for their helpful criticism and suggestions during my dissertation research. Furthermore, I would like to offer my special thanks to Dr. M. Teresa de la Morena as being like a second mentor to me.

To the former and current members of the van Oers lab, it has been a pleasure working with you. I am particularly grateful for the assistance given by Dr. Robert Silge, Jennifer Eitson, and Ashley Hoover throughout my studies. I also want to thank Dr. Igor Dozmorov, Dr. Kole Roybal, Dr. Shaheen Khan, Dr. Navin Chowdhury, Dr. Murat Balaban, Dr. Serkan Kir, Dr. Fatih Kocabas, Ty Troutman, Wei Hu, and Sean Murray for sharing their experience and knowledge.

I am deeply grateful to my immediate family, my uncle, Aytekin Butun, and my precious friends, Ebru Kaymak, Sezin Dagdeviren, Alpay Burak Seven, Felipe Andreas Piedra, Didem Agac, Duygu Saatcioglu, Jun Tsunezumi, Navin Chowdhury, Kole Roybal, Sean Murray, and Dicle Berfin Azizoglu, for their support and love.

CHARACTERIZATION OF STRESS RESPONSIVE MICRORNAS AND THEIR ROLES IN T CELL DEVELOPMENT

by

SERKAN BELKAYA

DISSERTATION

Presented to the Faculty of the Graduate School of Biomedical Sciences

The University of Texas Southwestern Medical Center at Dallas

In Partial Fulfillment of the Requirements

For the Degree of

DOCTOR OF PHILOSOPHY

The University of Texas Southwestern Medical Center at Dallas

Dallas, Texas

May, 2014

CHARACTERIZATION OF STRESS RESPONSIVE MICRORNAS AND THEIR ROLES IN T CELL DEVELOPMENT

Serkan Belkaya, Ph.D.

The University of Texas Southwestern Medical Center at Dallas, 2014

Supervising Professor: Nicolai S. C. van Oers, Ph.D.

Physiological stress evokes rapid changes in both the innate and adaptive immune responses. Immature αβ T cells developing in the thymus are particularly sensitive to stress, with infections and/or exposure to lipopolysaccharide or glucocorticoids eliciting a rapid apoptotic program. MicroRNAs (miRs) are short, non-coding RNAs that play critical roles in the immune system by targeting diverse mRNAs. We hypothesized that a subset of thymically encoded miRs would be stress responsive and modulate thymopoiesis. Thymic miR profiling revealed 18 distinct miRs that are dysregulated more than 1.5-fold in response to lipopolysaccharide or the synthetic glucocorticoid dexamethasone. These stress-responsive

miRs are dynamically regulated in distinct thymocyte subsets. We utilized both transgenic and gene-targeting approaches to study the impact of these miRs on thymopoiesis under normal and stress conditions.

MiR-181d is the most down-regulated thymic miR in response to stress. The over-expression of miR-181d in developing thymocytes reduced the number of immature $CD4^{+}CD8^{+}$ thymocytes. Lipopolysaccharide or dexamethasone injections caused a 4-fold greater loss of these cells than in the wild type controls. The targeted elimination of miR-181d resulted in a thymus stress-responsiveness similar to wild-type mice, suggesting a functional redundancy between miR-181 family members. Gene expression comparisons further indicated that miR-181d affects a number of stress, metabolic, and signaling pathways. These findings demonstrate that selected miRs enhance stress-mediated thymic involution *in vivo*.

MiR-185, another stress-responsive miR in murine thymus, is haploinsufficient in almost all individuals with 22q11.2 deletion/DiGeorge syndrome that can present with immune, cardiac, parathyroid, and psychological problems. The molecular targets of miR-185 in thymocytes are unknown. Transgenic expression of miR-185 attenuated thymopoiesis at the TCRβ-selection checkpoint and during positive selection. This caused a peripheral T cell lymphopenia. Mzb1, NFATc3, and Camk4 were identified as novel miR-185 targets. Elevations in miR-185 enhanced TCR-dependent intracellular calcium levels, while a knockdown of miR-185 diminished these calcium responses. These effects concur with reductions in Mzb1, an endoplasmic reticulum calcium regulator. Consistent with the haploinsufficiency of miR-185, Mzb1 levels were elevated in thymocyte extracts from

several 22q11.2 deletion/DiGeorge syndrome patients. These findings indicate that miR-185 regulates T cell development through its targeting of several mRNAs including Mzb1.

TABLE OF CONTENTS

LIST OF PUBLICATIONS

Belkaya, S., and N. S. van Oers. Transgenic expression of microRNA-181d augments the stress sensitivity of $CD4^+CD8^+$ thymocytes. Submitted.

Belkaya, S., S. E. Murray, J. L. Eitson, M. T. de la Morena, J. Forman, and N. S. van Oers. 2013. Transgenic expression of microRNA-185 causes a developmental arrest of T cells by targeting multiple genes including Mzb1. *J Biol Chem* doi: 10.1074/jbc.M113.503532.

de la Morena, M. T., J. L. Eitson, I. M. Dozmorov, **S. Belkaya**, A. R. Hoover, E. Anguiano, M. V. Pascual, and N. S. van Oers. 2013. Signature MicroRNA expression patterns identified in humans with 22q11.2 deletion/DiGeorge syndrome. *Clin Immunol* 147: 11-22.

Cevik, S. I., N. Keskin, **S. Belkaya**, M. I. Ozlu, E. Deniz, U. H. Tazebay, and B. Erman. 2012. CD81 interacts with the T cell receptor to suppress signaling. *PLoS One* 7: e50396.

Schmalstieg, A. M., S. Srivastava, **S. Belkaya**, D. Deshpande, C. Meek, R. Leff, N. S. van Oers, and T. Gumbo. 2012. The antibiotic resistance arrow of time: efflux pump induction is a general first step in the evolution of mycobacterial drug resistance. *Antimicrob Agents Chemother* 56: 4806-4815.

Belkaya, S., R. L. Silge, A. R. Hoover, J. J. Medeiros, J. L. Eitson, A. M. Becker, M. T. de la Morena, R. S. Bassel-Duby, and N. S. van Oers. 2011. Dynamic modulation of thymic microRNAs in response to stress. *PLoS One* 6: e27580.

DeFord-Watts, L. M., D. S. Dougall, **S. Belkaya**, B. A. Johnson, J. L. Eitson, K. T. Roybal, B. Barylko, J. P. Albanesi, C. Wulfing, and N. S. van Oers. 2011. The CD3 zeta subunit contains a phosphoinositide-binding motif that is required for the stable accumulation of TCR-CD3 complex at the immunological synapse. *J Immunol* 186: 6839-6847.

LIST OF FIGURES

LIST OF TABLES

LIST OF DEFINITIONS

ANOVA – Analysis of variance

Bcl2 – B-cell lymphoma 2 gene

BCR – B cell receptor

bp – Base pair

Btk – Bruton's tyrosine kinase

Camk4 – Calcium/Calmodulin-dependent protein kinase type IV

CD – Cluster of differentiation

cDNA – Complementary deoxyribonucleic acid

CDS – Coding sequence

CFSE – Carboxyfluorescein diacetate succinimidyl ester

COS-1 – Simian fibroblast cell line

Dex – Dexamethasone

DGCR8 – DiGeorge syndrome critical region 8

DMEM – Dulbecco's modified Eagle's medium

DN – Double negative ($CD4^-$ $CD8^-$)

DP – Double positive ($CD4^+$ $CD8^+$)

ds – Double stranded

ELISA – Enzyme-linked immunosorbent assay

ER – Endoplasmic reticulum

ES – Embryonic stem

FACS – Fluorescence activated cell sorting

FBS – Fetal bovine serum

GC – Glucocorticoid

GFP – Green fluorescent protein

GO – Gene ontology

HBSS – Hank's balanced salt solution

HEK293T – Human embryonic kidney 293T cell line

HPA – Hypothalamic-pituitary-adrenal

HRP – Horse radish peroxidase

hrs – Hours

icTCRβ – Intracellular TCRβ

IFN – Interferon

Ig – Immunoglobulin

IL – Interleukin

IP – Intraperitoneal

IPA – Ingenuity pathway analysis

KI – Knockin

KO – Knockout

l – Liter

LCR – Locus control region

Lif – Leukemia inhibitory factor

LN – Lymph nodes

LPS – Lipopolysaccharide

M – Molar

mAb – Monoclonal antibody

Mb – Million base pairs

MFI – Mean fluorescence intensity

MHC – Major histocompatibility complex

min – Minutes

miR – MicroRNA

mRNA – Messenger ribonucleic acid

Mzb1 – Marginal zone B an B1 cell-specific protein

Neo – Neomycin

NFAT – Nuclear factor of activated T cells

NK – Natural killer

NR – Nuclear receptor

nt – Nucleotides

OTII – Transgenic TCR specific for OVA presented by MHC class II

OVA – Ovalbumin

PAMP – Pathogen associated molecular pattern

PBS – Phosphate buffered saline

PCR – Polymerase chain reaction

pre – Precursor

pri – Primary

RPMI – Roswell Park Memorial Institute

RT-PCR – Real time PCR

SA – Streptavidin

SD – Standard deviation

sec – Seconds

self-pMHC – Self peptide-loaded MHC molecules

SEM – Standard error of mean

SERCA – Sarcoplasmic/endoplasmic reticulum calcium ATPase

SP – Single positive ($CD4^+$ $CD8^-$ or $CD4^-$ $CD8^+$)

t – Time

TCR – T cell receptor

TEC – Thymic epithelial cell

TF – Transcription factor

Tg – Transgenic

Th – T helper

TNF – Tumor necrosis factor

UTR – Untranslated region

UV – Ultraviolet

Vα – Variable alpha

WT – Wild type

7AAD – 7-Aminoactinomycin D

CHAPTER ONE

INTRODUCTION

T lymphocytes constitute an essential component of the adaptive immune system. The majority of T lymphocytes belong to the αβ lineage with $CD4^+$ helper and $CD8^+$ cytotoxic T cells evident in both mice and humans. αβ T cells express an antigen-specific T cell receptor (TCR) composed of one α-chain and one β-chain, along with either CD4 or CD8 co-receptors, and recognize antigen-bound major histocompatibility complex (MHC) class II or class I molecules on antigen presenting cells, respectively [1].

T cell development in the thymus

T cells are derived from hematopoietic progenitor cells that migrate from bone marrow to the thymus via the blood. The thymus is a bilobed organ, in which each lobe is composed of an inner medulla and a peripheral cortex surrounded by an outer capsule. Non-lymphoid cells including thymic epithelial cells (TECs) in the cortex and medulla provide an inductive microenvironment with various receptor ligands, growth factors, and cytokines to favor T cell specification and commitment [2,3,4]. Major stages of αβ T cell development are classified by the expression patterns of CD4 and CD8 co-receptors. The earliest lymphoid precursors, which enter the thymus as $CD4^-CD8^-$ (double-negative or DN) thymocytes, undergo a series of developmental stages further defined by differential surface expression of CD44 and CD25 [5]. Early thymopoiesis begins with extensive proliferation of DN1

($CD44^+CD25^-$) population, followed by the generation of DN2 ($CD44^+CD25^+$) thymocytes [6]. At the DN2 stage, thymocytes initiate rearrangement of TCRβ gene locus by Rag1/2-mediated VDJ recombination, which continues until these cells enter the DN3 ($CD44^-CD25^+$) stage [7]. DN3 thymocytes that complete successful arrangement of the TCRβ chain express a cell-surface pre-TCR complex consisting of the TCRβ chain and an invariant pre-TCRα subunit and the CD3 chains (γ, δ, ε, ζ) [8,9,10,11]. Signaling through the pre-TCR, which only occurs in those cells harboring a functional TCRβ subunit, triggers cell survival and differentiation into the DN4 ($CD44^-CD25^-$) thymocytes. Early thymopoiesis can also give rise to the γδ T cell lineage accompanied with the loss of alternative αβ-linage fate. Both T cell types originate from a common DN1 precursor and differ from one another through DN2 to DN3 stages [6,12,13]. Following TCRβ-selection checkpoint, αβ lineage-committed thymocytes expand rapidly by numerous rounds of cell division and progress into $CD4^+CD8^+$ (double positive or DP) thymocytes in the thymic cortex [14].

DP stage of thymopoiesis represents the largest cell population in the thymus. DP thymocytes undergo rearrangement of their TCRα gene locus via VJ recombination and become small, non-dividing cells expressing either MHC class-I or class-II restricted αβ TCR complex [15,16]. Mature TCR expressed on DP thymocytes can interact with endogenous (self) peptides bound to MHC molecules presented by cortical TECs. The affinity of this interaction will determine the further destiny of DP thymocytes: death by neglect, positive selection, or negative selection [14,17].

Most DP thymocytes do not recognize self-peptide-loaded MHC molecules (self-pMHC) and undergo a programmed cell death known as death by neglect. DP thymocytes

capable of recognizing self-pMHC are either positively or negatively selected depending on the ligand affinity of their cell-surface TCR. A low-affinity interaction results in weak TCR signals, promoting survival and further differentiation of DP thymocytes (positive selection) [18]. However, high-affinity self-pMHC leads to strong TCR signals, which in turn cause clonal deletion of DP thymocytes through apoptotic pathways (negative selection) [18]. Both modes of selection require proximal TCR signaling, which mediates the recruitment of LCK (Lymphocyte-specific protein tyrosine kinase) and ZAP70 (Zeta-chain-associated protein kinase 70) to the plasma membrane. LCK-activated ZAP70 phosphorylates a major downstream adapter protein, LAT (Linker of activated T cells) [18]. Low-affinity ligands result in partial phosphorylation of the LAT, elevating intracellular DAG and calcium levels through activation of PLCγ1 (Phospholipase C, gamma 1). DAG (Diacylglycerol) mediates weak, but sustained, activation of ERK, while calcium influx induces nuclear translocation of NFATs. These combine to elevate transcription of pro-survival factors, promoting positive selection of DP thymocytes [18]. In contrast, a strong TCR signal generates fully phosphorylated LAT proteins, driving stable localization of GRB2/SOS1 complex to the plasma membrane. This, in turn, leads to apoptosis of negatively selected DP thymocytes by activation of JNK and p38, and a strong, but transient, ERK activation [18].

The positively selected DP thymocytes migrate to the thymic medulla and differentiate into either MHC class-I restricted $CD8^+$ or MHC class-II restricted $CD4^+$ SP (single positive) thymocyte lineages through silencing the transcription of CD4 and CD8 co-receptor gene locus, respectively [19,20,21]. In the medulla, these immature thymocytes are subject to tissue-restricted antigens on MHC molecules presented by medullary TECs and/or

dendritic cells. This leads to a second round of negative selection, eliminating self-reactive T cells before exiting the thymus [22]. Upon successful completion of TCR-selection checkpoints, non-self reactive SP thymocytes egress to the periphery as naive T cells. Peripheral $CD4^{+}CD8^{-}$ and $CD4^{-}CD8^{+}$ T cells can further acquire effector, memory, or regulatory functions based on antigen and/or cytokine stimulations.

Strict selection pressure during thymopoiesis enables only a small percent of T cells to leave the thymus with an antigen-specific TCR. This indicates the significance of continuous thymic output in order to maintain the diversity of peripheral T cell repertoire against microbial invaders. However, thymus is extremely prone to acute, stress-induced and/or chronic, age-induced involution [23]. This leads to a reduction in T cell development, therefore limiting the host's ability to combat neo-antigenic threats.

Stress impairs T cell development

Stress has degenerative effects in the nervous and immune systems, and is particularly pronounced in thymopoiesis. Physiological and pathological stresses lead to a thymic atrophy, which is characterized by reductions in the thymus size and a substantial loss of DP thymocytes and in the egress of naive T cells to the periphery [23].

Acute thymic involution is a prevalent complication for patients undergoing surgery, irradiation, and/or treatments with immunosuppressive agents, such as synthetic glucocorticoids (GCs) including dexamethasone and prednisone [24,25,26,27,28]. Milder stress factors including pregnancy, emotional distress, alcoholism, and malnutrition exhibit varying degrees of impaired thymopoiesis [29,30,31,32,33]. These non-pathological stimuli elevate the systemic production of GCs through the HPA (Hypothalamic-pituitary-adrenal)

axis, which in turn leads to a programmed cell death of DP thymocytes [33,34]. Supporting this, adrenalectomy completely hinders stress-induced thymic atrophy by preventing the production of GCs [35].

GCs easily diffuse across the plasma membrane and bind to the glucocorticoid receptor, NR3C1, (nuclear receptor subfamily 3, group C, member 1) in the cytoplasm [34]. This binding leads to the dissociation of the multimeric receptor complex, followed by subsequent translocation of GC-bound NR3C1 into the nucleus. NR3C1 can act both as a trans-activator by binding GC-response elements in the promoter of anti-inflammatory genes including IκB and IL-10 and as a trans-repressor by binding to other transcription factors, such as NF-κB and AP-1 [36,37,38]. NR3C1 is more highly expressed in DP thymocytes compared to all other T cell subsets. T cell-specific deficiency of this receptor leads to a complete resistance to GC-induced apoptosis, while sustaining normal T cell development and effector functions in mice [39,40]. This clearly indicates the important role of this pathway in GC-mediated DP cell death.

There are a number of GC-modulated genes identified to date. These included up-regulation of pro-apoptotic genes, such as Bim and Puma, and down-regulation of c-Myc [41,42,43]. Bim and Puma are known to mediate apoptosis of neglected and/or negatively selected DP thymocytes [44,45,46], whereas c-Myc is implicated in positive selection during thymopoiesis [47,48]. In addition to the above, Bcl2, an anti-apoptotic gene, functions as a rheostat of GC-sensitivity in immature thymocytes [49]. Low levels of Bcl2 render DP thymocytes more sensitive to GCs, compared to other thymocyte subsets. Nevertheless, how

GCs induce DP cell death is still unclear and the physiological role of this pathway during thymopoiesis remains an enigma.

Multiple pathological stresses are also known to induce thymic involution, evident from studies investigating bacterial, fungal, and viral infections in mice and humans [50]. The host's innate immune cells recognize a diverse range of pathogen-associated molecular patterns (PAMPs) through their pattern-recognition receptors, such as Toll-like receptors (TLRs) and NOD-like receptors (NLRs). PAMP-activated TLR signaling culminates in production of multiple inflammatory cytokines including IL-1, TNF, and IL-6 family proteins [51,52]. The release of these inflammatory mediators subsequently elicits the intrathymic secretion of GCs, which in turn leads to the direct apoptosis of DP thymocytes [53].

One other mechanism implicated in thymic atrophy is through thymic epithelial cells (TECs). TECs are essential components of thymic microenvironment by providing key signals for proper development and differentiation of thymocytes. In particular, Notch signaling, induced by TEC ligands, plays an indispensible role in T-cell lineage commitment during early thymopoiesis [2,54,55]. Activation of Notch signaling pathway renders DP thymocytes resistant to GC-induced apoptosis [56]. In addition to this, TECs are thought to sense inflammatory cytokines and transmit involution signals to the thymocytes during microbial infections [57,58]. Nevertheless, TEC-dependent thymic involution is more common with chronic stresses such as aging [23,59]. In rodents and humans, an aged thymus is characterized by the loss of TECs and the emergence of ectopic fat tissue, which in turn lead to a decline in thymopoietic efficiency [59,60]. In addition, inflammation-mediated

reductions in growth factors and sex hormones were shown to exaggerate thymic atrophy in elderly, indicating the involvement of other signaling pathways (Leptin, ghrelin, etc.) in thymocytes during stress-induced cell death [53].

In summary, acute thymic atrophy is a complication of multiple physiological and pathological conditions. This is even more pronounced in patients undergoing immunosuppressive treatments and surgery, and in individuals with HIV/AIDS [23]. Attenuated thymopoiesis and the limited peripheral T cell pool render these individuals extremely susceptible to opportunistic microbial infections, significantly increasing their morbidity and mortality [23]. These complications necessitate a better understanding of molecular mechanisms behind the stress-induced thymic involution and thymic recovery following stress removal. Most studies to date have been focused on classical mRNAs, however little is known about the role of small non-coding RNAs, microRNAs, in the course of thymic-atrophy.

MicroRNAs: Micro-managers of gene expression

MicroRNA biogenesis

MicroRNAs (miRs) are small non-protein coding RNA molecules (22 to 24 nucleotides in length) found in almost all metazoans. MiR genes have either intragenic or intergenic localizations in the genome. Intragenic miRs can be located in introns and/or exons of their host mRNAs, whereas intergenic miRs have their own promoters [61,62,63]. MiRs are transcribed from the genome, usually by RNA polymerase II, as long primary transcripts (pri-miRs) in the form of step-loop structures with the 5'-cap and a 3'-poly (A)

tail [64,65]. In the nucleus, these pri-miRs undergo an enzymatic cleavage by the RNase III enzyme, Drosha, and its mutual partner DGCR8 (DiGeorge syndrome critical region gene 8), generating a hairpin RNA of ~70 nucleotides known as pre-miRs [66,67]. These nuclear pre-miRs are transported by exportin-5 and a Ran-GTPase into the cytoplasm where they are further cleaved into ~22-24 bp RNA duplexes by another RNase III enzyme, Dicer [68,69,70]. One arm of this RNA duplex, the mature miR, is incorporated into the RNA-induced silencing complex (RISC), which is composed of multiple proteins. The core component of this ribonucleoprotein complex is an argonaute family member protein (Ago). Ago-associated miR mediates targeting of multiple genes based on the complementary binding between the miR and the mRNA. The target specificity of a mature miR is usually mediated through its seed region (nucleotides 2-8 at the 5'end) [71]. MiRs base pair with their targets mostly in the 3' untranslated region (3' UTR); several miRs have been reported to also bind 5' UTR and/or coding sequences of mRNAs [72,73,74,75,76]. Thus, the sequence-specific binding of miRs leads to degradation and/or translational inhibition of target mRNAs [77].

More than thousands of miRs have been identified in mammals (miRBase v.20.0). These miRs have been implicated in regulating a wide range of biological processes including development, metabolism, cell differentiation, proliferation, and apoptosis [78,79].

MicroRNAs in the immune system

The importance of miRs in the immune system became more evident with the studies using different mouse models in which Dicer was conditionally deleted in specific

hematopoietic lineages. For example, targeted deletion of Dicer in immature thymocytes leads to a defective early thymopoiesis, with a dramatic reduction in thymus cellularity [80]. In the case of B cell development, Dicer ablation results in an almost complete block at the pro-B to pre-B cell transition [81]. Genetic manipulation of individual miRs further helped to reveal their critical roles in lymphocyte development and subsequent responses [82]. Over-expression of miR-155 resulted in aberrant B cell proliferation and leukemia, whereas loss of miR-155 modulated lineage commitment of T-helper cells and negatively affected B cell differentiation in germinal centers [83,84,85]. Genetic gain- and loss- of function studies of miR-17-92 cluster have demonstrated that these miR family members play critical roles in controlling lymphopoiesis at the early stages [86,87]. Another crucial miR involved in B cell development, miR-150, was also shown to differentially regulate natural killer (NK) and invariant NK T (iNKT) cell generation and functions [88,89,90]. In the course of thymopoiesis, miR-181 family members are differentially expressed through distinct developmental stages [91,92,93]. This family includes miR-181a, miR-181b, miR-181c, and miR-181d, differing from each other by a few nucleotides [94,95]. Specifically, miR-181a is implicated in regulating TCR signaling strength and deletion of autoreactive T cell clones by targeting multiple phosphatases [96,97]. Recent studies with targeted elimination of miR-181a/b in mice demonstrated that these miRs are indispensible for NK T cell development, whereas deficiency of miR-181a/b or miR-181c/d appeared to have no effect on thymopoiesis [98,99,100,101]. Furthermore, several miRs including miR-10, miR-182, miR-21, miR-214, and miR-29 have been shown in controlling peripheral T cell activation and differentiation [102,103].

MicroRNAs in human diseases

Many miR genes reside within unstable chromosomal locations and cancer-associated genomic regions, which explains their differential expression in several human diseases [104,105]. A haploinsufficiency of the miR-17-92 cluster causes skeletal and growth defects, while mutations in miR-137 and miR-96 lead to schizophrenia and progressive hearing loss in humans, respectively [106,107,108]. Human miR-185 is encoded within an intronic region at chromosome 22q11.2, which undergoes a monoallelic deletion (~1.5 to 3 Mb) in patients with the 22q11.2 deletion/DiGeorge syndrome. MiR profiling of peripheral blood samples from 22q11.2 deletion/DiGeorge syndrome patients revealed that miR-185 was significantly reduced in almost all patients compared to normal individuals, consistent with its haploinsufficiency at the 22q11.2 locus [109]. The 22q11.2 deletion/DiGeorge syndrome is a heterogeneous congenital disorder associated with thymic and parathyroid gland hypo- or aplasia, cardiac abnormalities, schizophrenia, and/or cognitive impairment [110,111,112]. A subset of these patients has increased prevalence of autoimmune disorders and age-dependent alterations in T helper cell (Th1 and Th2) commitment [113,114]. In the mouse models of 22q11.2 deletion/DiGeorge syndrome, 50% normal expression of miR-185 results in elevated levels of SERCA2 (Sarcoplasmic/endoplasmic reticulum calcium ATPase 2) in hippocampal neurons [115]. Higher levels of SERCA2 enhance pre-synaptic neurotransmitter release in hippocampal neurons, leading to an age-dependent cognitive impairment [115]. Structural alterations in the neuronal morphology, often noted in schizophrenia, have been linked to the increased expression of a novel miR-185 target, 2310044H10Rik, an uncharacterized Golgi

associated neuronal inhibitor [116]. Thus, these findings could explain, at least in part, the high incidence of schizophrenia and/or learning disabilities in 22q11.2 deletion/DiGeorge syndrome patients as adults. Moreover, the elimination of Dicer in mature $CD19^{+}$ B cells causes elevated autoantibody production [117]. MiR-185 was identified as a key miR mediating this effect, as its loss increases the expression of Btk (Bruton's tyrosine kinase) [117]. This could account for the autoreactive antibodies noted in 22q11.2 deletion /DiGeorge syndrome patients. However, the genetic elements that contribute to poor thymocyte development and autoimmune susceptibility in this syndrome remain unknown.

MicroRNAs in stress responses

MiRs are emerging as key, stress-responsive regulators of biological processes in the cardiac, thyroid, auditory, immune, and hematopoietic systems [118,119,120,121,122]. For example, several miRs (miR-29, miR-92a, miR-195, miR-208) control cardiac stress responses during hypertrophy and myocardial infarctions [121,122,123,124]. Moreover, miR-146 and miR155 are dramatically elevated in the innate immune cells upon bacterial infections and/or lipopolysaccharide (LPS) treatment [120,125,126]. MiR-146 attenuates TLR signaling pathways by down-modulating the expression of IRAK1 and TRAF6, whereas miR-155 is involved in positive regulation of innate immune responses by targeting SHIP1 and SOCS1 [125,126,127]. In contrast, miR-125b and let-7 are reduced in macrophages following LPS stimulation. Inhibition of these two miRs results in elevated production of inflammatory cytokines [127,128].

Thymus is a hyper-stress-sensitive organ, with massive depletion of DP thymocytes in response to various stress stimuli, such as LPS and synthetic GCs (Dexamethasone) [129,130]. Presence of stress-responsive miRs in the thymus first became evident with the transient paucity of key miR-processing enzymes (Drosha, DGCR8, and Dicer) in immature thymocytes within hours of GC exposure [131]. At later time points, I reported that several miRs, such as miR-181d and miR-185, exhibited dynamic expression patterns in murine thymus following stress [132]. In addition to the above, deficiency of Dicer and/or miR-29a in TECs increases IFN-α sensitivity of these cells with elevated IFN-α receptor levels. This, in turn, impairs their integrity to support thymopoiesis upon exposure to poly(I:C), a synthetic mimic of viral dsRNA [58]. All together, these findings indicate that miRs could be critical in modulating thymopoiesis during initiation and recovery phases of acute thymic atrophy.

Concluding remarks

Given the role of thymus in T cell development, continuous and effective thymopoiesis is of significance in the maintenance of a robust immune system against various antigenic challenges across a lifetime. Multiple stress factors negatively influence this development with barely understood mechanisms. MiRs are emerging regulators in many aspects of the immune system, however little is known about their contribution to the stress-induced thymic atrophy. The work presented in this dissertation provides the identification of stress-responsive miRs in the thymus and characterization of their functional roles during T cell development by utilizing both transgenic and knockin mouse models.

CHAPTER TWO

MATERIALS AND METHODS

Ethics statement

All mouse procedures were carried out in accordance with the Institutional Animal Care and Use Committee at the University of Texas Southwestern Medical Center (IACUC #2010-0053). Animal use adheres to applicable requirements such as the Animal Welfare Act, the Guide for the Care and Use of Laboratory Animals, and the US Government Principals regarding the care and use of animals. The mice were housed in the specific pathogen free facility on the North campus of UT Southwestern Medical Center.

Mice

The miR-185 and miR-181d transgenic (Tg) lines were generated by the UT Southwestern Medical Center Transgenic Core facility. The VA-hCD2 transgenic cassettes containing genomic DNA with pri-miR-185 (~600 bp) or pri-miR-181d (~394 bp) were injected into C57BL/6 fertilized eggs as described [133,134]. These pri-miR fragments were cloned from genomic DNA, isolated from C57BL/6 mice, using standard PCR reactions. The VA-hCD2-pri-miR-181d transgenic construct was designed with the first 28 nucleotides of pri-miR-181c lacking. This eliminates a significant segment of miR-181c, while leaving the pri-miR-181d intact. MiR-185 and miR-181d transgenic founders were identified using DNA probes for the VA-hCD2 transgenic cassette using previously described assays [133].

Transgenic expression of miRs was confirmed by performing Northern blotting and real time PCR techniques. Based on their miR over-expression levels, 3 miR-185 transgenic (Tg-25, Tg-35, and Tg-6) and 2 miR-181d transgenic lines (Tg-8 and Tg-38) were selected for further characterization and analysis. OTII/miR-185 double Tg mice were obtained from crosses between the OTII Tg and miR-185 Tg-35 lines.

For the generation of the miR-181d knockin construct, PCR reactions were performed to amplify a 3.56 kb genomic DNA fragment containing miR-181d followed by miR-181c (reverse orientation). Bam HI and Bgl II restriction sites were incorporated at the 5' and 3' ends, respectively. All genomic PCR reactions were undertaken with LA-Taq polymerase (Takara Inc., Thermo-Fisher Scientific, Pittsburgh, PA), and the constructs were directly cloned into pCR2.1-TOPO-TA cloning vectors according to the manufacturers' instructions (Invitrogen, Grand Island, NY). dsDNA sequencing reactions confirmed nucleotide sequence information. A 3.03 kb genomic piece that continued from miR-181c, included new Nhe I and Hind III restriction sites, was PCR amplified and also cloned into a pCR2.1 TOPO-TA cloning vector. This piece was subcloned into the targeting vector, pGKnexloxP2dta that was linearized with Hind III (vector was a kind gift from Dr. Toru Miyazaki, University of Tokyo, Japan). Site-directed mutagenesis (QuikChange Site-directed Mutagenesis Kit, Stratagene, La Jolla, CA) was used to modify miR-181d, with total 11 nucleotide replacements to eliminate the seed region and the hairpin loop. A new Pst I restriction site was cloned into this region. The original miR-181d sequence was ACAATTAACATTCATTGTTGTCGGTGGGTTGTG and the new sequence was ACAATTAAGTGCTAATGTTGTCC**CTGCAG**TGTG, with the underlined nucleotides

changed and the bold region high-lighting the Pst I site. This region was subcloned into the left arm of pGK-neomycin using a Bgl II linearized vector. The pGK-neo-miR-181d knockin construct was linearized with Not I, purified, and electroporated into C57BL/6-derived embryonic stem cells (LR2.6.1) by the UT Southwestern Medical Center Transgenic and Knockout Core facility. Embryonic stem (ES) cell clones were selected with G418 and gancyclovir, and correct insertion of the targeted allele was determined by Southern blotting following digestion of ES cell DNA with Xba I. Of the 600 clones screened, 4 ES cell lines that contained the correctly sized targeted allele were identified (6B12, 5C1, 2B7, and 2C9). The wild-type allele is 5.3 kb, while the targeted allele is 3.9 kb. Two of the ES cell lines, 5C1 and 2B7, were separately used for injections into C57BL/6 blastocyts. The resulting chimeric male mice were mated with C57BL/6 female mice. Following subsequent interbreeding between heterozygous mice, homozygous mice (miR-181d KI^{neo}) were crossed with CAG-Cre transgenic lines, eliminating the neomycin cassette and leaving a loxP site. MiR-181d KI progeny mice were further confirmed for the mutated miR-181d sequence by PCR reactions and subsequent DNA sequencing as well as Southern blotting. The miR181d KI line is currently being deposited with the mouse mutant resource center (C57BL/6-Mir181d $^{tm1Oers/Mmucd}$, #036959-UCD).

Lipopolysaccharide (LPS from E. coli 0111:B4, Sigma L4391) and dexamethasone (Dex, Sigma D2915, Sigma Chemical Co, St. Louis, MO) were prepared at 1 mg/ml in PBS and at 0.06 mg/ml in water, respectively. Mice with 5-8 weeks of age were used in all experiments including intraperitoneal injections of PBS, LPS, and Dex.

Human thymus tissues

Human thymus samples were obtained from patients undergoing corrective heart surgery at Children's Medical Center in Dallas, TX from 2012-2013. Informed consent was obtained for all patients and control subjects. The Institutional Review Board at UT Southwestern Medical Center approved this study (IRB # 072010-003).

Cell isolation, culture, and flow cytometry

Single cell suspensions were freshly prepared from isolated lymphoid organs, followed by FACS staining as described previously [135]. Total organ cellularity was determined by counting live cells upon Trypan blue staining. Absolute cell numbers were calculated using total cellularity and percentages of subsets in the lymphoid organs.

FACS antibodies used were from BD Biosciences (San Jose, CA), unless otherwise indicated. Thymocytes from PBS- and LPS-treated mice were stained with anti-CD4 and anti-CD8, followed by sorting with a Mo-Flo High Speed Cell Sorter (Cytomation). One hundred thousand $CD4^-CD8^-$ (DN), $CD4^+CD8^+$ (DP), $CD4^+CD8^-$ (CD4 SP), and $CD4^-CD8^+$ (CD8 SP) thymocytes were sorted to > 95 % purity, and processed for total RNA isolation. In certain experiments, T cells were enriched from single cell suspensions with the EasySep T cell Enrichment Kit following the manufacturers' guidelines (StemCell Technologies, Vancouver, Canada). One to two million $CD44^-CD25^+$ ($CD4^-CD8^-TCR\gamma\delta^-NK1.1^-B220^-CD11b^-CD11c^-$) DN3 thymocytes from the control and miR-185 Tg mice were sorted and processed for total RNA isolation.

Intracellular TCRβ staining was performed using Cytoperm/Cytofix Kit (BD Biosciences). Quantification of apoptosis was determined by staining with Annexin V and 7AAD antibodies in Annexin V Binding Buffer (BD Biosciences). Intracellular staining of natural regulatory T cells was performed using the Mouse Regulatory T Cell Staining Kit (eBioscience, San Diego, CA).

Total $CD4^+$ T cells, purified from the lymph nodes using magnetic beads (BD Biosciences), were stimulated at a density of 5 x 10^5 cells/ml in 96-well plates with anti-CD3ε (3 mg/ml; 145.2C11) and anti-CD28 (3 mg/ml; 37.51). Following a 48 hrs culture period at 37°C in complete RPMI (supplemented with 10% FBS, 1% L-glutamine, and 1% penicillin/streptomycin), IL-2 levels were measured using the Mouse IL-2 ELISA Max Kit (Biolegend, San Diego, CA).

Naive $CD4^+$ T cells were purified from the lymph nodes using the Dynal Mouse CD4 Negative Isolation Kit (Invitrogen), followed by magnetic-activated cell sorting for CD62L expression (Miltenyi Biotec, Auburn, CA). Naive ($CD4^+CD62L^{high}$) T cells were labeled for 10 min at 37°C with 300 nM CFSE (Carboxyfluorescein diacetate succinimidyl diester, Invitrogen), followed by three washes with culture medium. Labeled cells were stimulated at 0.5-1 x 10^6 cells/ml in 96-well plates with varying amounts of anti-CD3ε (0.3-3 μg/ml; 145.2C11) and anti-CD28 (0.3-3 μg/ml; 37.51) in complete RPMI for 2-3 days at 37°C.

Thymocytes from OTII Tg and OTII/miR-185 Tg-35 mice were isolated and incubated (2 x 10^6 cells/ml; 24-well plate) with 10 μM of SIINFEKL or OVA class II peptides in complete RPMI for 20 hrs at 37°C. Live percentage of DP thymocytes was determined by gating on Annexin V^- $7AAD^-$ cells.

Ten thousand to 1 x 10^6 cells per sample were acquired on FACS-Calibur and LSRII flow cytometers (BD Biosciences). Data was analyzed using FlowJo software (Tree Star, Ashland, OR).

Northern blotting

Total RNA (including microRNAs) was isolated from various murine tissues and/or cell types using the miRNeasy Kit (Qiagen, Valencia, CA), based on the manufacturers' instructions. Five to 15 μg of total RNA was resolved on 15 % urea/polyacrylamide gels and transferred to Zeta-probe membranes (Bio-Rad, Hercules, CA). Following UV- or carbodiimide-mediated cross-linking [136], the membranes were hybridized with miR specific probes labeled with [^{32}P]-dATP using the StarFire microRNA Detection Kit (Integrated DNA Technologies, Coralville, IA). A U6 probe was used as the endogenous control to normalize total RNA input. Bands were visualized with a phosphorimager (GE Healthcare Biosciences, Pittsburgh, PA), followed by quantification using ImageQuant (Bio-Rad).

Real-time PCR

For the microRNA real-time PCR, total RNA was isolated with the miRNeasy Kit (Qiagen) and subsequently treated with DNase (Turbo-DNAse, Ambion, Grand Island, NY). cDNA was made from 10 ng of total RNA using the TaqMan MicroRNA Reverse Transcription Kit (Applied Biosystems, Grand Island, NY). Real-time PCR analysis was performed using TaqMan Gene Expression Master Mix, and miR-specific TaqMan probes on

an ABI 7300 series PCR machine (Applied Biosystems) according to the manufacturers' recommendations. U6 probe was used as the endogenous control. To determine mRNA levels by real-time PCR, RNA was isolated from sorted DN3 thymocytes using the Ambion RNAqueous Micro-Kit (Invitrogen) and treated by DNase (Ambion). cDNA was made from 100 ng of RNA using High Capacity cDNA Reverse Transcription Kit (Applied Biosystems). The real-time PCR steps were performed with 5 ng of cDNA, 2X Maxima SYBR Green qPCR Master Mix, and 100 nM ROX passive reference dye (Thermo Scientific). The real-time cycling parameters were as follows: 1 cycle at 95^{o}C for 10 min, followed by 40 cycles of 95^{o}C for 15 sec and 60^{o}C for 60 sec on an ABI 7300 series PCR machine. All real-time quantitative PCR reactions were performed in triplicates. Relative expression of miRs and mRNAs was calculated by the comparative threshold method ($\Delta\Delta C_T$).

MicroRNA arrays

MiR arrays were from LC Sciences (LS Sciences, Houston, TX). In brief, 6 total thymic RNA samples were prepared from 3 control (PBS) and 3 LPS-treated C57BL/6 male mice of 6-8 weeks of age. Total 5 μg RNA per sample for each group were sent to LC Sciences for miR profiling. The various labeled samples were analyzed on the microarray platform with a probe set containing 649 murine miRs, based on the Sanger Version 12.0 and 13.0 database release.

Microarray analysis

For gene expression comparisons between the wild type and miR-185 Tg mice, total thymocytes from control (n=6) and miR-185 Tg-6 (n=6) mice were pooled and DN3 thymocytes were sorted. RNA was isolated with the RNAqueous Micro-Kit (Ambion). RNA samples (3 samples per group; total 6 samples) were examined for quality and integrity using Bioanalyzer Chip. cDNA synthesis and hybridization onto Illumina SingleColor MouseWG-6_V2_0_R1 platform was performed at the UTSW Genomics and Microarray Core Facility. GenomeStudio Data Analysis Software Version 1.8.0 was used to analyze raw image files from the scanned to get signal intensity values. Sample probe profiles were generated without normalization. Using GeneSpring GX 11 Version 4.0 (Agilent Technologies, Santa Clara, CA), quantile normalization of all samples was performed to obtain a gene-level expression profile. Following the normalization of raw data, unpaired Student's *t*-test was performed to identify differentially expressed genes among the wild type and miR-185 Tg samples. 1.5-fold change was used as the cut-off value to determine range of significantly deregulated genes ($p < 0.05$). The microarray data were submitted to the GEO (Gene Expression Omnibus) database with the accession number: GSE49057.

For gene expression comparisons between the miR-181d Tg and miR-181d KI mice, whole thymus tissues from the miR-181d Tg-8 (n=2) and miR-181d KI (n=2) mice were isolated and homogenized. Total RNA was isolated with the Qiagen miRNeasy Kit. RNA quality and integrity was examined using Bioanalyzer Chip. cDNA synthesis and hybridization onto Illumina SingleColor MouseWG-6_V2_0_R1 platform was performed at the UTSW Genomics and Microarray Core Facility. Subsequent analysis of microarray raw data was performed as described previously, followed by associative *t*-test analysis to

identify significantly ($p < 0.05$) deregulated genes among the miR-181d Tg and miR-181d KI samples [109,137]. The microarray data were submitted to the GEO database with the accession number: GSE50113. Gene expression data were analyzed for enrichment of canonical pathways through the use of IPA (Ingenuity Systems, www.ingenuity.com). Gene Ontology Slim classification and Transcription Factor Target analysis (based on the MsigDB) were performed through the WebGestalt (Web-based Gene Set Analysis Toolkit, http://bioinfor.vanderbilt.edu/webgestalt/) [138,139]. 576 down- and 315 up-regulated genes more than 1.25-fold ($p < 0.05$) were used in the enrichment analyses with at least 5 genes for each category through the hyper-geometric test and Benjamini & Hochberg as multiple test adjustment.

MicroRNA target validation

Genetic fragment encompassing pri-miR-185 (~600 bp) were PCR-amplified and cloned into the pCDNA3.1 vector (Invitrogen). The 3'UTRs of target genes (Btk, Mzb1, Mcm10, Camk4, Hmga1, NFATc3, Igf1r, and Dusp4) were amplified by PCR and ligated into the firefly luciferase reporter construct (pMIR-REPORT, Invitrogen). Reporter constructs and a beta-galactosidase vector were co-transfected into COS-1 cells (1×10^5 cells/ml in complete DMEM; 24-well plate) along with either pCDNA3.1 or pCDNA3.1-miR-185, using the Fugene 6 Transfection Reagent (Roche, Indianapolis, IN). Cells were processed using the Luciferase Assay Kit (Promega, Madison, WI) at 48 hrs post-transfection. Relative luciferase activity was calculated by normalizing the firefly luciferase to the beta-galactosidase. Murine Mzb1 CDS (excluding the stop codon) was cloned into the

pEF1/myc-His B plasmid in frame with the myc epitope (Invitrogen). Along with the Mzb1/myc fusion plasmid, a GFP expression vector (pEGFP) with either empty pCDNA3.1 or pCDNA3.1/miR-185 plasmids were transfected in HEK293T cells (1 x 10^5 cells/ml in complete DMEM; 24-well plate) using the X-tremeGENE 9 DNA Transfection Reagent (Roche). Twenty-four hrs post-transfection, cells were lysed at 1 x 10^7 cells/ml for immunoblotting. For all transfections, the total amount of DNA per well was kept equivalent by adding empty vector (pCDNA3.1). Mutations in the 3' UTR and CDS of Mzb1 were introduced with QuikChange Site-Directed Mutagenesis Kit (Stratagene).

MicroRNA knockdown

Jurkat T cells (2-2.5 x 10^5 cells/ml in complete RPMI) were transfected with 10-40 nM of control inhibitor (miRNA Hairpin Inhibitor Negative Control 1, cel-miR-67) or miR-185 inhibitor, a-miR-185, (miRIDIAN, ThermoScientific, Waltham, MA) using PepMute siRNA Transfection Reagent (SignaGen, Rockville, MD). Transfected cells were lysed for immunoblotting and/or analyzed for induction of calcium responses at 48 hrs post-transfection.

Immunoblotting

A 1% Triton X-100–containing lysis buffer, pH 7.6 was used for lysing cells, and immunoblotting was performed as previously described [135]. The following antibodies were used: Mzb1 (#11454-1-AP, Proteintech, Chicago, IL), NFATc3 (SC-8321, Santa Cruz Biotechnology, Dallas, Texas), β-actin (#4967, Cell Signaling Technology, Danvers, MA),

GFP (#632380, Clontech, Mountain View, CA), myc epitope (#2272, Cell Signaling Technology), anti-rabbit HRP-conjugated secondary antibody, and anti-mouse IgG HRP-conjugated secondary antibody [135]. Expression levels were quantified using the ImageJ software (version 1.46r). X-ray films, developed using chemiluminescence, were scanned with the Canon CanoScan 8800r. They were saved as TIFF images with a resolution of 300 dpi. These files were converted to 8-bit gray- scale images using ImageJ software. Band quantifications were performed as detailed (http://rsbweb.nih.gov/ij/). For the Western blots, multiple exposures were obtained.

Measurement of intracellular calcium responses

Freshly isolated total thymocytes (1 x 10^7 cells/ml) were loaded with 4 mM final concentration of Fluo-3-AM (Invitrogen) in 1X HBSS (1.2 mM Ca^{2+}, Cellgro, Manassas, VA) and incubated at 37^{o}C for 30 min. Labeled thymocytes were resuspended in 1X HBSS (2 x 10^6 cells/ml) and kept at room temperature until the analysis. Baseline fluorescence was monitored for 45 sec before adding biotinylated anti-CD3ε (Biolegend) and anti-CD4 (Biolegend) with a final concentration of 1 mg/ml of each. The fluorescence intensity was measured for 45 sec, followed by streptavidin addition at 2 mg/ml and monitoring for an additional 330 sec. In certain experiments, the SERCA pump inhibitor thapsigargin was added at 1 mM after 105 sec. Maximal calcium responses were determined by adding Ionomycin at 2 mM for 90 sec, with the fluorescence signal subsequently quenched by the addition of $MnCl_2$ at 1 mM for 60 sec. Jurkat T cells (1 x 10^7 cells/ml) following 48 hrs after transfection with antagomirs were loaded with 4 mM final concentration of Fluo-3-AM in 1X

HBSS (1.2 mM Ca^{2+}) at 37°C for 30 min. Baseline fluorescence of these cells (2 x 10^6 cells/ml in 1X HBSS) was monitored for 45 sec. Upon the addition of C305.2 at 1 mg/ml, the fluorescence intensity was measured for 270 sec. Maximal calcium responses were determined by adding Ionomycin at 1 mM for 60 sec, and the fluorescence signal was subsequently quenched by the addition of $MnCl_2$ at 1 mM for 60 sec. All sample acquisition during measurements of intracellular calcium responses was performed at 37°C.

Statistical analysis

Mean values, standard deviation (SD), and standard error of the mean (SEM), and Student's *t*-test were calculated with GraphPad Prism Software (GraphPad Software Inc., La Jolla, CA). The statistical significance was designated with asterisks (*$p < 0.05$, **$p < 0.01$, ***$p < 0.001$) and *p*-values more than 0.05 were considered non-significant (n.s.).

Primers and probes

All primers and probes used in this study are listed in Table 2.1.

Table 2.1. List of primers and probes.

Northern blot probes (5'-3')		**Real-time PCR primers (5'-3')**	
miR-106a	ctacctgcactgttagcactttg	Camk4 Fwd	tagccacaccagcatccaagagaa
miR-1224	ctccacctcccagtcctcac	Camk4 Rev	agaagatctgtgctgtccttggca
miR-125b-5p	tcacaagttagggtctcaggga	NFATc3 Fwd	accaggtgcatcggattactggaa
miR-15a	cacaaaccattatgtgctgcta	NFATc3 Rev	acctgcacagtcaatactcgctga
miR-150	cactggtacaagggttgggaga	Mzb1 Fwd	agtggattgcaggagctgagtgaa
miR-17	ctacctgcactgtaagcactttg	Mzb1 Rev	tcatcacgctgattcttggctctg
miR-181a	actcaccgacagcgttgaatgtt	**Primers used in the target validation (5'-3')**	
miR-181b	acccaccgacagcaatgaatgtt	Btk 3'UTR Fwd	gagctcgctggctgctaagc
miR-181c	actcaccgacaggttgaatgtt	Btk 3'UTR Rev	aagcttttccaataattttattg
miR-181d	acccaccgacaacaatgaatgtt	Camk4 3'UTR Fwd	ttactagtgatgccggtgaagctcttctgc
miR-185	tcaggaactgcctttctctcca	Camk4 3'UTR Rev	ttactagtgccaagctgggcttaacacacc
miR-20a	ctacctgcactataagcacttta	Dusp4 3'UTR Fwd	ttactagtcgtctctggaccccaaatccag
miR-20b	ctacctgcactatgagcactttg	Dusp4 3'UTR Rev	ttgagctcgggagggcgtttcagagtattc
miR-205	cagactccggtggaatgaagga	Hmga1 3'UTR Fwd	ttactagtgcctgctccatagccactgag
miR-26b	acctatcctgaattacttgaa	Hmga1 3'UTR Rev	ttgagctcagaaaccagggaggaagccc
miR-128	aaagagaccggttcactgtga	Igf1r 3'UTR Fwd	ttactagttcctcggacacaccgaagcac
miR-342-3p	acgggtgcgatttctgtgtgaga	Igf1r 3'UTR Rev	ttgctagctgcatcctggggactcagcag
miR-705	tgcccaccccacctcccacc	Mcm10 3'UTR Fwd	ttactagtctctcttcagacaccgcccaacc
miR-709	tcctcctgcctctgcctcc	Mcm10 3'UTR Rev	ttgagctccccacactaaaggtgaggagagc
Primers used in cloning of miRs (5'-3')		Mzb1 3'UTR Fwd	ttactagtccaacctgctgcacttctgg
miR-181d Fwd	atgaattcgtcggtgagtttgggcagc	Mzb1 3'UTR Rev	ttgagctcagaaaggcagcctcagtccc
miR-181d Rev	tggaattccatccccccagagtctccc	Mzb1 CDS Fwd	ttggatccatgagactgcctctgccactg
miR-185 Fwd	gaattcgcgatcagaaggctaggg	Mzb1 CDS Rev	tatctaga**ct**aagctcttctctctgggccag
miR-185 Rev	gaattccctcctatcagctgcc	NFATc3 3'UTR Fwd	ttactagtcttttgcccaccacggactg
		NFATc3 3'UTR Rev	ttgagctcagaagcagcagcagcagcac

CHAPTER THREE

DYNAMIC MODULATION OF THYMIC MICRORNAS IN RESPONSE TO STRESS

The work presented in this chapter was originally published as: **Belkaya, S.**, R. L. Silge, A. R. Hoover, J. J. Medeiros, J. L. Eitson, A. M. Becker, M. T. de la Morena, R. S. Bassel-Duby, and N. S. van Oers. 2011. Dynamic modulation of thymic microRNAs in response to stress. *PLoS One* 6: e27580.

Introduction

The thymus is the critical organ required for the production of the αβ T lymphocytes of the immune system, a developmental process maintained throughout life [18,29,140]. Selection mechanisms within the thymus ensure the development of naive T cells capable of recognizing foreign peptides bound to self-MHC molecules, which are presented in the peripheral lymphoid organs [18]. These self-restricted T cells are essential for effective immune responses to infections. Interestingly, developing thymocytes are exquisitely sensitive to physiological and pathological stresses, which cause a rapid programmed cell death termed apoptosis [23,141]. This response is evident during infections, as well as in humans undergoing immunosuppressive treatments, radiation therapy, and/or surgery [27,142,143]. Even milder stress such as pregnancy, emotional anxiety, malnutrition, or alcoholism can reduce thymic cellularity [30,144,145,146]. All these forms of stress increase

the systemic and/or intrathymic production of glucocorticoids, which are major regulators of lymphocyte apoptosis [147,148]. In the case of bacterial infections, the innate immune system responds to pathogen associated molecular patterns (PAMPs), releasing inflammatory cytokines, such as interferon, IL-1β, TNF-α, IL-6, and leukemia inhibitory factor (Lif) [144,149,150]. The IL-6 family (oncostatin-M, IL-6, leukemia inhibitory factor) induces the production of corticosteroids (glucocorticoids (GC)) from the Hypothalamic-pituitary-adrenal (HPA) axis and intrathymically [151,152,153]. Influenza virus also elevates GCs systemically, albeit via undefined mechanisms [154]. Clinically, synthetic GCs (e.g. dexamethasone, methylprednisone) are routinely used to suppress immune functions in transplant recipients, during autoimmune and systemic inflammatory disorders, and for treating certain malignancies [155,156,157]. The effects of these treatments on thymopoiesis are becoming better understood with the identification of down-regulated genes that are coupled to T cell development, cell cycle, and cell activation [129]. Functionally, GCs, lipophilic steroids, diffuse across the plasma membrane and complex a specific member of the nuclear receptor family, designated nuclear receptor 3, group C, member 1 (NR3C1) [141]. This GC-bound receptor complex dimerizes and translocates into the nucleus where it interacts with GC-response elements, culminating in the trans-activation of apoptotic effector genes [141,147,158,159]. DP thymocytes are very sensitive to GC-induced cell death because of high levels of NR3C1 [40,141].

MicroRNAs (miRs) are key, stress-responsive regulators in the immune, hematopoietic, cardiac, thyroid, and auditory systems [118,119,120,121,122]. They are small, non-coding RNA molecules (20-24 nucleotides in length) that repress global mRNA

translation and/or induce mRNA degradation [119,160]. Within hrs of exposure to GCs, the protein levels of three miR-processing enzymes, Drosha, DGCR8, and Dicer are reduced significantly in thymocytes [131]. These enzymes/miR-binding proteins generate mature miRs from the larger pre-miRs processed from primary miR transcripts. The targeted deletion of Dicer and Drosha in developing thymocytes causes a significant loss of cells, and results in a lethal lymphoid inflammatory disorder, partly from the loss of T regulatory cells [161,162,163]. Thus, a transient loss of Dicer and Drosha following GC treatment could modulate T cell development. There are several additional miRs with key roles in thymopoiesis. MiR-181a is highly expressed in DP thymocytes, representing 15% of the total miR pool [92,93,97]. This particular miR targets genes that regulate T cell receptor signaling pathways [93,97]. The normal levels of miR-181a maintain T cell tolerance to self-peptide/MHC molecules, with a reduction in this miR increasing the number of self-reactive T cells [96]. Less is known about the role of the three other miR-181 family members (miR-181b, miR-181c, and miR-181d), two of which are expressed in developing thymocytes [92]. While little is known about the effects of stress on the thymic miRs, certain miRs are up-regulated in innate effector cells following bacterial infections and/or LPS exposure (miR-146a, miR-155) [120,125,126,164,165,166]. The targeted deletion of miR-146a in T regulatory cells results in rampant autoimmunity [165]. Given the critical function of T cells in the immune system, the modulation of miRs during thymopoiesis could have important clinical consequences.

The work in this chapter describes 18 thymic miRs that are dysregulated > 1.5-fold in mice exposed to LPS or dexamethasone for one to three days. Many of these miRs exhibited

a distinct responsiveness in immature versus mature thymocyte subsets, with the $CD4^-CD8^+$ subset the most refractory to miR down-regulation. MiR-181d, a member of the miR-181 family, had an up to 15-fold reduced expression following LPS or dexamethasone treatment, suggesting an important functional role for this miR in thymopoiesis. These experiments indicate that stress can have a profound impact on thymopoiesis, altering the expression of miRs involved in apoptosis, tolerance, and proliferation.

Results

LPS and synthetic steroids reduce $CD4^+CD8^+$ thymocyte numbers

Stress, resulting from infections, induces thymocyte apoptosis and suppresses peripheral T cell responses [149,150,151,152,159]. A single intraperitoneal (IP) injection of 100 μg lipopolysaccharide (LPS), used to mimic a bacterial infection, caused a significant reduction in the percentage of $CD4^+CD8^+$ (DP) thymocytes within 24 hrs (Figure 3.1A). These DP cells were almost completely eliminated by 72 hrs (Figure 3.1A). The reduced percentage of DP cells results from LPS-induced elevations in glucocorticoids [152]. Consistent with this, an IP injection of 60 μg dexamethasone (Dex), a synthetic glucocorticoid, also caused a significant loss of the DP thymocytes that was revealed within 24 hrs (Figure 3.1A). While both treatments increased the percentage of $CD4^+CD8^-$ and $CD4^-CD8^+$ (SP) thymocytes, the absolute numbers of these SP cells were not altered (Figure 3.1A-C). This indicated that the DP subset was selectively targeted (Figure 3.1B-C). Unlike thymocytes, the consequences of LPS and Dex injections on peripheral lymphocytes were distinct. LPS increased the number of mature B cells ($B220^+$) at 48 hrs while Dex caused a

depletion of both B and T cells (Figure 3.2A-D). Taken together, these results indicate that DP thymocytes are acutely sensitive to stress induced by both LPS and Dex.

Selected thymic microRNAs are differentially regulated in diverse tissues following stress

Three miR processing enzymes, Drosha, DGCR8, and Dicer, are significantly reduced in thymocytes within 6-12 hrs of glucocorticoid treatment, leading to an overall reduction in the miRs in the thymus [131]. These findings suggested that the most dramatic changes in thymocyte subset composition occurred at 72 hrs. To profile the miRs at this time point, total RNA was prepared from the thymus of mice at 72 hrs after treatment with PBS or LPS. Murine microRNA arrays were used to profile over 600 miRs [132]. Seven and 11 distinct miRs were up- and down-regulated, respectively, at levels greater than 1.5-fold ($p < 0.05$, 3 mice/group) (Figure 3.3A). The changes in 14 of the 18 miRs were confirmed by northern blotting using probes specific for each miR, with U6 RNA as an internal control for RNA levels. MiR-125b-5p, miR-150, miR-205, and miR-342-3p were consistently up-regulated in the thymic tissue from the LPS injected mice (Figure 3.3B). MiR-15a, miR-17, mir-20a, miR-20b, miR-106a, miR-128, miR-181a, miR-181b, and miR-181d were consistently down-regulated (Figure 3.3C). While miR-26b appeared down-regulated, based on the microRNA array data, northern blots did not consistently reveal this change (Figure 3.3C). MiR-1224, miR-709, and miR-705 could not be characterized by northern blotting due to high, non-specific background issues with the probes (data not shown). MiR-185 gave a weak signal when assessed by northern blotting (data not shown). Of note, the fold changes

revealed in the miR microarrays were much greater than that identified by northern blotting because the arrays are more sensitive, specific, and quantitative [167].

We next examined whether any of the miRs identified in the thymus were stress responsive in other tissues [92]. Northern blotting was performed using RNA isolated from the heart, kidney, liver, brain, spleen, and thymus of PBS-, LPS- and Dex-treated mice at 72 hrs post-injection (Figure 3.4). While miR-150 was identified in both the spleen and thymus, it only appeared up-regulated in the thymic tissue following LPS or Dex treatments. MiR-205 and miR-181d were uniquely expressed and stress responsive in the thymic tissue. MiR-128, identified in the brain and thymus, was only down-regulated in the latter following a stress response. Of the miR-181 family members that were stress responsive in the thymus, miR-181a and miR-181b were also weakly expressed in the brain and spleen. Many of the other miRs were stress responsive in diverse tissues (Figure 3.4). For example, miR-15a, miR-17, miR-20b, and miR-26b were stress responsive in nearly every tissue examined. MiR-342-3p, primarily brain- and spleen- specific, was reduced upon LPS and Dex treatment. MiR-20b, miR-106a, and miR-150 were stress responsive, but were only identified in the thymus and spleen. MiR-125b-5p was highly expressed in the brain and heart, but it was detected at low levels in other tissues (Figure 3.4). Taken together, these experiments reveal that many of the miRs identified in the thymus are stress responsive in different tissues.

The miR array profiling was undertaken at a single time point (72 hrs). To determine the temporal alterations in miR levels following LPS or Dex treatments, northern blots were performed with RNA extracted from the thymus at 24, 48, and 72 hrs. MiR-125b-5p and miR-150 exhibited a transient, 2-fold increase 24 hrs post-LPS and -Dex injections (Figure

3.5A; *lanes 2 and 5 versus 1*). MiR-150 continued to increase and plateaued between 48 and 72 hrs (Figure 3.5B; *lanes 6-7*). Unlike miR-150, miR-125b-5p was primarily expressed in stromal tissue, as it was not detected in purified thymocytes (Figure 3.5A-B; *lanes 8-9*). MiR-181a transiently increased in the LPS-treated mice at 24 hrs, but thereafter dropped 1- and 5-fold upon LPS and Dex treatments, respectively (Figure 3.5C; *lanes 4-7*). MiR-181d exhibited the most dramatic down-regulation after both LPS and Dex treatments, with an up to 15-fold reduction by 72 hrs (Figure 3.5D; *lanes 3, 5-7*). The other miRs exhibited time dependent changes in expression (Figure 3.6). In summary, at least 18 distinct miRs expressed in the thymus are dynamically regulated following LPS- and Dex-induced stress responses.

MicroRNA expression patterns are differentially affected by stress in specific thymocyte subsets

To determine whether the stress-responsive miRs were equivalently or differentially regulated in particular T cell subsets, thymocytes from control and LPS-injected mice were sorted into the DN, DP, CD4 SP, and CD8 SP subsets. MiR profiling was performed using quantitative real-time PCR (RT-PCR) with miR-specific probes (Figure 3.7A-D). With the exception of miR-150 and miR-342-3p, the majority of the miRs were down-regulated in the DN subset. The reduced expression of the miR-17-90 cluster and the miR-181 family was even more pronounced in the DP population (Figure 3.7B). Comparing all the thymocyte subsets, the CD8 SP was the most divergent, with the miR-17-90 cluster up-regulated 2-fold and the miR-181 group unaffected by the LPS treatment (Figure 3.7D). It should be noted

that the down-regulation of the miR-181 family was not as obvious with the RT-PCR assays as with the arrays. This is because miR-181a, miR-181b, miR-181c, and miR-181d are very conserved, with only 1-4 bp differences within this family. Since the PCR amplification is not as stringent as the arrays, and it is likely that miR-181a/b can be amplified to a small degree when using a miR-181d specific primers, causing a less obvious down-regulation. In summary, LPS exposure induces a dynamic, time-dependent modulation of miRs that is distinct in each of the thymocyte subsets.

Discussion

MiRs have critical roles in the development, differentiation, and expansion of cells in many organ systems. Stress directly affects the biogenesis and functionality of miRs [168]. We describe a set of miRs expressed in the thymus that are differentially regulated following the introduction of systemic stress *in vivo*. The stress was induced by LPS to mimic bacterial infections, and by Dex, the known modulator of LPS-induced thymocyte apoptosis. Many of the miRs present in the thymus that were down-regulated following LPS or Dex injection belong to the miR-17-92 cluster, which are anti-apoptotic [169]. The miR-17-92 cluster includes miR-17, miR-20a, miR-20b, and miR-106a. Their down-regulation is consistent with the increased apoptotic program initiated in the thymocytes. Previous work has shown that this same cluster is significantly down-regulated in thymocytes within 6 hrs of glucocorticoid treatment [131]. The short-term (6 hrs) Dex treatments cause a reduction in most miRs due to diminished levels of three key MiR processing enzymes: Drosha, DGCR8, and Dicer [131]. Consequently, no thymic miRs are increased in expression. We examined

the longer-term consequences of stress on thymic miRs. As the thymocyte subpopulations are dramatically altered following stress, we also examined the miRs changes in individual thymocyte subsets. For the DP population, the miR-17-92 cluster is reduced at all time points examined. This reduction is unique to the DP subset since the cluster is unchanged in the CD4 SP cells, and up-regulated in the CD8 SP population. The loss of this cluster in the DP subset is consistent with the increased programmed cell death evident in these cells. We hypothesize that such a change is necessary to prevent tolerogenic signals in the DP cells during infections when foreign antigens are present. Furthermore, we speculate that the up-regulation of the miR-17-92 cluster in the CD8 SP cells may be important in preventing these cells from dying during infections, providing for a new source of naive T cells required for maintaining an ongoing immune response. It is interesting to note that even among DP thymocytes several miRs are up-regulated after 24 hrs of stress. MiR-709, miR-1224, and miR-342-3p/5p are increased several-fold in the DP subset, while miR-150 and miR-342-3p are increased in all the thymocyte subsets. Contrasting these findings, miR-150 is up-regulated 2 to 3.5-fold in the mature SP subsets, while remaining unchanged in the DP population. It is noteworthy that elevations of miR-150 in the hematopoietic system, via retroviral transduction, cause early developmental arrest of B cells and contribute to myeloid leukemia's [170]. This suggests that long-term stress could promote a developmental arrest of the DN cells via the up-regulation of miR-150, the target of which is c-Myb [89]. A number of stress responsive miRs have been characterized in innate effector cells following LPS exposure or infections, including miR-146, and miR-155 [120,166]. Interestingly, these miRs are not modulated significantly in the thymocyte subsets, implying that stress has

distinct effects on the innate versus adaptive immune system. It was noted that the magnitude of miR modulation was not as accurate when using real-time RT-PCR assays compared to the microRNA arrays. This is consistent with the known RT-PCR disadvantages for quantitating miRs [167].

Of the stress responsive miRs identified in the thymus, miR-181d is the most dramatically down-modulated miR. This miR is a member of the miR-181 family, with all four members sharing an almost identical seed sequence. MiR-181d is the most divergent of the four, and is located approximately 85 bp downstream of miR-181c. While both miR-181c and miR-181d are expected to arise from the same polycistronic message, miR-181c is not highly expressed in thymocytes, suggesting additional post-transcriptional processes [92]. In addition, miR-181c and miR-181d are encoded on a chromosome (murine chromosome 8) distinct from the miR-181a and miR-181b cluster, which have undergone gene duplication on two separate chromosomes (murine chromosomes 1 and 2). This difference could also explain why miR-181d expression levels are very susceptible to stress compared to miR-181a or miR-181b. The entire family has a complex regulation and function. Thus, the pre-miR loop nucleotides of miR-181a versus miR-181c result in the differential ability of miR-181a to regulate thymocyte development compared to miR-181c [95]. The stem-loop structure of miR-181d is the most distinct of all members. These findings suggest important functional distinctions between miR-181a and miR-181d. MiR-181d is more highly expressed in induced T regulatory cell populations and pre-B cells, compared to the other family members [92].

The differentially regulated miRs expressed in the thymus may have functions systemically, especially since miRs are very stable and are detected in the plasma and tissue fluids, indicating that miRs are not restricted to their site of production [171]. From a physiological perspective, we suggest that stress-responsive miRs have crucial roles in the specific elimination of DP thymocytes following stress, thereby preventing tolerance to foreign, pathogen-derived antigens.

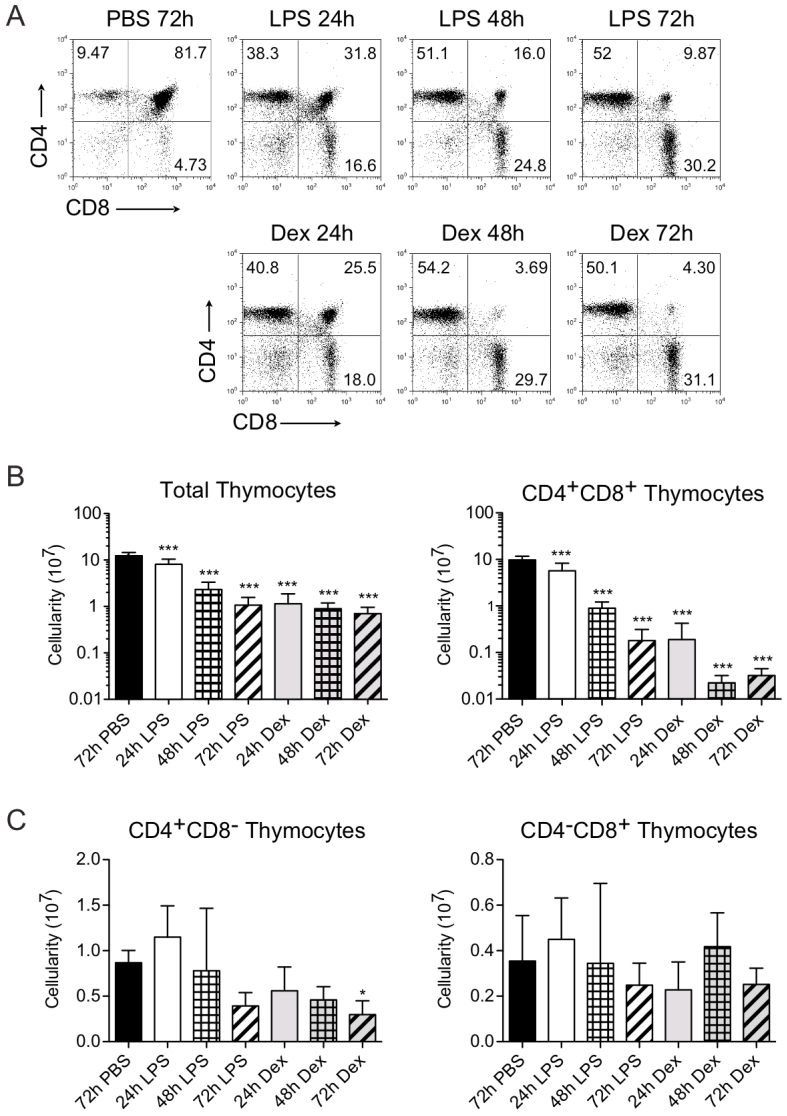

Figure 3.1. Lipopolysaccharide and dexamethasone deplete immature $CD4^+CD8^+$ thymocytes. (**A**) Thymocytes were isolated from either control (PBS injected, t= 72 hrs), or LPS and dexamethasone (Dex) injected mice (t= 24, 48 and 72 hrs). The cells were stained for CD4 and CD8, and analyzed by flow cytometry. The percentage of $CD4^-CD8^-$ (DN), $CD4^+CD8^+$ (DP), $CD4^+CD8^-$ (CD4 SP), and $CD4^-CD8^+$ (CD8 SP) subsets are provided in each quadrant of the dot plot profiles. (**B**) The total thymic cellularity and the number of $CD4^+CD8^+$ cells were calculated at 24, 48, and 72 hrs post-injection and are shown in a log scale. (**C**) The absolute number of mature $CD4^+CD8^-$ and $CD4^-CD8^+$ SP cells after PBS, LPS, and Dex treatments were calculated at t= 24, 48 and 72 hrs post-injection. Data are representative of the mean +/- SD from at least 8 mice per group (*$p < 0.05$, **$p < 0.01$, ***$p < 0.001$, versus the PBS control; One-way ANOVA analysis).

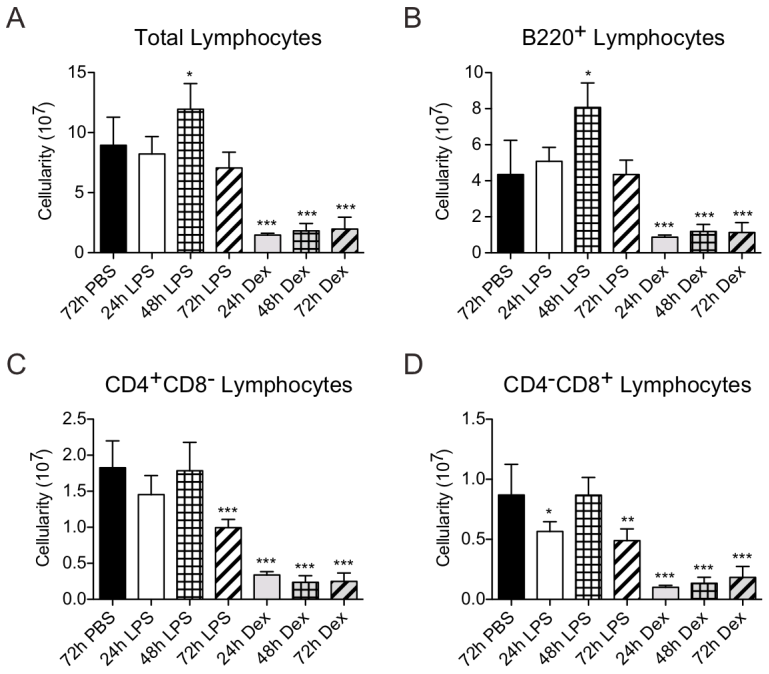

Figure 3.2. Lipopolysaccharide and dexamethasone have differential effects on peripheral lymphocytes. (**A**) Lymphocytes were isolated from control (PBS injected, t= 72 hrs), LPS, or Dex injected mice (t= 24, 48 and 72 hrs). The total lymphoid cellularity was determined. (**B**-**D**) The splenic cells were stained with fluorochrome-labeled anti-B220, anti-CD3, anti-CD4, and anti-CD8 mAbs and analyzed by flow cytometry. The absolute number of $B220^+$ B cells (**B**), $CD4^+CD8^-$ T cells (**C**), and $CD4^-CD8^+$ T cells (**D**) were calculated at 24, 48, and 72 hrs post-injection, after appropriate electronic gating to determine the percentage of each population. Data are representative of the mean +/- SD from at least 5 mice per group (*$p < 0.05$, **$p < 0.01$, ***$p < 0.001$ versus the PBS control; One-way ANOVA analyses).

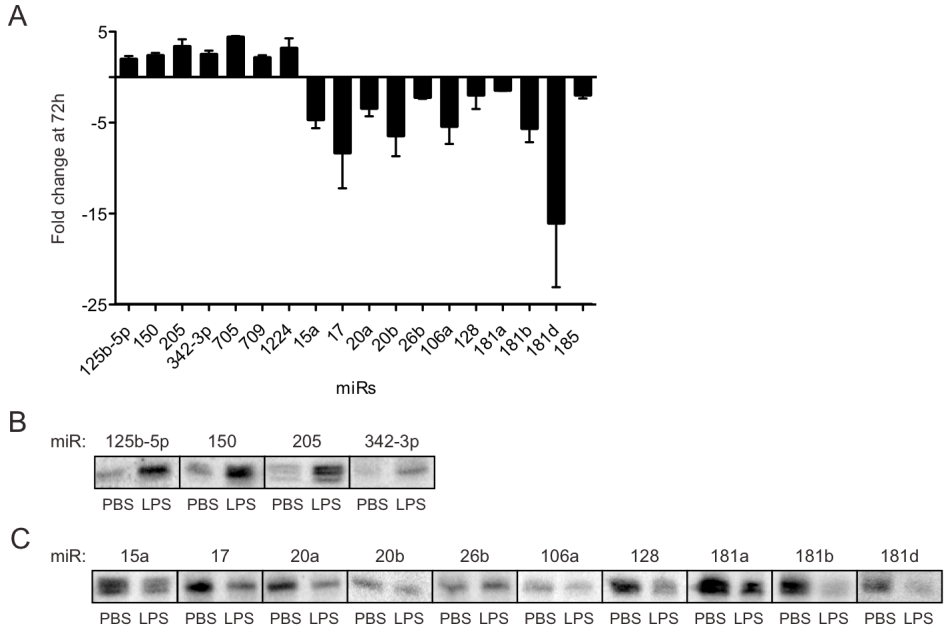

Figure 3.3. Stress-responsive signature microRNAs in the thymic tissue. (**A**) Graph shows 18 distinct miRs with a statistically significant fold change ($p < 0.05$) in expression. Fold change indicates the change in miR expression in LPS-treated sample relative to PBS-treated thymus sample. (**B**) Northern blots of 4 miRs that were upregulated in the thymic tissue at 72 hrs after LPS injection. (**C**) Northern blots were performed on 10 miRs that were down-regulated at 72 hrs after LPS injection. (**B-C**) Data are representative of at least 3 independent experiments.

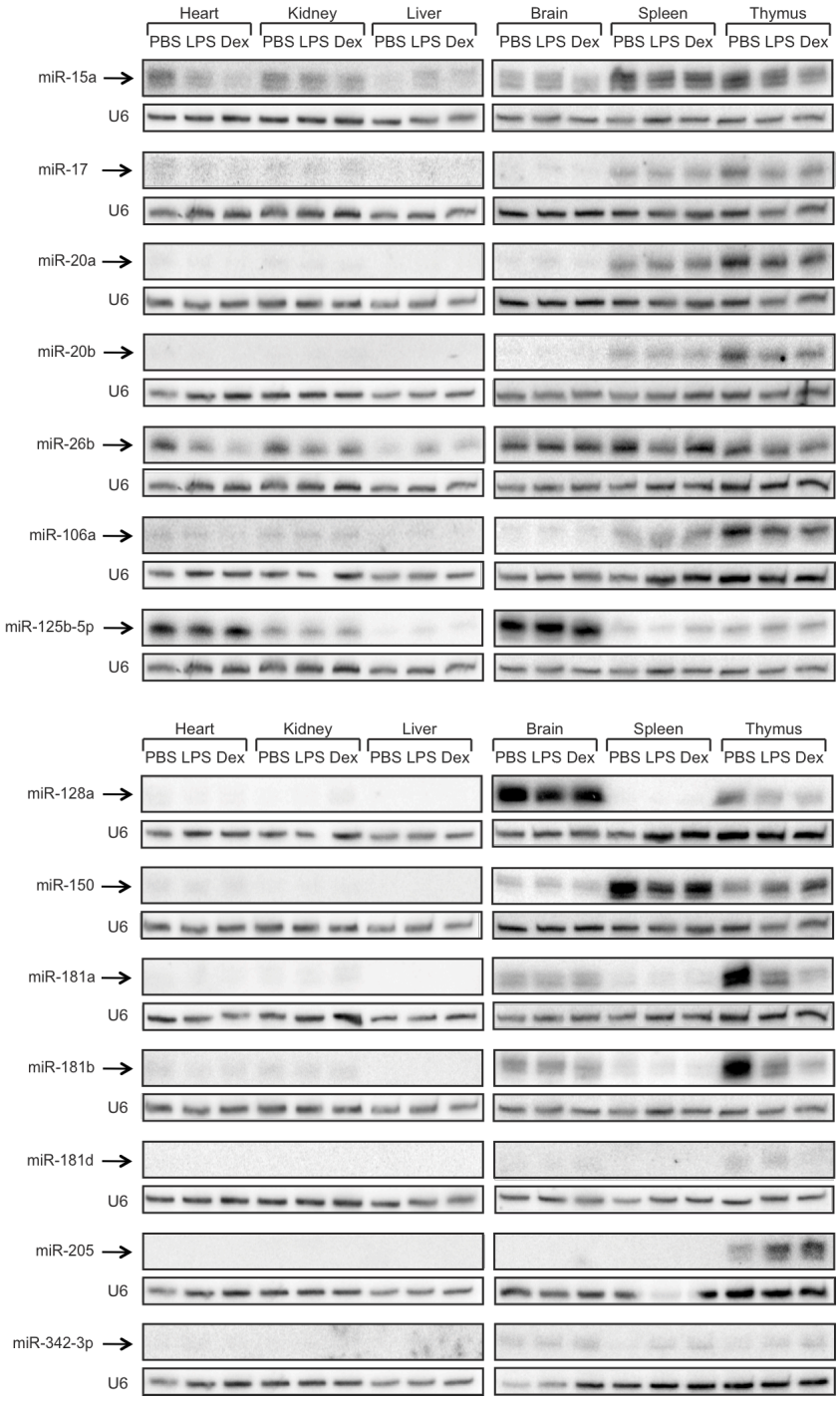

Figure 3.4. Differential expression of stress-responsive microRNAs in diverse tissues. Total RNA was isolated from the heart, kidney, liver, brain, spleen, and thymus of PBS-, LPS-, or Dex-treated mice at 72 hrs post-injection. The individual miRs were detected by Northern blotting. The relative amounts of RNA input were determined by blotting for U6. Data are representative of at least 3 independent experiments.

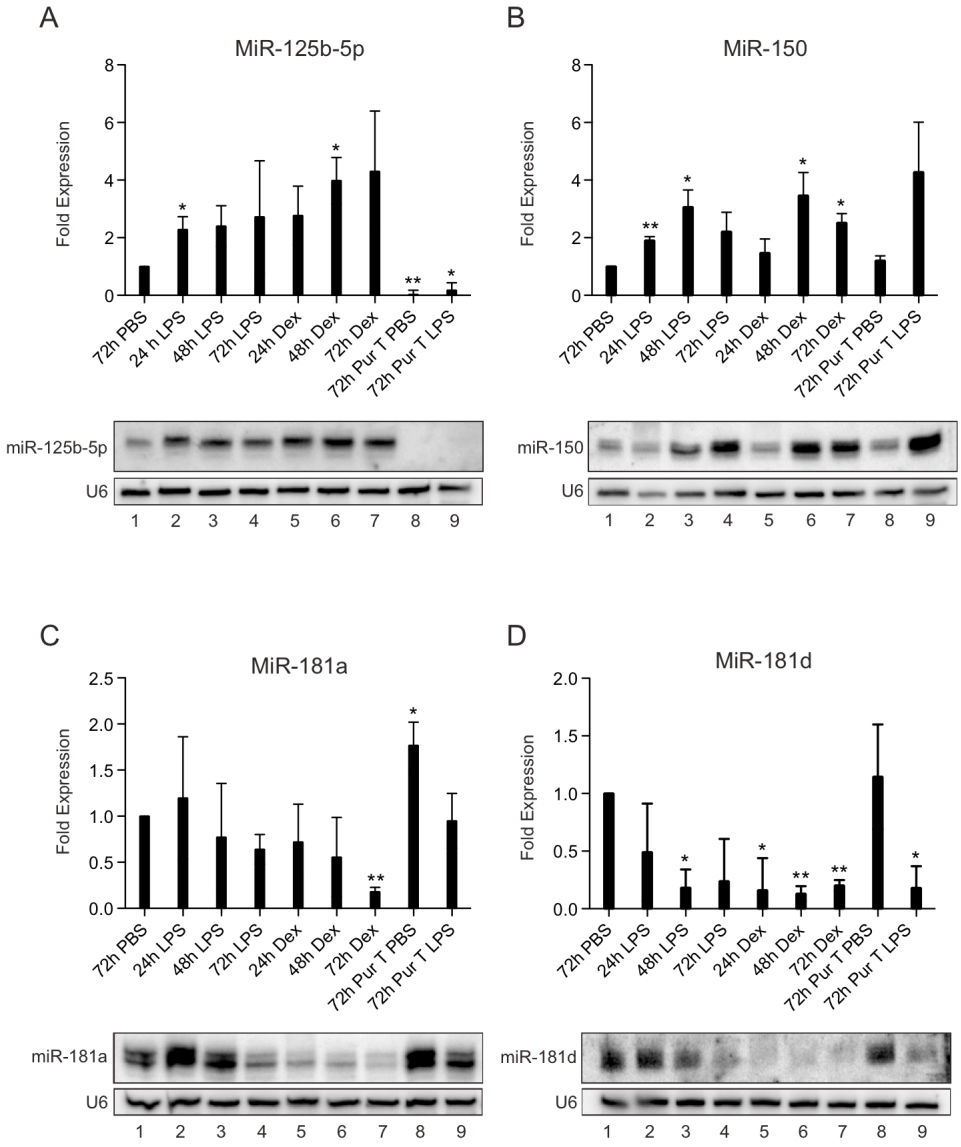

Figure 3.5. Time-dependent alterations in the expression of miR-125b-5p, miR-150, miR-181a, and miR-181d upon stress. (**A**-**D**) Total RNA was isolated from thymic tissue prepared from PBS- (lane 1), LPS- (lanes 2-4), and Dex- (lanes 5-7) treated mice at 24 hrs (lanes 2, 5), 48 hrs (lanes 3, 6), and 72 hrs (lanes 1, 4, 7). In lanes 8-9, RNA was prepared from purified T cells isolated from the thymus. Northern blots were performed for the selected miRs: miR-125b-5p (**A**), miR-150 (**B**), miR-181a (**C**), and miR-181d (**D**). The samples were normalized for total RNA amounts with a U6 probe. Data shown are the mean +/- SD of relative fold changes in miR expression levels of PBS- versus LPS- or Dex-treated samples from 3 to 5 independent Northern blots (*$p < 0.05$, **$p < 0.01$, ***$p < 0.001$, versus the PBS control; Two-tailed unpaired Student *t*-test).

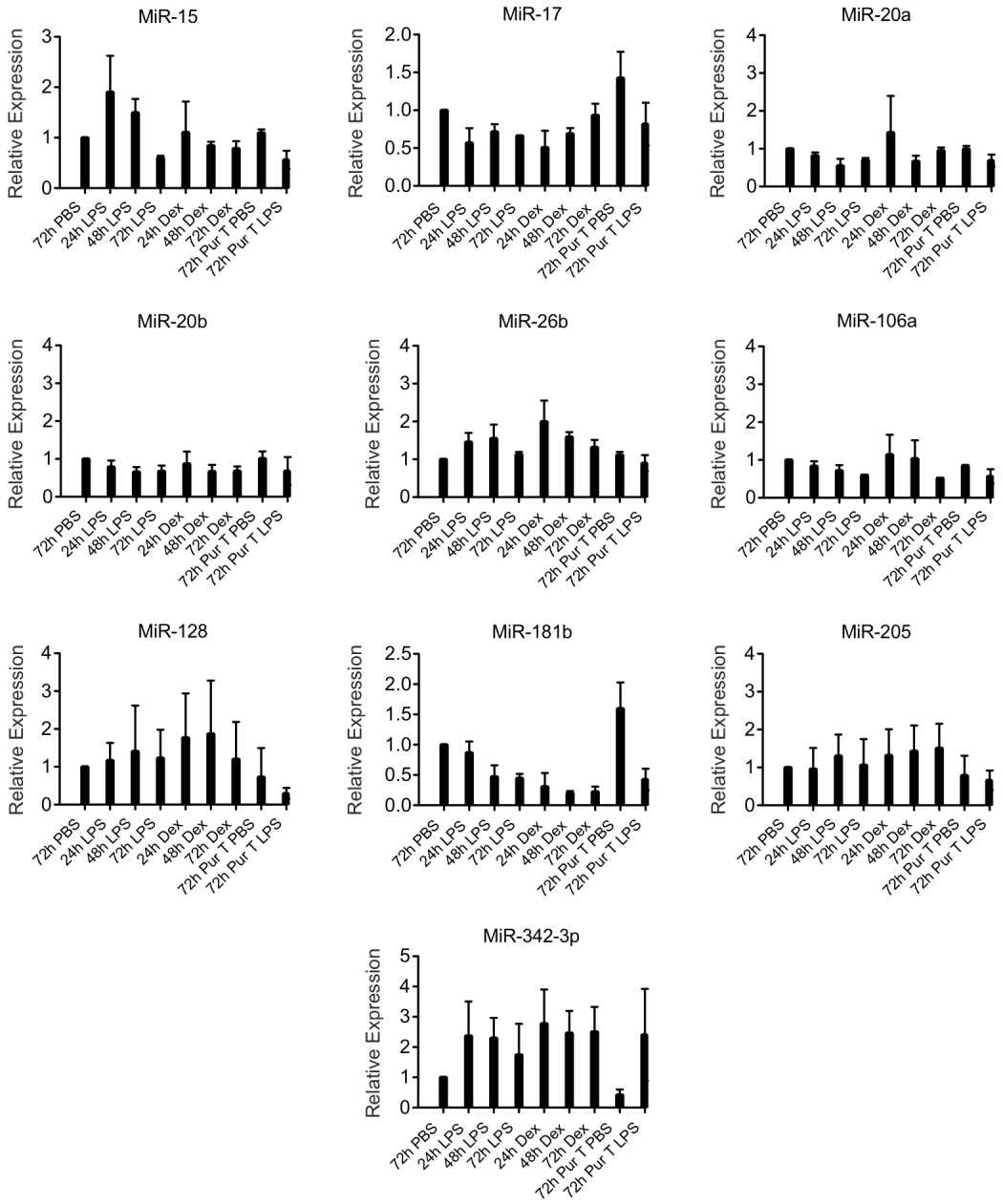

Figure 3.6. Stress responsive changes in thymic microRNA profiles are time dependent. Total RNA was isolated from thymic tissue prepared from PBS- (lane 1), LPS- (lanes 2-4), and Dex-treated (5-7) mice at 24 hrs (lanes 2, 5), 48 hrs (lanes 3, 6), and 72 hrs (lanes 1, 4, 7). In lanes 8-9, T cells were purified from the thymus preparation prior to Northern blotting for the selected miRs. The samples were normalized for total RNA amounts with a U6 probe. Data shown is mean +/- SD of relative fold changes in miR expression levels of PBS- versus LPS- or Dex-treated samples from 3-5 independent northern blots.

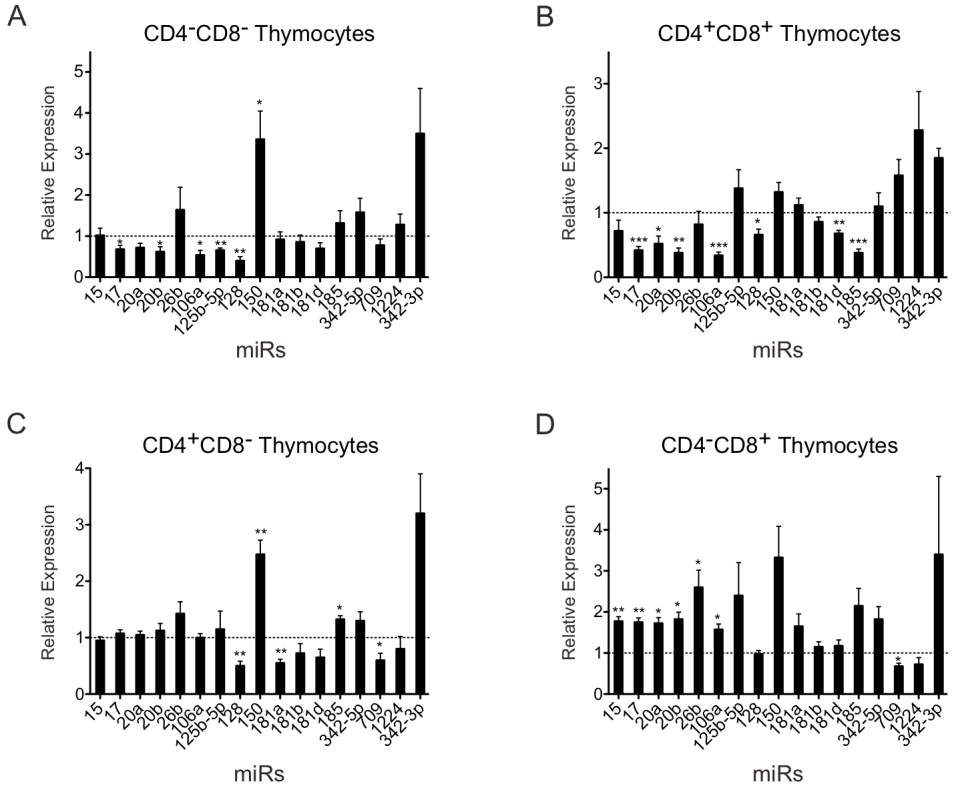

Figure 3.7. Stress-responsive thymic microRNAs are differentially regulated in thymocyte subsets. (**A-D**) Thymocytes from PBS and LPS injected mice (72 hrs) were sorted into $CD4^-CD8^-$ (DN) (**A**), $CD4^+CD8^+$ (DP) (**B**), $CD4^+CD8^-$ (CD4 SP) (**C**), and $CD4^-CD8^+$ (CD8 SP) (**D**) subsets. RNA was isolated from the sorted sub-populations. Real-time microRNA RT-PCR was used to detect the levels of the indicated miRs in various subsets. The vertical line on the figure indicates the control (PBS) threshold set as 1. Data represent the average fold changes +/- SD in miR expression levels of PBS- versus LPS-treated samples normalized to the endogenous U6 levels, of 4 independent experiments performed in triplicate (*$p < 0.05$, **$p < 0.01$, ***$p < 0.001$, versus the threshold; One sample Student *t*-test).

CHAPTER FOUR

TRANSGENIC EXPRESSION OF MICRORNA-181D AUGMENTS THE STRESS SENSITIVITY OF $CD4^+CD8^+$ THYMOCYTES

This chapter presents unpublished data submitted as: **Belkaya, S.**, and N. S. van Oers. Transgenic expression of microRNA-181d augments the stress sensitivity of $CD4^+CD8^+$ thymocytes.

Introduction

The thymus is the primary organ responsible for T cell development, providing for a continuous output of effector and regulatory T cells. Interestingly, this tissue is hyper-responsive to stress resulting from infections, trauma, pregnancy, starvation, and alcoholism [27,29,30,140,142,143,146]. These diverse forms of stress induce a thymic involution, caused by the deletion of immature $CD4^+CD8^+$ thymocytes and a ensuing reduction in thymic cellularity [23,172]. In the case of infections, the release of pathogen-associated molecular patterns, such as lipopolysaccharide (LPS) activates Toll-like receptor 4 signaling pathways, releasing inflammatory cytokines that cause thymocyte cell death [52,129,132]. Elevations in these inflammatory cytokines (IL-1β, IL-6, and LIF) induce the production and release of glucocorticoids (GC) via the hypothalamic-pituitary-adrenal axis and intrathymically [33,147,148,151,152]. The GCs, as lipophilic steroids, diffuse across the plasma membrane and trigger apoptosis of thymocytes by binding to GC-receptors (NR3C1)

that are expressed at high levels within the $CD4^+CD8^+$ (DP) thymocytes [35,36,141]. Synthetic GCs (e.g. Prednisone and Dexamethasone) are widely used for the treatment of patients with malignancies and autoimmune diseases, although their effects on thymocytes are not often realized [155,173]. A second mechanism underlying the stress-induced thymic atrophy is the direct sensing of microbial molecules by pattern-recognition receptors expressed on thymic epithelial cells (TECs) [26,172,174]. Activation of these pathways reduces the ability of TECs to support thymopoiesis [58,172].

Several microRNAs (miRs) can modulate stress responses in tissues such as the thymus, heart, and brain [168,175,176]. MiRs are a class of small, non-coding RNA molecules that regulate gene expression at the post-transcriptional level by degrading mRNAs and/or repressing mRNA translation [77,78]. In the thymus, reductions in the pre-miR Rnase, Dicer, and/or just miR-29a increase the levels of the IFN-α receptor on TECs, decreasing their ability to support thymopoiesis following viral infections [58]. LPS and/or dexamethasone injections cause a transient loss of both Dicer and DGCR8 in TECs and immature thymocytes within the first 6-12 hrs, significantly reducing miR biogenesis [131]. At later time points, there is a selective up- and down-modulation of 18 thymically-encoded stress responsive miRs [132]. MiR-181d is one of the most stress-responsive miRs identified in the thymus, declining 15-fold after several days post-LPS injection [132]. It is a member of miR-181 family that includes miR-181a, miR-181b, and miR-181c. These four miRs are produced from three different polycistronic clusters: 181ab1, 181ab2, and 181cd [94,95]. In contrast to miR-181d, miR-181c remains unchanged while miR-181a and miR-181b are reduced 2- and 6-fold upon stress, respectively [132]. Such results reveal a differential

regulation of miR-181 family members under both steady and disease states [91,92,132]. Reductions in miR-181a increase the cell survival of astrocytes from ischemia-like injury upon glucose deprivation, in part via elevations in one of its targets, Bcl2 [177]. In developing thymocytes, miR-181a controls T-cell repertoire selection by targeting CD69, Bcl2, Dusp5, Dusp6, Ptpn11, Ptpn22, Nrarp, and Pten [97,98,99,100,101,131,177]. While miR-181a/b knockout (KO) mice have normal αβ T cell development, their NK T cell development is blocked [100,101]. Contrasting this, the complete deficiency of all miR-181 family members is embryonic lethal, suggesting a functional compensation or redundancy [99].

To study the contribution of miR-181d to stress-induced thymic atrophy, we generated two transgenic (Tg) mouse models with increasing levels of miR-181d in immature thymocytes and peripheral T cells. The miR-181d Tg mice exhibited a statistically significant reduction in DP thymocytes. *In vivo* LPS and Dexamethasone (Dex) injections caused a substantial increase in the stress-sensitivity of the DP thymocytes, in a miR-181d dose-dependent manner. The targeted mutation of the miR-181d sequence in the mouse genome revealed a similar stress-mediated thymic atrophy as control mice. These results suggest that multiple miR-181 family members function in a compensatory manner.

Results

Generation of miR-181d transgenic mice

The miR-181 family comprises four members, miR-181a, miR-181b, miR-181c, and miR-181d, generated from three separate genomic clusters (miR-181ab1, miR-181ab2, miR-

181cd) [94,95]. While all share an identical seed sequence at their 5' end, miR-181d is the most divergent member with between 1 and 5 nucleotide differences (Figure 4.1A). All miR-181 family members are primarily expressed in the thymus, at levels at least 10-20 fold higher than the brain and liver [92]. In most other tissues, they were very low or undetectable (Figure 4.1B). Although miR-181c and miR-181d are transcribed from the same cistron, miR-181d is expressed at least 5-10 fold higher in the hematopoietic lineages, including immature thymocytes and T-helper cells [91,92]. It is one of the most stress responsive miRs in the thymus, with reductions of 15-fold occurring following LPS treatment. MiR-181c expression was unaffected upon stress [132]. This indicates that additional post-transcriptional mechanisms exist for the processing of miR-181d.

In order to identify the contribution of miR-181d to thymopoiesis under normal and stress conditions, we first utilized a gain of function approach. Since miR-181c and miR-181d are separated by only 85 nucleotides, the expression of miR-181d could only be achieved by including 146 bases upstream of miR-181d [132]. This excluded the first 28 nucleotides of miR-181c, eliminating the seed sequence of mature miR-181c and the sense-antisense base pairing involved in pre-miR-181c formation (Figure 4.1C). With this construct, transgenic mice were generated in which the murine pri-miR181d was over-expressed in thymocytes and peripheral T cells (Figure 4.1C) [134]. Two transgenic lines (Tg-8 and Tg-38) were selected based on their increasing levels of miR-181d expression. Relative to the wild-type control, which was set as 1, miR-181d was over-expressed 2- and 6-fold in Tg-8 and Tg-38, respectively (Figure 4.1D). Interestingly, we also detected increased levels of miR-181c in miR-181d transgenic thymocytes although the transgenic construct

excluded a significant portion of the mature miR-181c (data not shown). This is likely due to the cross-reactivity between RT-PCR probes designed for these highly homologous miRs.

Elevated levels of miR-181d perturb T cell development

The total thymic cellularity was decreased in both the Tg-8 and Tg-38 lines (Figure 4.2A). This was matched with an increased percentage of $CD4^-CD8^-$ (DN) cells, an effect directly correlated with elevated levels of miR-181d (Figure 4.2B-C). Both the percentage and number of $CD4^+CD8^+$ (DP) thymocytes in Tg-8 and Tg-38 lines were significantly lower than in control mice (Figure 4.2B-D). While the percentages of $CD4^+CD8^-$ (CD4 SP) and $CD4^-CD8^+$ (CD8 SP) thymocytes were increased significantly, their overall cell numbers were similar, reflecting the decreased percentage of DP thymocytes (Figure 4.2E). The DN cells were next characterized for CD44 and CD25 expression, markers used to define 4 subsets, DN1-DN4. The miR-181d transgenic mice had a similar profile of DN1-DN4 cells as wild type mice (data not shown). In addition, similar levels of intracellular TCRβ and surface CD5 expression were detected in the DN3 ($CD44^-CD25^+$) thymocytes from the control and miR-181d Tg mice, indicating normal TCR rearrangements and pre-TCR signaling, respectively (data not shown). Finally, the proportion and numbers of γδ T cells and $NK1.1^+$ cells were normal in miR-181d Tg mice (data not shown).

The reduced number DP thymocytes in the miR-181d transgenic mice could be caused by accelerated positive selection, diminished cell survival, and/or increased sensitivity to stress. DP thymocytes had a normal expression of CD5, CD69, and TCRβ (Figure 4.2F). In contrast, the expression of CD69 on CD4 SP and CD8 SP thymocytes was significantly

decreased in a miR-181d dose-dependent manner (Figure 4.2G-H). Moreover, the ratio of $CD69^{+}TCR\beta^{high}$ (early stage) to the $CD69^{-}TCR\beta^{high}$ (late stage) SP thymocytes was lower in miR-181d Tg mice (Figure 4.2I). This suggests that elevations in miR-181d levels might alter further maturation and/or egress of SP thymocytes. Furthermore, Annexin V and 7-AAD staining showed no alterations in cell death of immature thymocytes in the Tg-8 and Tg-38 lines (data not shown).

MiR-181d transgenic mice have slightly reduced peripheral T cell numbers

The total cellularity of lymph nodes and spleen was similar in all the Tg lines compared to normal mice (Figure 4.3A-B). Both percentages and numbers of $CD4^{+}CD8^{-}$ T cells were slightly lower with increased miR-181d levels (Figure 4.3C-H), but this reduction only reached statistical significance in the Tg-38 line when comparing percentages of $CD4^{+}CD8^{-}$ T cells in the lymph nodes, and for the absolute numbers of $CD4^{+}CD8^{-}$ T cells in the spleen (Figure 4.3D, H). The reductions in peripheral $CD4^{-}CD8^{+}$ T cells were more pronounced in miR-181d Tg lines (Figure 4.3C-H). Both the percentages and numbers of mature $CD4^{-}CD8^{+}$ T cells were significantly decreased in lymph nodes and spleen of the Tg-38 line (Figure 4.3D-E, G-H). While the cellularity was marginally altered, the percentages of peripheral $B220^{+}$ B cells were equivalent in the control and miR-181d Tg mice (data not shown). The activation and memory phenotypes were not different when comparing the mice, as revealed with the similar CD44 and CD62L profiles (data not shown). In addition, the naive miR-181d Tg-8 and Tg-38 T cells displayed similar survival and proliferative responses as wild type controls upon anti-CD3/CD28 stimulations *in vitro* (data not shown).

Taken together, these results suggested that once the T cells egressed from the thymus, they had normal functions.

Transgenic expression of miR-181d augments stress-induced thymic atrophy

To study the impact of miR-181d on stress-induced thymic atrophy, we analyzed the effects of LPS injections on thymic cellularity (Figure 4.4A). LPS treatment (100 μg/mouse) resulted in 2- and 4-fold greater reduction in both percentages and numbers of DP thymocytes in the Tg-8 and Tg-38 lines, respectively, compared to wild-type control (Figure 4.4B-D). While the percentages of CD4 SP and CD8 SP thymocytes were increased in the transgenic lines after LPS injection, the absolute numbers of these SP thymocytes remained equivalent to the wild type control (Figure 4.4C-D). The decreased ratio of DP thymocyte numbers in LPS- versus PBS-treated control and transgenic mice further supported the findings that miR-181d enhanced stress sensitivity of DP thymocytes (Figure 4.4E). The DP thymocytes in the miR-181d Tg lines had elevated cell death markers upon stress (Figure 4.4F). Moreover, a dose response analysis using varying amounts LPS indicated an accelerated depletion of DP thymocytes at all doses (Figure 4.5A). Peripheral T and B cell numbers were similar in the control and miR-181d Tg mice following LPS injections, indicating that the miR-181d effects are specific to the thymus (data not shown) [132].

Consistent with LPS-induced thymic atrophy, an IP injection of dexamethasone (Dex), a synthetic glucocorticoid, also results in a dramatic elimination of the DP thymocytes [131,132]. Forty-eight hrs after Dex injection (60 μg/mouse), Tg-38 mice had more than 2-fold reduction in total thymic cellularity and DP thymocyte numbers (Figure 4.5B-E). Taken

together, these findings indicate that miR-181d over-expression selectively elevates the stress-sensitivity of DP thymocytes.

T cell development and effector functions in miR-181d knockin mice are normal

Since miR-181c and miR-181d are separated by only 85 nucleotides, we utilized a knockin (KI) approach in which only the miR-181d sequence was modified (miR-181d KI) (Figure 4.6). A total of 11 base-replacements (five in the 5' seed region) were introduced into the miR-181d sequence in order to disrupt the formation and processing of the pre-miR-181d stem-loop structure (Figure 4.7A). The miR-181d KI mice had normal T cell development, with similar percentages and numbers of thymocyte subsets (Figure 4.7B-F). Consistent with their normal thymopoiesis, the number and percentage of peripheral lymphocytes in these mice were similar to wild-type controls (Figure 4.7G-I). Of note, percentages of $CD4^+$ and $CD8^+$ T cells were significantly increased in the spleen of miR-181d KI mice (Figure 4.7I). While the transgenic expression of miR-181d augmented stress-induced thymic atrophy, its selective elimination had no preventative effect on thymic involution following LPS or Dex injections (Figure 4.8A-H). Moreover, there was a similar level of Annexin V induction in the KI compared to normal mice in response to stress (Figure 4.8E). Finally, the percentage and number of SP thymocytes appeared normal in the miR-181d KI mice following LPS and Dex treatments (Figure 4.8C, G-H). These experiments suggest that the targeted elimination of one miR-181 family member is insufficient to modulate the stress responsiveness of developing thymocytes.

Analysis of differential gene expression in miR-181d transgenic and miR-181d knockin mice

While a number of mRNA targets of miR-181 have been reported, it is not known whether miR-181d has overlapping and/or distinct targets. Therefore, gene expression comparisons were done with the miR-181d transgenic line, Tg-8 and the miR-181d KI lines. Of the 26,000 genes probed on the array, 78 were down- and 60 were up-regulated more than 1.5-fold in the thymus of miR-181d Tg-8 mice compared to the miR-181d KI ($p < 0.05$) (data not shown). Ingenuity Pathway Analysis (IPA) was applied to the genes significantly modulated more than 1.25-fold. The top 20 over-represented canonical pathways are listed for both down- and up-regulated genes (Figure 4.9A-B). The most significant pathways affiliated with down-regulated genes included PPAR (Peroxisome proliferator-activated receptor) signaling, Cdc42 signaling, and PI3K/Akt signaling. IL-1 signaling, phospholipase C signaling, and T cell signaling pathways matched the up-regulated genes in miR-181d Tg thymus (Figure 4.9A-B). We also performed Gene Ontology Slim (GO Slim) analysis with the Web-based Gene Set Analysis Toolkit (WebGestalt) to obtain a broad summary of the dysregulated genes (miR-181d Tg versus miR-181d KI thymocytes) [138,139]. GO Slim classification was provided with the number of genes for each biological process category (Figure 4.9C). Most of the up- and down-regulated genes in miR-181d Tg thymocytes were represented within the metabolic process category (Figure 4.9C). 211 down-regulated genes were annotated in response to stimulus, whereas 104 were within the category of response to stress with a *p*-value of 2.84×10^{-14} (Figure 4.9C and data not shown). These data confirm

the involvement of miR-181d-targeted genes in cell metabolism and stress responses, consistent with the phenotypes revealed in the Tg mice.

We next performed Transcription Factor (TF) Target enrichment through the WebGestalt, to identify the genes sharing similar TF target motifs among the dysregulated genes in miR-181d Tg versus KI thymocytes (Table 4.1). A significant number of these genes had predicted binding sites for Foxo4 and Myc, both of which are direct targets of the PI3K/Akt signaling pathways [178,179,180].

Discussion

MiR-181d is one of the most down-regulated miRs detected in the thymus following stress [132]. We used both transgenic and gene targeting approaches in mouse models to determine the role of miR-181d in thymopoiesis under normal and stress conditions. While over-expression of miR-181d resulted in a slight reduction in thymic cellularity under normal conditions, the depletion of $CD4^{+}CD8^{+}$ thymocytes following LPS or Dex injections was significantly increased. Such experiments indicate that miR-181d potentiates programmed cell death. This would suggest that the down-modulation of miR-181d occurring following stress could protect thymocytes from cell death.

Most DP thymocytes undergo a process of death by neglect, partly through the systemic and intrathymic production of glucocorticoids. Stress elevates these glucocorticoid levels, enhancing the magnitude and kinetics of cell death. Within the first 12 hrs, stress causes a global reduction in miRs by the degradation of Drosha, DGCR8, and Dicer [131]. By 48-72 hrs, and once Dicer levels are restored, there is a differential regulation of mature

miRs, some up- and others down-regulated. Interestingly, while miR-181d was down-modulated around 15-fold, the much more abundantly expressed miR-181a and miR-181b family members were only minimally affected [132]. This indicates that the processing of the miR-181c/d locus during stress is very distinct from the two miR-181a/b loci. In fact, the processing is specific to miR-181d, as miR-181c is marginally affected even though it arises from the same cistron and is only separated by 85 nucleotides.

Most studies to date have focused on miR-181a, the most abundant miR in thymocytes [92]. It targets mRNAs encoding TCR signaling proteins, controlling repertoire selection by establishing signaling thresholds [96,97]. A gene analysis of mice deficient in miR-181a/b revealed a distinct set of miR-181 targets, with Pten, a regulator of PI3K/Akt signaling, one of the principal targets [100]. In our study, PI3K/Akt and PPAR signaling were the most significant pathways enriched among the miR-181d down-regulated genes. Furthermore, many of the targeted genes had Foxo4 or Myc binding motifs, and these two transcription factors are regulated by PI3K/Akt. Such results strongly suggest that miR-181d targets genes responsible for cell metabolism and survival. Since stress and metabolic rates are intricately linked, the altered expression of miR-181d would modulate energy and nutrient demands within the cell.

MiR-181a is also implicated in regulating Notch1 down-stream signaling [98,99]. Notch1 is a critical regulator of T cell development [55]. In fact, Notch1 signaling increases the resistance of DP thymocytes to GC-induced cell death [54,56,181]. Elevations of miR-181d would attenuate the Notch1 signaling pathway, increasing the magnitude of DP cell death in response to stress. MiR-181 family members also target Bcl2, with its reduction

increasing the GC-sensitivity of DP thymocytes [36,93,177]. Therefore, it is likely that the diverse miR-181d targets in TCR-, PI3K/Akt-, Notch1-, and anti-apoptotic-signaling pathways combinatorially modulate the stress responses of thymocytes. CD69 is one of the overlapping targes of miR-181a and miR-181d [93,132]. Transgenic expression of miR-181d led to decreased levels of CD69 expression on SP thymocytes, reducing the ability of T cells to leave the thymus. The additional effects on the SP thymocytes likely result from additional known and unidentified miR-181d targets.

To specifically define the role of miR-181d in thymopoiesis, we developed a miR-181d gene-targeted mouse in which the miR-181d seed sequence and hairpin loop were changed. There was no effect of this knockout on either normal or stress-modulated thymopoiesis. This finding is consistent with recent reports that miR-181c/d knockout mice have normal T cell development [99,100]. This strongly indicates a functional redundancy/compensatory mechanism exists among the miR-181 family members. Consistent with this, a complete targeting of all miR-181 family members causes a presumed embryonic lethality [99]. Besides miR-181d, we identified 17 additional stress-responsive miRs in the thymus. All have known targets that could influence stress responses, including the miR-17-92a family that targets pro-apoptotic genes [87,169]. MiR-185 is another stress-responsive thymic miR that is haploinsufficient in 22q11.2 deletion syndrome patients and down-regulated following LPS or Dex exposure [109,132]. The role of miR-185 during thymopoiesis will be discussed in the next chapter.

Together with previous reports, this study further supports the involvement of miRs in stress-induced thymic involution. In particular, elevated levels of miR-181d lead to

increased loss of DP thymocytes upon stress. Nevertheless, this may be advantageous in preventing toleragenic signalings in immature thymocytes to foreign antigens derived from infectious agents. Overall, these findings potentiate the importance of miR-181d as therapeutic agents for hematological malignancies exhibiting resistance to GC-induced apoptosis.

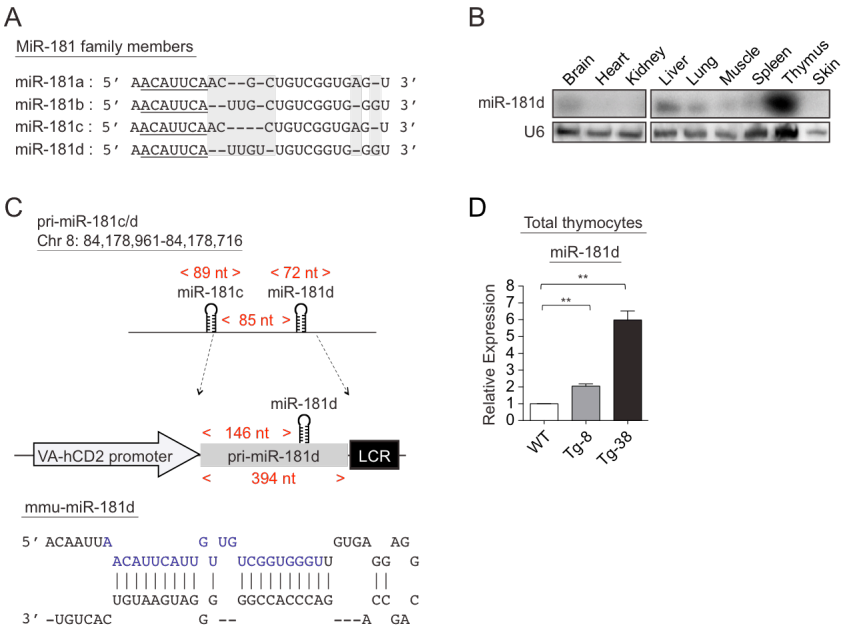

Figure 4.1. Generation of miR-181d transgenic mice. (**A**) Schematic shows the sequence homology between mature miR-181 family members. 5' end seed region is underlined. Base differences are shaded with gray. (**B**) MiR-181d expression in various tissues examined by Northern blotting. U6 probe was used as the endogenous control. (**C**) Cloning of the pri-miR-181d into the VA-hCD2 transgenic cassette. Stem-loop structure of pre-miR-181d is shown, in which mature miR-181d is highlighted in blue. (**D**) Relative miR-181d levels were determined by real-time quantitative PCR. Littermate control values were set to 1. Graph represents the mean fold changes +/- SEM normalized to the U6 levels from 3 independent samples, performed in triplicates (n.s. = non-significant, $*p < 0.05$, $**p < 0.01$, $***p < 0.001$; Two-tailed unpaired Student's t-test).

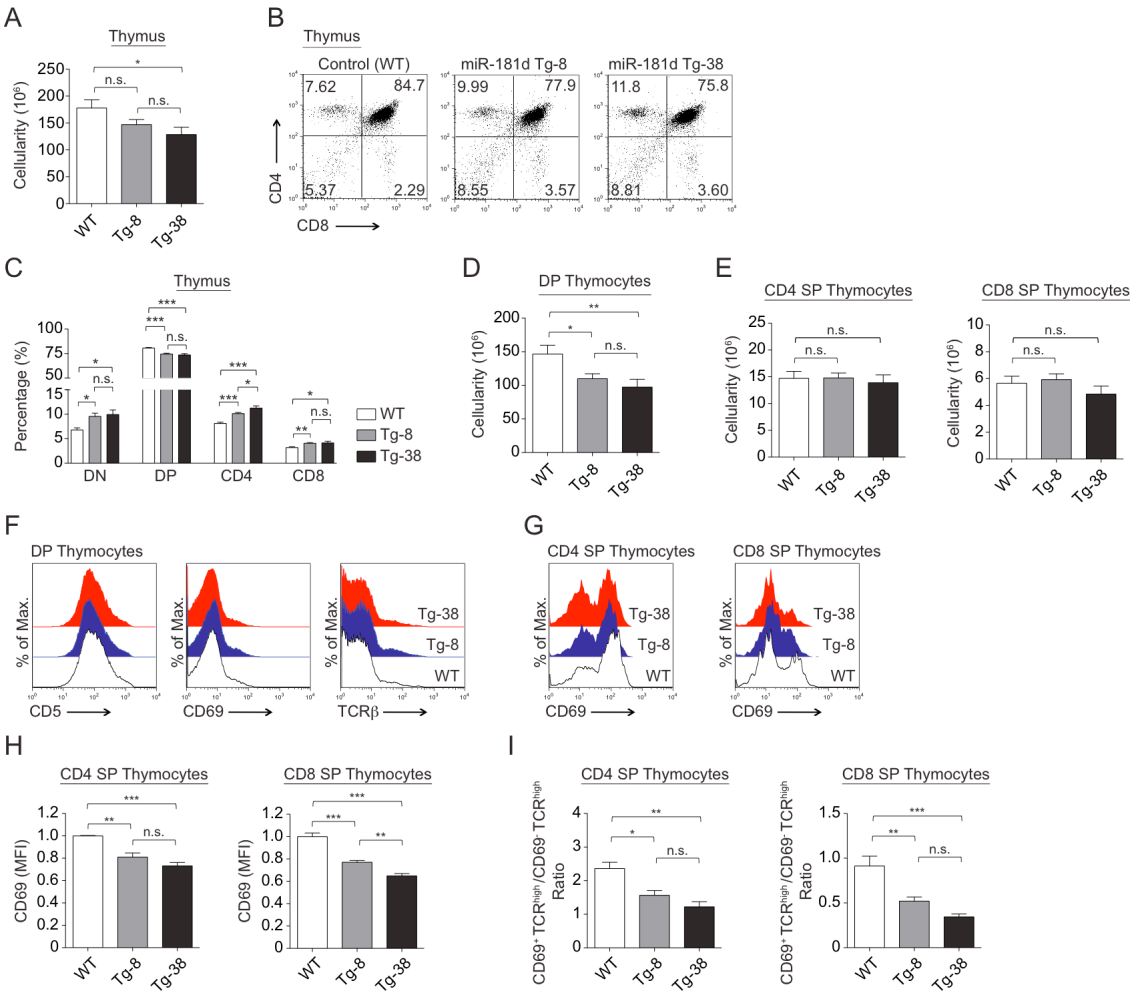

Figure 4.2. MiR-181d over-expression reduces the number of CD4$^+$CD8$^+$ thymocytes. (**A**) Total thymus cellularity in the control and miR-181d Tg mice. (**B**) Representative plots show CD4 by CD8 profiles of thymocytes in the control and miR-181d Tg mice, analyzed by FACS. (**C**) Average percentages of thymocyte subsets (DN, DP, CD4 SP, and CD8 SP) from control and miR-181d Tg mice. (**D**) Absolute cell numbers of DP thymocytes. (**E**) Absolute cell numbers of CD4 SP and CD8 SP thymocytes. (**A**-**E**) Data are from WT (n=18), Tg-8 (n=25), and Tg-38 (n=16) mice. (**F**) Histograms show CD5, CD69, and TCRβ expression gated on DP thymocytes. (**G**) Histograms show CD69 expression on CD4 SP and CD8 SP thymocytes from the WT (white), Tg-8 (blue), and Tg-38 (red) mice. (**H**) Relative MFI (Mean Fluorescence Intensity) levels of CD69 on SP thymocytes. (**I**) Ratio of the CD69$^+$TCRβ^{high} to CD69$^-$TCRβ^{high} thymocyte numbers shown for CD4 SP and CD8 SP thymocytes. (**F**-**I**) Data are of at least 3 mice per group. All bar graphs represent the mean +/- SEM values (n.s. = non-significant, *$p < 0.05$, **$p < 0.01$, ***$p < 0.001$; One-way ANOVA followed by Tukey's post-hoc test).

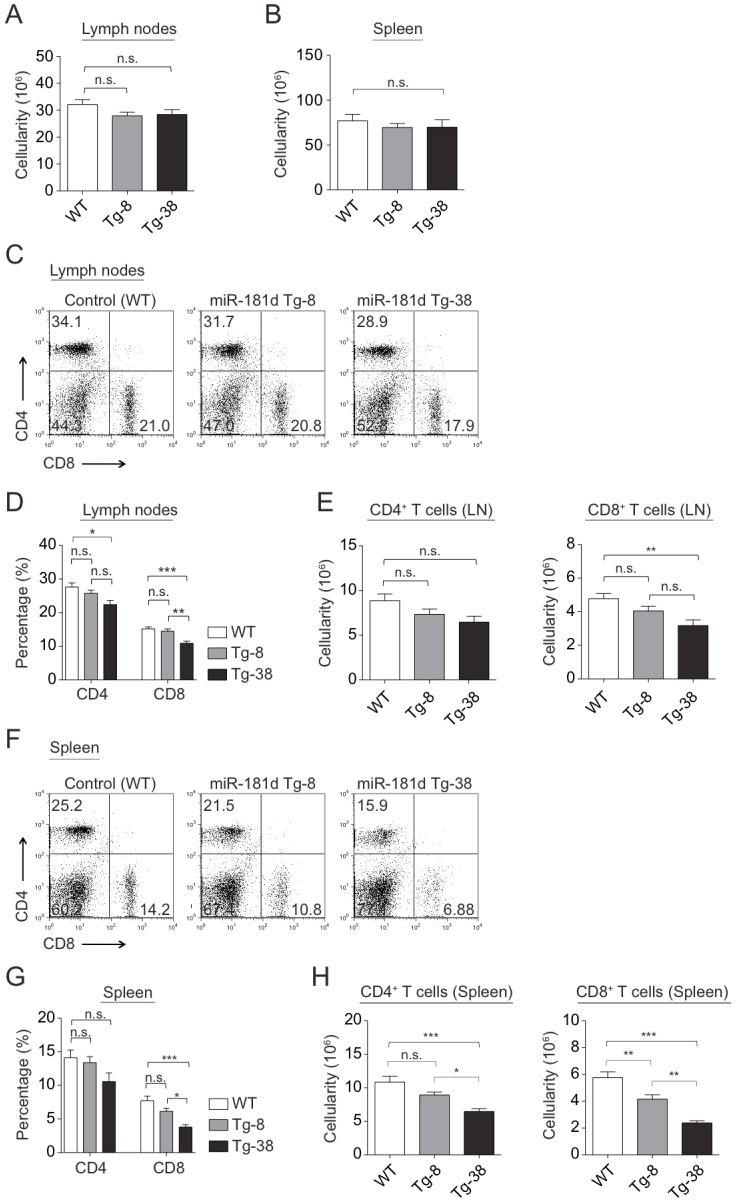

Figure 4.3. Characterization of peripheral lymphocytes in miR-181d transgenic mice. (**A**-**B**) Total cellularity in the lymph nodes (**A**) and spleen (**B**) of the wild type and miR-181d Tg mice. (**C**) Representative FACS plots of $CD4^+$ and $CD8^+$ T cells in the lymph nodes. (**D**-**E**) Average percentages (**D**) and absolute numbers (**E**) of $CD4^+$ and $CD8^+$ T cells in the lymph nodes of WT (n=17), Tg-8 (n=23), and Tg-38 (n=14) mice. (**F**) Representative FACS plots show CD4 by CD8 profiles in the spleen. (**G**-**H**) Average percentages (**G**) and absolute numbers (**H**) of $CD4^+$ and $CD8^+$ T cells in the spleen of WT (n=16), Tg-8 (n=16), and Tg-38 (n=11) mice. All bar graphs show the mean +/- SEM (n.s. = non-significant, $*p < 0.05$, $**p < 0.01$, $***p < 0.001$; One-way ANOVA followed by Tukey's post-hoc test).

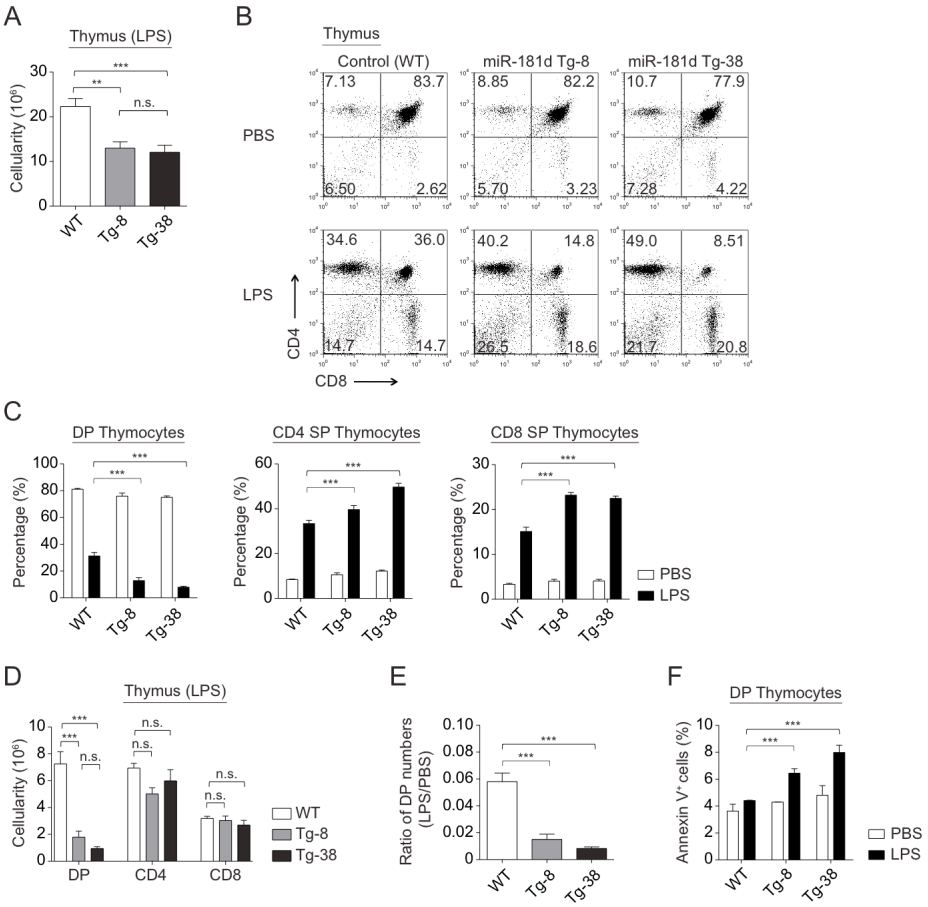

Figure 4.4. Over-expression of miR-181d elevates stress-induced thymic atrophy. (**A**) Total thymic cellularity in the control and miR-181d Tg mice at 72 hrs upon LPS injection (100 μg/mouse) from at least 4 independent experiments using at least 3 mice per injection (n.s. = non-significant, *$p < 0.05$, **$p < 0.01$, ***$p < 0.001$; One-way ANOVA followed by Tukey's post-hoc test). (**B**) Representative CD4 by CD8 profiles of total thymocytes at 72 hrs after PBS or LPS injections. (**C**) Average percentages of DP thymocytes, CD4 SP, and CD8 SP thymocytes post-injection (PBS, white; LPS, black) (n.s. = non-significant, *$p < 0.05$, **$p < 0.01$, ***$p < 0.001$; Two-way ANOVA followed by Bonferroni's post-hoc test). (**D**) Absolute cellularity of thymocyte subsets (DP, CD4 SP, and CD8 SP) upon LPS injection (n.s. = non-significant, *$p < 0.05$, **$p < 0.01$, ***$p < 0.001$; One-way ANOVA followed by Tukey's post-hoc test). (**E**-**F**) Data were calculated from the experiments shown in the panels A and B. (**E**) Ratios of DP thymocyte numbers upon LPS treatment to the numbers of DP thymocytes upon PBS treatment (n.s. = non-significant, *$p < 0.05$, **$p < 0.01$, ***$p < 0.001$; One-way ANOVA followed by Tukey's post-hoc test). (**F**) Average percentages of Annexin V^+ cells gated on DP thymocytes following PBS or LPS injections. (n.s. = non-significant, *$p < 0.05$, **$p < 0.01$, ***$p < 0.001$; Two-way ANOVA followed by Bonferroni's post-hoc test). All bars are of the mean +/- SEM.

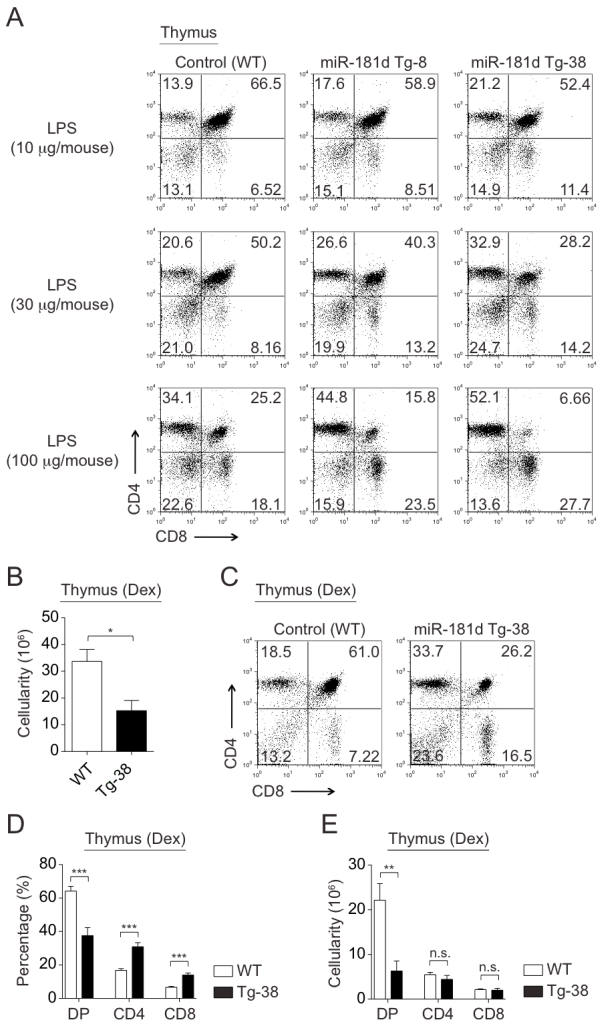

Figure 4.5. Thymic atrophy in miR-181d transgenic mice upon various stress stimuli. (**A**) Representative FACS plots show CD4 by CD8 profiles in the thymus of the control and miR-181d Tg mice at 72 hrs upon LPS injection at varying concentrations (10, 30, and 100 μg/mouse). (**B**) Total thymic cellularity in the control and miR-181d Tg-38 mice at 48 hrs upon Dex injection (60 μg/mouse). (**C**) CD4 by CD8 profiles of thymocytes after 48 hrs post-Dex injections. (**D**-**E**) Average percentages (**D**) and absolute numbers (**E**) of thymocyte subsets following Dex treatment at 48 hrs. All the bar graphs show the mean +/- SEM from at least 4 mice per treatment (n.s. = non-significant, *$p < 0.05$, **$p < 0.01$, ***$p < 0.001$; Two-tailed unpaired Student's *t*-test).

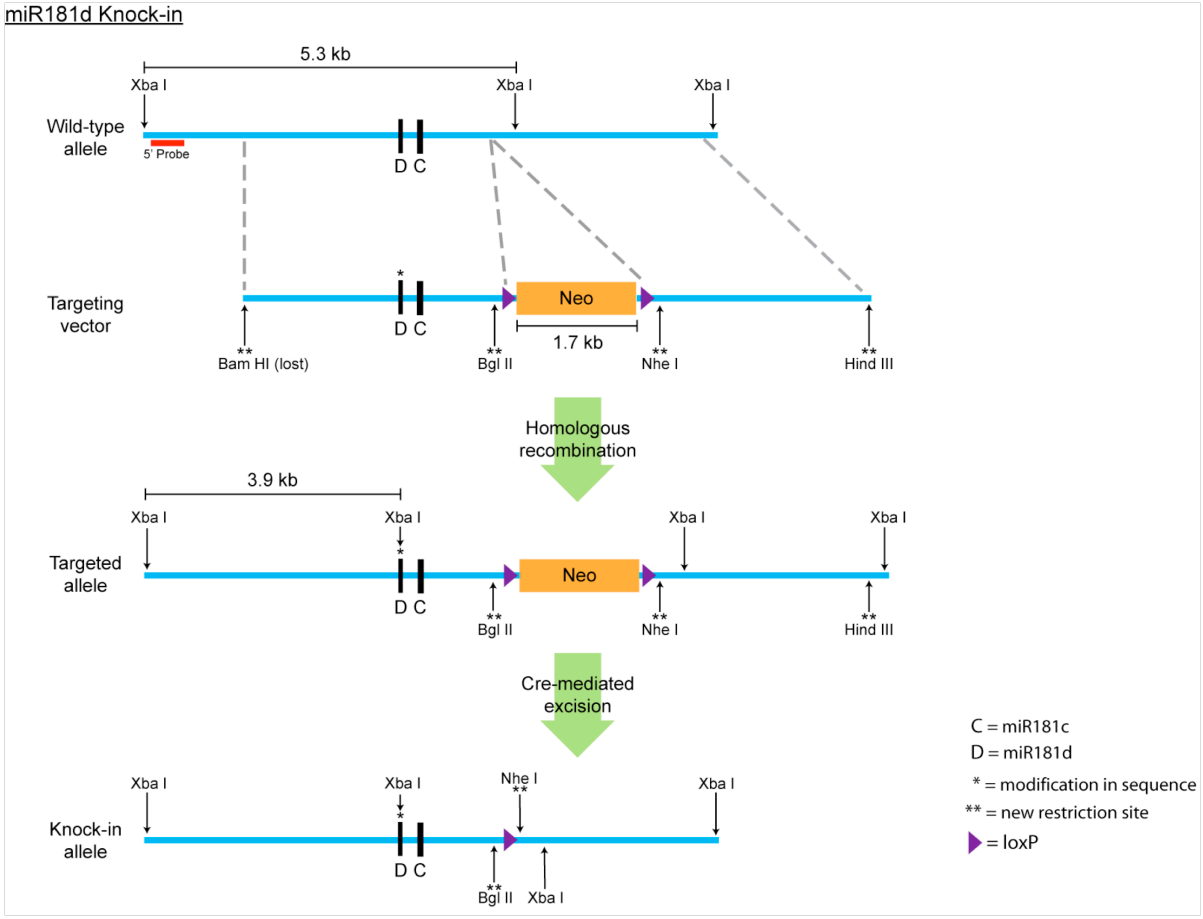

Figure 4.6. Generation of miR-181d knockin mice. Schematic represents the miR-181d knockin strategy. Details are described in the methods section.

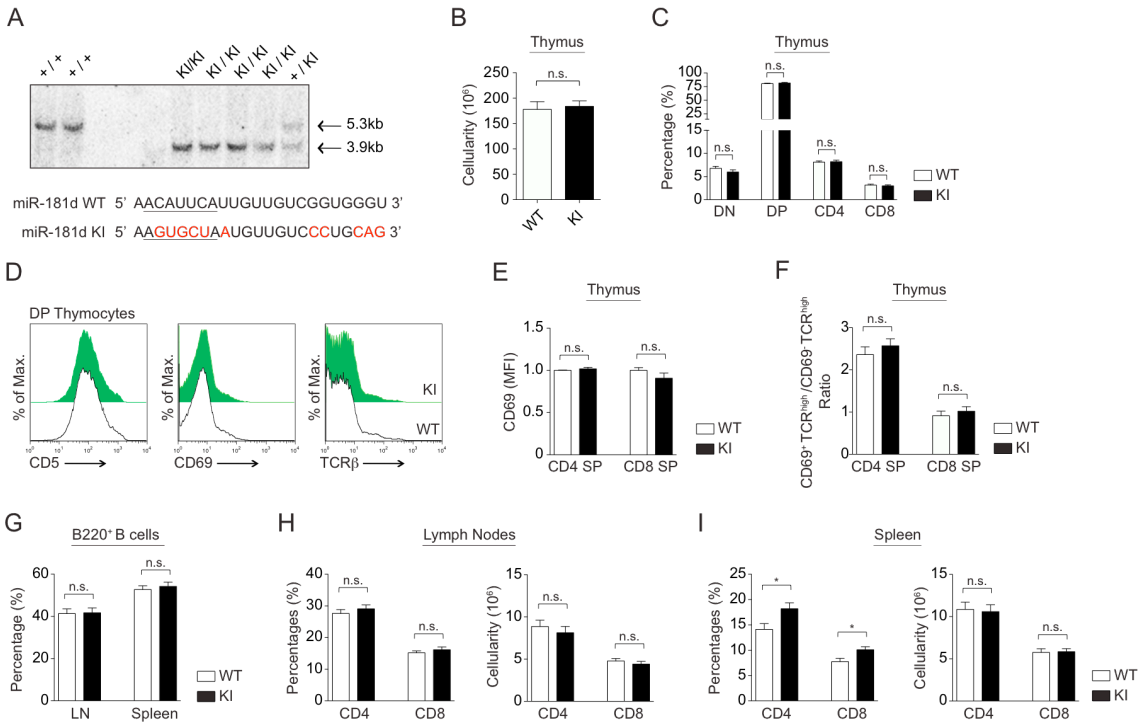

Figure 4.7. T cell development is normal in miR-181d knockin mice. (**A**) Confirmation of miR-181d knockin by a representative southern blot. Comparison of the wild type and mutated (miR-181d KI) sequences are provided. 5' end seed region is underlined. Base replacements are highlighted in red. (**B**) Total thymus cellularity in the control and miR-181d KI mice. (**C**) Average percentages of thymocyte subsets (DN, DP, CD4 SP, and CD8 SP) are shown for the WT (white) and miR-181d KI (black) mice. (**B-C**) Data are of the mean +/- SEM from the WT (n=18) and miR-181d KI (n=17) mice (n.s. = non-significant; Two-tailed unpaired Student's *t*-test). (**D**) Histograms show CD5, CD69, and TCRβ expression gated on DP thymocytes from the WT (white) and miR-181d KI (green) mice. (**E**) Relative MFI (Mean Fluorescence Intensity) levels of CD69 on SP thymocytes. (**F**) Ratio of the $CD69^{+}TCR\beta^{high}$ to $CD69^{-}TCR\beta^{high}$ thymocyte numbers gated on CD4 SP and CD8 SP thymocytes. (**E-F**) Data show the mean +/- SEM values from at least 3 mice per group (n.s. = non-significant; Two-tailed unpaired Student's *t*-test). (**G**) Average percentages of $B220^{+}$ B cells in the lymph nodes and spleen. (**H-I**) Average percentages and absolute cell numbers of $CD4^{+}$ T and $CD8^{+}$ T cells in the lymph nodes (**H**) and spleen (**I**). (**G-I**) Bar graphs show the mean +/- SEM from the WT (n= >16) and miR-181d KI (n= >13) mice (n.s. = non-significant, $*p < 0.05$; Two-tailed unpaired Student's *t*-test).

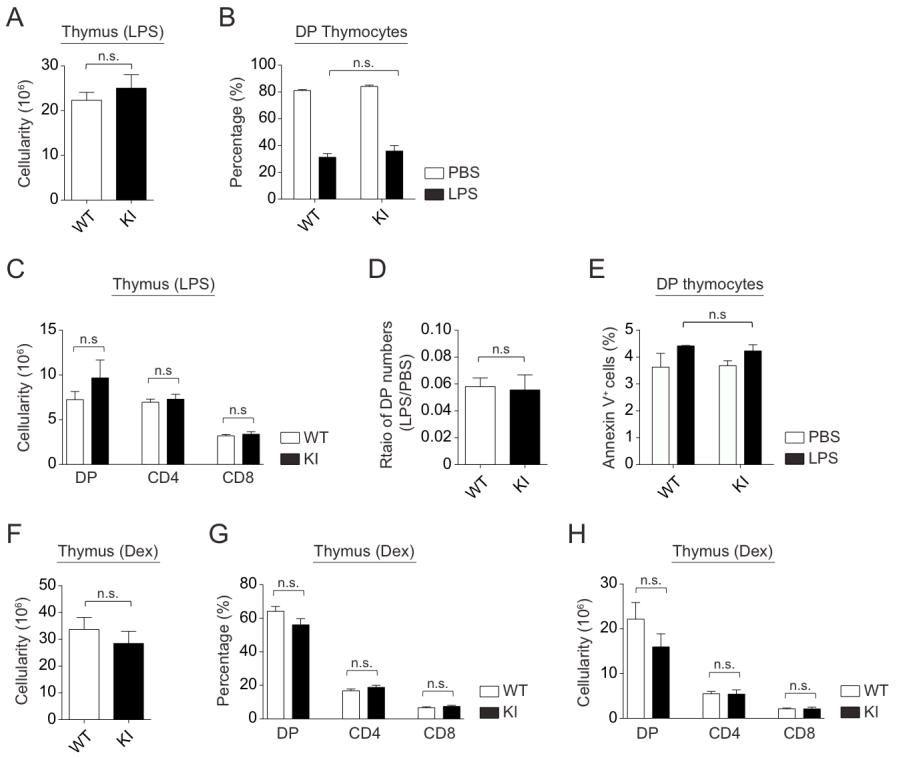

Figure 4.8. Stress-induced thymic atrophy in miR-181d knockin mice. (**A**) Total thymus cellularity in the control and miR-181d KI mice at 72 hrs post-LPS (100 μg/mouse) injection (n.s. = non-significant; Two-tailed unpaired Student's *t*-test). (**B**) Average percentages of DP thymocytes at 72 hrs after PBS or LPS treatment (n.s. = non-significant; Two-way ANOVA followed by Bonferroni's post-hoc test). (**C**) Absolute cell numbers of thymocyte subsets at 72 hrs post-LPS injection (n.s. = non-significant; Two-tailed unpaired Student's *t*-test). (**A-C**) Data are of the mean +/- SEM from at least 4 independent experiments using at least 3 mice per treatment. (**D-E**) Data were calculated from the experiments shown in the panels A and B. Each bar shows the mean +/- SEM. (**D**) Ratios of DP thymocyte numbers upon LPS treatment to the numbers of DP thymocytes upon PBS treatment (n.s. = non-significant; Two-tailed unpaired Student's *t*-test). (**E**) Average percentages of Annexin V^+ cells gated on DP thymocytes (n.s. = non-significant; Two-way ANOVA followed by Bonferroni's post-hoc test). (**F**) Total thymic cellularity in the control and miR-181d KI mice at 48 hrs upon Dex injections (60 μg/mouse). (**G-H**) Average percentages (**G**) and absolute numbers (**H**) of thymocyte subsets following Dex treatment at 48 hrs. (**G-H**) Bar graphs show the mean +/- SEM from at least 4 mice per treatment (n.s. = non-significant; Two-tailed unpaired Student's *t*-test).

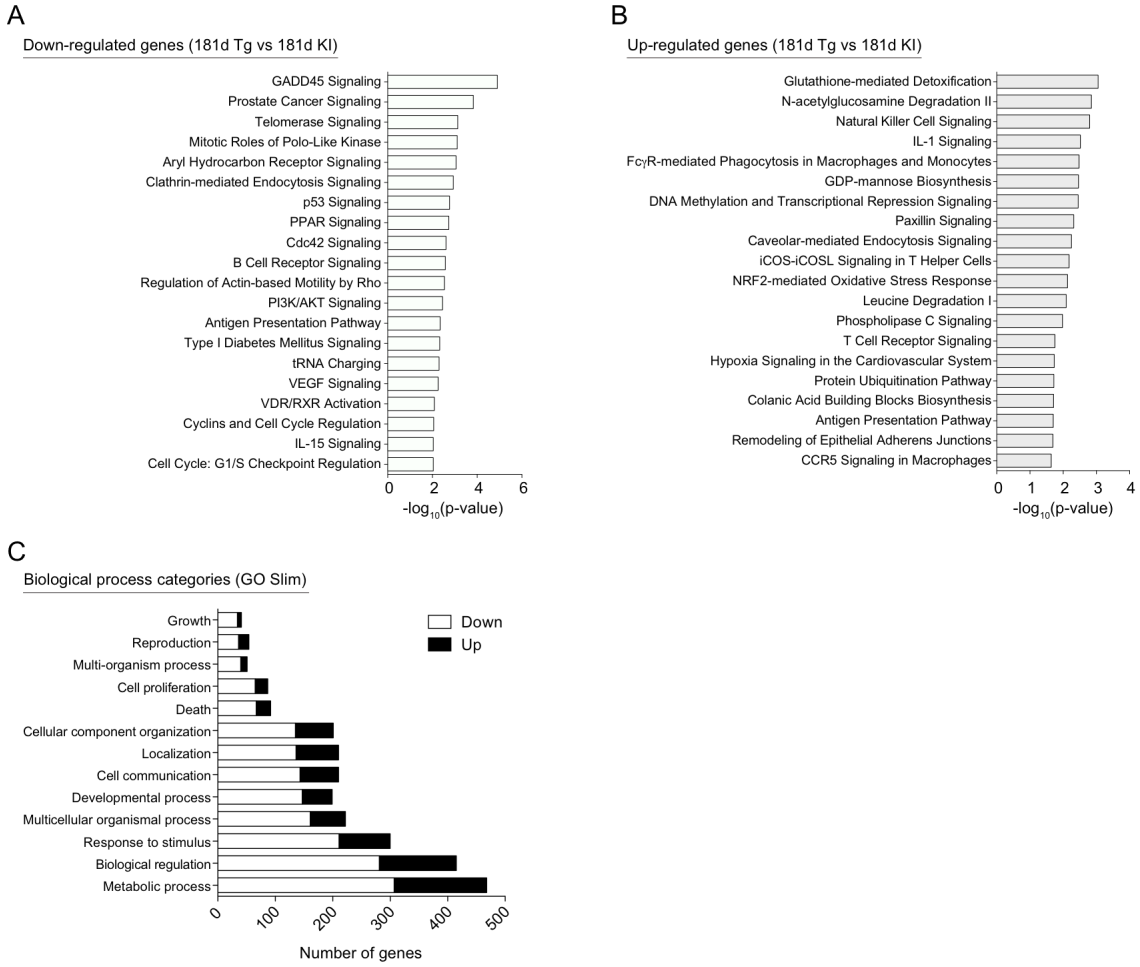

Figure 4.9. Canonical pathway and Gene Ontology analyses of differentially regulated genes in miR-181d transgenic and miR-181d knockin thymocytes. (**A-B**) Top 20 over-represented canonical pathways are shown based on their statistical significance for down-regulated (**A**) and up-regulated (**B**) genes with more than 1.25-fold ($p < 0.05$) in miR-181d Tg thymocytes compared to the miR-181d KI. Pathway enrichment analysis was performed using the IPA software. (**C**) Biological process categories over-represented within the dysregulated genes are shown. White and black bars are of down- and up-regulated genes in the miR-181d Tg thymocytes, respectively. Gene ontology Slim (GO Slim) analysis was performed using the Web-based Gene Set Analysis Toolkit.

Table 4.1. The top 10 transcription factors with predicted target motifs among differentially regulated genes in miR-181d transgenic and miR-181d knockin thymocytes. This enrichment analysis was performed using at least 5 genes for each category with hyper-geometric statistical test and Benjamini & Hochberg multiple test adjustment. Top 10 transcription factors with binding motifs are listed based on their significance level (adjusted p-value).

Down-regulated genes in miR-181d Tg thymocytes			
Transcription factors	**Number of genes**	**Enrichment ratio**	**Adjusted p-value**
SP1 (GGGCGGR)	109	4.50	5.33×10^{-38}
LEF1 (CTTTGT)	82	5.05	1.74×10^{-31}
MAZ (GGGAGGRR)	87	4.62	6.78×10^{-31}
E12 (CAGGTG)	89	4.34	8.98×10^{-30}
FOXO4 (TTGTTT)	77	4.58	4.59×10^{-27}
ELK1 (SCGGAAGY)	51	5.32	1.69×10^{-20}
NFAT (TGGAAA)	64	4.16	2.69×10^{-20}
MYC (CACGTG)	44	5.18	2.87×10^{-17}
LEF1 (CTTTGA)	47	4.74	5.21×10^{-17}
AP4 (CAGCTG)	51	4.11	6.13×10^{-16}
Up-regulated genes in miR-181d Tg thymocytes			
Transcription factors	**Number of genes**	**Enrichment ratio**	**Adjusted p-value**
GABP (MGGAAGTG)	21	6.16	1.20×10^{-8}
ELK1 (SCGGAAGY)	26	4.92	1.20×10^{-8}
FOXO4 (TTGTTT)	32	3.45	2.18×10^{-7}
ETS	12	10.56	2.18×10^{-7}
FREAC2 (RTAAACA)	21	4.97	2.18×10^{-7}
ETS2 (RYTTCCTG)	22	4.50	4.68×10^{-7}
AP4 (CAGCTG)	25	3.65	1.96×10^{-6}
NFY (GATTGGY)	21	4.01	4.72×10^{-6}
MYC (CACGTG)	19	4.05	1.52×10^{-5}
NFAT (TGGAAA)	26	3.06	2.00×10^{-5}

CHAPTER FIVE

TRANSGENIC EXPRESSION OF MICRORNA-185 CAUSES A DEVELOPMENTAL ARREST OF T CELLS BY TARGETING MULTIPLE GENES INCLUDING MZB1

The work presented in this chapter was originally published as: **Belkaya, S.**, S. E. Murray, J. L. Eitson, M. T. de la Morena, J. Forman, and N. S. van Oers. 2013. Transgenic expression of microRNA-185 causes a developmental arrest of T cells by targeting multiple genes including Mzb1. *J. Biol. Chem. doi: 10.1074/jbc.M113.503532*

Introduction

MicroRNAs (miRs) are small non-coding RNAs (20 to 24 nucleotides in length) that regulate gene expression at the post-transcriptional level by base pairing with target mRNAs, causing mRNA degradation and/or translational inhibition [77,78]. Functional roles of the miRs in the immune system are being partly elucidated with loss- and gain-of-function approaches. For example, conditional knockout lines of Dicer, an RNase III enzyme critical for miR biogenesis, in thymic epithelial cells, causes a premature thymic involution and an ensuing T cell lymphopenia, in part via the diminished expression of miR-29 [58]. The elimination of Dicer at the DN3 stage ($CD4^-CD8^-CD44^-CD25^+$) of thymopoiesis reduces thymic cellularity [80]. For pro-B cells, this knockout impairs their transition to pre-B cells, while its loss in mature $CD19^+$ B cells causes B cell autoantibody production [81,117]. In the latter case, the formation of autoreactive B cells was linked to the loss of miR-185 and the

up-regulation of its target, Bruton's tyrosine kinase (Btk) [117]. Gain-of-function approaches have uncovered roles for miR-146 and miR-155 in regulating IL-2 production in T cell and increasing NK cell numbers and cytokine production, respectively [164,182].

MiR-185 is a stress responsive miR expressed in the thymus [132]. It is encoded on human chromosome 22q11.2, and is haploinsufficient in patients with 22q11.2 deletion/DiGeorge syndrome [109]. Such patients present with varying clinical complications, including a T cell lymphopenia linked to a thymic hypoplasia, hypoparathyroidism, cardiac anomalies, and/or learning disabilities [110]. The patients also have an increased frequency of autoimmune disorders and age-dependent alterations in T helper cell (Th1 and Th2) commitment [113,114]. One third of 22q11.2 deletion syndrome patients will develop schizophrenia as adults [112]. Individuals with a duplication of chromosome 22q11.2 (Trisomy 22q11.2) can have similar clinical presentations as those with the deletions, suggesting that both reductions and elevations in miR-185 are clinically relevant [183,184]. Mouse models of this syndrome have shown that the haploinsufficiency of miR-185 elevates the expression of one of its neuronal targets, SERCA2 (Sarcoplasmic/endoplasmic reticulum calcium ATPase 2) [115]. High levels of SERCA2 enhance pre-synaptic neurotransmitter release in hippocampal neurons [115]. This contributes to an age-dependent cognitive impairment. A second target increased in neurons is 2310044H10Rik; a Golgi associated inhibitor [116]. While many miR-185 targets have been identified, it remains unknown whether altered miR-185 levels can affect T cell development and functions.

We developed a series of transgenic mice with increasing levels of miR-185 expressed in thymocytes and peripheral T cells. A miR-185 dose-dependent developmental block occurred at both the pre-TCR checkpoint and the positive selection stage. This attenuated both pre-TCR and positive selection, with an ensuing peripheral T cell lymphopenia. Several novel targets of miR-185 were identified, including Marginal zone B and B1 cell-specific protein (Mzb1), Nuclear factor of activated T cells, cytoplasmic, calcineurin-dependent 3 (NFATc3), and Calcium/calmodulin-dependent protein kinase IV (Camk4). MiR-185 transgenic thymocytes had higher levels of calcium influx upon TCR stimulation. A knockdown of miR-185 resulted in reduced TCR-driven calcium responses, with corresponding increases in Mzb1. The protein levels of Mzb1 were also elevated in thymocytes from the majority of the 22q11.2 deletion syndrome samples. Taken together, these findings indicate that alterations in the expression of miR-185 can affect T cell development and activation by controlling the expression of several novel mRNA targets including Mzb1.

Results

Elevations in miR-185 attenuate T cell development

MiR-185 is highly conserved and expressed in most tissues including the thymus, brain, heart, kidney, liver, lung, skin, and spleen (Figure 5.1A-B). It is expressed in immature thymocytes, mature $CD4^{+}CD8^{-}$ and $CD4^{-}CD8^{+}$ T cells, and in B cells [91,92,117,132]. To determine whether miR-185 levels impact T cell functions, we utilized a gain-of-function transgenic approach in which the murine pri-miR-185 was over-expressed in thymocytes and

peripheral T cells [134] (Figure 5.1C). Three transgenic lines, designated as miR-185 Tg-25, miR-185 Tg-35, and miR-185 Tg-6, were selected from 40 transgenic founders based on their increasing levels of miR-185 expression and dramatic effects on thymocyte development. MiR-185 was over-expressed 130-, 175-, and 250-fold in Tg-25, Tg-35, and Tg-6 lines, respectively, when compared to non-transgenic littermates (Figure 5.1D-E). Overall thymic cellularity was slightly reduced in Tg-25 and Tg-35 lines, whereas a severe thymic hypoplasia was noted in the Tg-6 line (Figure 5.2A). Further analyses revealed that over-expression of miR-185 caused a statistically significant dose-dependent decrease in the percent and number of $CD4^{+}CD8^{-}$ and $CD4^{-}CD8^{+}$ SP cells compared to control WT mice (Figure 5.2B-E). However, similar numbers of DP thymocytes observed in the wild type and two of the miR-185 lines (Tg-25 and Tg-35) suggested a developmental impairment at the DP stage (Figure 5.2F). The highest over-expressing line, miR-185 Tg-6, had statistically significant reductions in the DP and SP subsets, reflected as a dramatic loss in overall thymic cellularity (Figure 5.2B-G). Elevated DN percentages in the Tg-6 line further indicated a developmental block by miR-185 at early stages of thymopoiesis (Figure 5.2G). In addition, the Tg-6 line had no defined cortical region, an absent cortico-medullary junction, and a pronounced stromal component in the medulla. Hassall's corpuscles and dendritic cells were evident, and on increased magnification, mitotic activity was observed (Figure 5.3A-B).

Thymopoiesis in miR-185 transgenic lines is affected at two development checkpoints

The attenuated T cell development in the miR-185 transgenic mice appeared to be during pre-TCR and TCR selection stages. To assess whether there was a defect at the pre-

TCR checkpoint, $CD4^-CD8^-$ (DN) thymocytes were profiled for CD44 and CD25 cell surface expression, which marks 4 DN subsets, including those thymocytes at pre-TCR selection stage (DN3). Increasing miR-185 levels matched the severity of the block at the DN3 ($CD44^-CD25^+$) stage, with the percentage of DN3 cells increasing from 25% in controls to 40%, 51%, and 73% in the miR-185 Tg-25, Tg-35, and Tg-6 lines, respectively (Figure 5.4A). This was statistically significant for all the Tg lines compared to the wild type controls, and between Tg-6 versus Tg-35 and Tg-25 (Figure 5.4B). No change in intracellular TCRβ expression was detected in the DN3 subsets (Figure 5.4C). To induce TCR signals, the mice were injected intraperitoneally with anti-CD3ε. This induces a differentiation of DN3 thymocytes to the DP stage in Rag1-deficient mice, which is coupled with an increased thymic cellularity (Figure 5.4D-E). The DN3 thymocytes in the miR-185 Tg-6 mice were unable to progress to the DP stage following anti-CD3ε injection, indicating a complete block at the DN3 stage (Figure 5.4D-E). Surface expression levels of CD5 on DN3 thymocytes were normal in Tg-25 and Tg-35 lines, but slightly elevated in the Tg-6 line, an indication of normal pre-TCR engagement and signal strength (Figure 5.4F-G). With regards to other cell populations in the thymus, percent and number of NK T cells were similar in the miR-185 Tg lines, except for the Tg-6 line that had very low NK T cell numbers (Figure 5.5A-B). γδ T cell numbers in all Tg lines were similar to the control, while their percentages were slightly increased (Figure 5.5A, C).

The reduced SP thymocytes in all the miR-185 Tg lines suggested an impairment of positive selection. Consistent with this, the percentages of $CD69^+TCR\beta^{high}$ total thymocytes, including $CD69^+TCR\beta^{high}$ CD4 and CD8 SP thymocytes, were reduced in a statistically

significant manner (Figure 5.6A-C). The reduction in positive selection was consistent with an increased percentage of DP thymocytes that were gated on $CD69^{-}TCR\beta^{high}$ total thymocytes (Figure 5.6D). Differences between the closely matched Tg-25 and Tg-35 lines were also of statistical significance once the reductions in $CD4^{+}CD8^{-}$ and $CD4^{-}CD8^{+}$ subsets were compared (Figure 5.6D-E). Negligible numbers of mature $CD69^{-}TCR\beta^{high}$ SP thymocytes were found in the miR-185 Tg-6 line (Figure 5.6D-E). Moreover, CD5 expression on $CD69^{-}TCR\beta^{high}$ DP thymocytes was lower in miR-185 Tg lines, supporting impaired positive selection (Figure 5.6F-G). Attenuated positive selection was further established by comparing the number of OTII-specific TCR transgenic T cells developing in the miR-185 Tg-35 lines. Their numbers were significantly reduced in the OTII/miR-185 Tg-35 double Tg lines compared to the OTII Tg parental line (Figure 5.7A-B), and those residual SP cells lost the expression of the transgenic TCRα subunit (Figure 5.7C-D). Severe loss of CD4 SP thymocytes in the OTII/miR-185 Tg-35 line could reflect enhanced negative selection. However, the total number of thymocytes was equivalent in both the OTII and OTII/miR-185 Tg-35 lines (Figure 5.7E). Furthermore, *in vitro* treatment of thymocytes from the OTII/miR-185 Tg-35 line with an OVA-class II peptide induced DP cell death, indicating that negative selection was intact and similar (Figure 5.7F). The ability to induce negative selection in the miR-185 Tg lines was also consistent with the significant loss of DP thymocytes in all the miR-185 Tg-25 lines following anti-CD3ε injections *in vivo* (Figure 5.7G). In addition, the impairment at DN3 and DP stages of thymopoiesis in miR-185 Tg mice was not due to increased cell death since Annexin V^{+} percentages were normal in these

lines (Figure 5.7H). Taken together, these findings demonstrate that increases in miR-185 reduce the effectiveness of TCRβ and positive selection.

MiR-185 transgenic lines have a peripheral T cell lymphopenia

A miR-185 dose-dependent reduction in the percent and number of mature peripheral $CD4^+CD8^-$ and $CD4^-CD8^+$ T cells occurred in all three miR-185 Tg lines and was most pronounced in the Tg-6 (Figure 5.8A-F). The number of natural T regulatory ($Foxp3^+$ $CD25^+$ $CD4^+$) cells was also reduced gradually in the spleen of all miR-185 Tg lines (Figure 5.8G-H). As a consequence of the T cell lymphopenia, the percentages of peripheral $B220^+$ B cells increased in all miR-185 Tg lines (Figure 5.8I). Peripheral T cells from all the miR-185 Tg lines displayed spontaneous hyper-activated phenotype with increased CD25, CD44 expression, and decreased CD62L expression (Figure 5.9A-B). Consistent with this activated phenotype, total $CD4^+$ T cells had a statistically significant increase in IL-2 production that occurred in a miR-185-dose dependent manner (Figure 5.9C). Total $CD4^+$ T cells from the miR-185 Tg-6 line were unable to proliferate, while $CD4^+$ T cells from the miR-185 Tg-25 and Tg-35 lines had a slightly diminished proliferative response, evident only after 48 hrs but not 72 hrs of stimulation, likely due to decreased percentages of naive T cells in miR-185 Tg mice (Figure 5.10A). *In vitro* TCR-stimulation with anti-CD3ε/CD28 led to an increase in apoptosis of total $CD4^+$ T cells, the severity of which matched increasing miR-185 levels (Figure 5.10B). However, naive $CD4^+CD62L^{high}$ T cells from the miR-185 Tg-35 and Tg-25 lines did not exhibit significant changes in proliferation (Figure 5.10C). Finally, a significant

reduction was also noted both in numbers and TCR-density of mature peripheral $CD4^+CD8^-$ T cells from the OTII/miR-185 Tg-35 mice (Figure 5.11A-F).

MiR-185 targets a number of genes implicated in thymopoiesis

The effects of miR-185 over-expression on T cell development suggested that genes coupled to pre-TCR- and TCR-driven selection were targeted by this miR. Gene expression comparisons were performed on sorted DN3 thymocytes from wild type mice and pooled miR-185 Tg-6 mice. Of the 26,000 genes probed, 234 were down- and 317 were up-regulated more than 1.5-fold in the DN3 thymocytes of miR-185 Tg-6 mice compared to normal controls ($p < 0.05$) (data not shown). A miR target prediction database (miRWalk) parsed the down-regulated genes to those containing putative miR-185 binding sites on their 3' untranslated regions (3' UTRs) and/or coding sequences (CDS) [185]. The top 25 candidates are listed (Table 5.1), and those with implicated roles in thymopoiesis were analyzed further. Quantitative RT-PCR with gene specific probes for Mzb1 (also known as 2010001M09Rik, PACAP, or pERp1), NFATc3, and Camk4 revealed a direct, and statistically significant, miR-185 dose-dependent decrease in the expression of each target (Figure 5.12A). Protein expression comparisons confirmed a substantial loss of Mzb1 and NFATc3 in sorted DN3 cells (Figure 5.12B). Patients with the 22q11.2 deletion are haploinsufficient in miR-185 [109]. To determine if the levels of Mzb1 were altered in their thymocytes, immunoblotting was performed using protein extracts prepared from 5 independently prepared normal controls and 4 individuals with confirmed deletions on 22q11.2. Mzb1 was up-regulated >2-fold in 3 of the 4 patient samples (Figure 5.12C).

Prediction software suggests there are 2 miR-185 target sites in Mzb1 mRNA, one actually in the coding sequence (Figure 5.13A). To confirm if the CDS was targeted, a myc epitope-tagged Mzb1 expression vector was transfected along with an empty control plasmid or a plasmid expressing miR-185. MiR-185 reduced Mzb1 levels compared to the vector control in a statistically significant manner (Figure 5.13B-C). Mutating the target sequence in Mzb1 prevented its down-regulation (Figure 5.13B-C). To confirm targeting of the 3'UTR of Mzb1, luciferase reporter assays were performed. Relative to the control, the luciferase activity of Mzb1-3'UTR was decreased more than 2-fold (Figure 5.13D). Mutations of the target sequence within the Mzb1 3' UTR restored control luciferase levels (Figure 5.13D). A number of additional targets identified in the microarray (Mcm10, Camk4, Hmga1, NFATc3, Igf1r, and Dusp4) were validated as novel miR-185 targets in luciferase reporter assays, with the Btk 3' UTR included as a positive control (Figure 5.13E).

MiR-185 levels affect TCR-driven intracellular calcium responses

MiR-185 targets Mzb1, an endoplasmic reticulum (ER) associated protein involved in calcium regulation. In marginal zone B cells, knockdown of Mzb1 augments intracellular calcium (Ca^{2+}) levels following BCR stimulation, whereas over-expression of Mzb1 in T cells decreases TCR-mediated Ca^{2+} influx [186]. We examined the changes in TCR-driven intracellular Ca^{2+} responses of DP thymocytes from the miR-185 Tg lines. DP thymocytes from normal mice increased intracellular Ca^{2+} responses 30-40 seconds after TCR/CD4 cross-linking (Figure 5.14A). The magnitude of the TCR-induced Ca^{2+} response was significantly higher in the Tg-25 and Tg-35 lines (Figure 5.14A-B). The addition of the

calcium ionophore, ionomycin, revealed an identical capacity of all groups of thymocytes to internalize Ca^{2+}, indicating that the differences in the cells were TCR signaling dependent. The thymocytes were also treated with thapsigargin, an inhibitor of the SERCA that pumps Ca^{2+} into the ER. Thymocytes with varying levels of miR-185 exhibited similar Ca^{2+} responses following thapsigargin addition (data not shown). In a complementary loss-of-function approach, chemically modified miR inhibitors (antagomirs) were used to reduce miR-185 activity in Jurkat T cells. Inhibiting miR-185 increased Mzb1 protein expression in a dose-dependent and statistically significant manner, compared to the control inhibitor (cel-miR-67) (Figure 5.14C-D). The knockdown of miR-185, which resulted in higher Mzb1 levels, reduced TCR-mediated intracellular calcium levels in Jurkat T cells (Figure 5.14E-F). In summary, miR-185 directly affects TCR-triggered calcium responses in developing thymocytes and Jurkat T cells.

Discussion

Gain- and loss- of-function approaches were used to characterize the function role of miR-185 in T cells. A transgene driven over-expression of miR-185 caused a developmental impairment at two crucial stages of thymopoiesis: pre-TCR- and TCR-selection. The block was specific to αβ T cells, as the numbers of γδ T cells were similar. The consequence of the attenuation of αβ T cells was a severe peripheral T cell lymphopenia, with the cells phenotypically similar to those developing in lymphopenic mice.

The most down-regulated target, Mzb1, was first identified as a novel gene induced during B to plasma cell differentiation, regulating proper assembly and secretion of mature

IgM [187,188]. It is highly expressed in marginal zone B cells and regulates intracellular Ca^{2+} flux upon BCR stimulation [186]. These findings indicate that Mzb1 is also highly expressed in DN3 thymocytes, and is present in Jurkat T cells, consistent with prior Northern blotting results [187,188,189]. MiR-185 targets two highly conserved sites in Mzb1. This likely contributes to the developmental block in thymopoiesis, resulting from pre-TCR- and αβ TCR-driven intracellular calcium responses that are too high to support positive selection. The dramatic attenuation of T cell development is further compounded by reductions in NFATc3 and Camk4. Of note, the targeted elimination of NFATc3 causes a very similar development block at the pre-TCR selection stage and during positive selection. In fact, a peripheral T cell lymphopenia is also seen in these knockout mice [190,191].

Our data raise important questions as to whether miR-185 affects T and B cell functions in humans. Patients with 22q11.2 deletion syndrome, haploinsufficient for miR-185, have an increased prevalence of autoimmune disorders and B cell defects [109]. Reductions in miR-185 might affect the expression of both Btk and Mzb1 in B cells, enhancing autoantibody production [117,186]. These patients have abnormal T helper cell skewing [192]. Further experiments are needed to elucidate the contribution of miR-185 in both thymocytes and thymic epithelial/mesenchymal cells. Mouse models of 22q11.2 deletion syndrome confirm a reduction of miR-185, with an age-dependent reduction in other miRs [115]. Such mice have neurological abnormalities resulting from enhanced calcium regulated neurotransmitter release, which is linked to elevations in a distinct miR-185 target, the calcium regulator, SERCA2 [115]. Since SERCA2 is expressed at very low levels in thymocytes, we hypothesize that the principal targets of miR-185 in thymocytes are distinct

and depend on target mRNA abundance [193]. In fact, Mcm10, Hmga1, Igf1r, and Dusp4 were additional targets in the developing thymocytes. MiR-185 also targets Six1, RhoA, and Cdc42 genes involved in controlling cell cycle progression in various cancer cell lines [194,195,196]. Interestingly, while these were not identified in our thymocyte screen, they may play a role in the peripheral T cells [193]. It will be important to assess the consequences of both the haploinsufficiency and trisomy of miR-185 on the novel targets reported herein as NFATc3 and Camk4 are expressed in many tissues and organs affected by the deletions on chromosome 22q11.2.

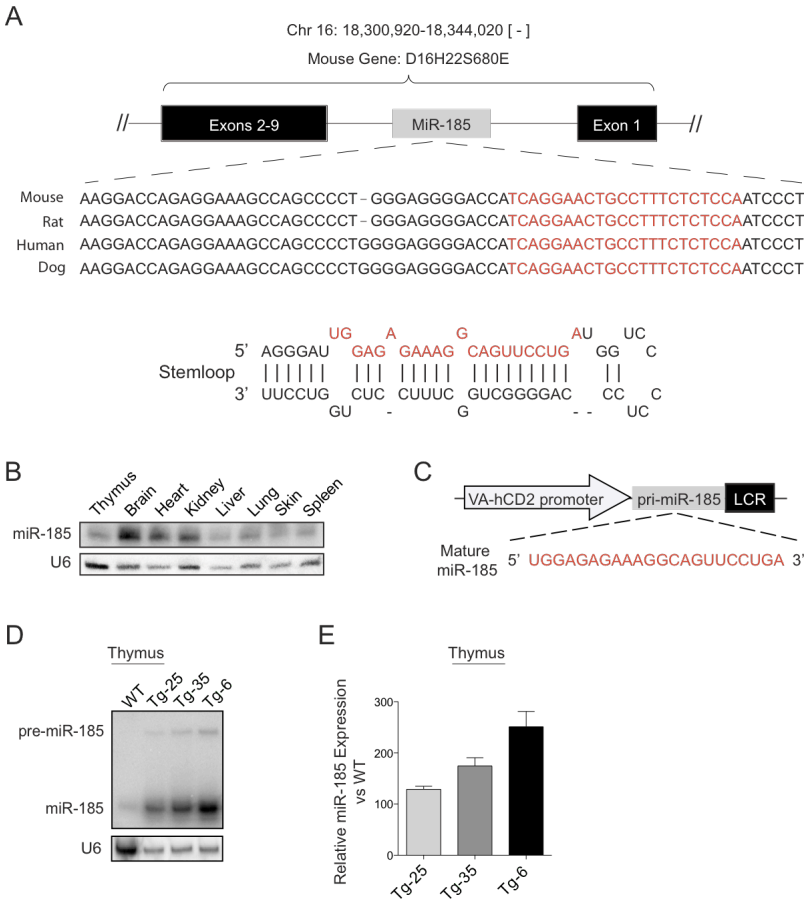

Figure 5.1. Generation of miR-185 transgenic mice. (**A**) MiR-185 is encoded on mouse chromosome 16, within the first intron of the gene, D16H22S680E. The mature miR-185 sequence is highlighted in red. The homology between the human, mouse, rat and dog are shown. The stem loop structure of pre-miR-185 is provided. (**B**) MiR-185 expression in various tissues assessed by Northern blotting. U6 probe was used as the endogenous control. (**C**) VA-hCD2 transgenic cassette. Pri-miR-185 was cloned under control the human CD2 promoter, which enables mature miR-185 (highlighted in red) expression in T cells. (**D**) A representative northern blot demonstrating the expression levels of miR-185 in the thymus of the control and transgenic lines. (**E**) Relative over-expression levels of miR-185 in different transgenic lines determined by Northern blotting. The wild type control was set as 1. Bars show the mean fold changes +/- SEM normalized to the U6 levels from 2 independent experiments.

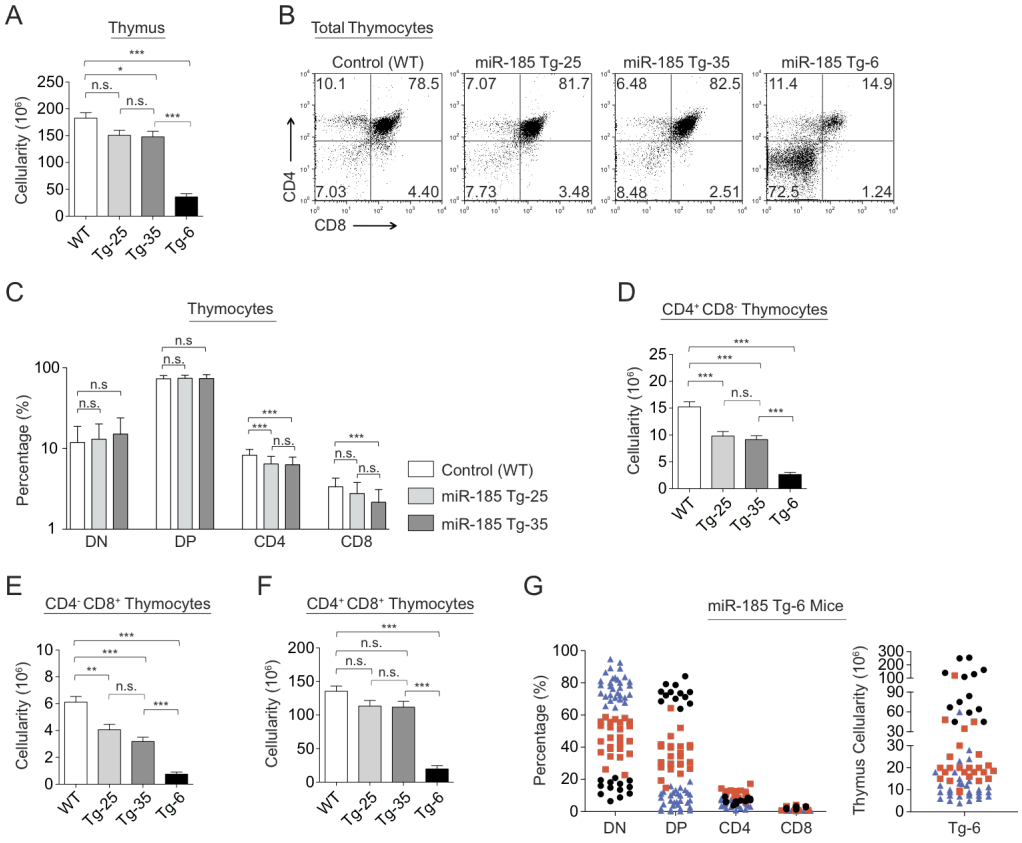

Figure 5.2. Elevations in miR-185 impair T cell development. (**A**) Total thymus cellularity in the control and miR-185 Tg mice. (**B**) Total thymocytes from the control and miR-185 Tg mice were stained for CD4 and CD8, and analyzed by FACS. (**C**) Average percentages of DN, DP, CD4 SP, and CD8 SP thymocytes in the control (white), miR-185 Tg-25 (light gray), and Tg-35 (dark gray) mice. (**D-F**) Bar graphs show absolute cell numbers of the $CD4^+CD8^-$ thymocytes (**D**), $CD4^-CD8^+$ thymocytes (**E**), and $CD4^+CD8^+$ thymocytes (**F**) in the control and miR-185 Tg mice. Data are of the mean +/- SEM from WT (n=50), Tg-25 (n=20), Tg-35 (n=40), and Tg-6 (n=70) mice (n.s. = non-significant, $*p < 0.05$, $**p < 0.01$, $***p < 0.001$; One-way ANOVA followed by Tukey's post-hoc test). (**G**) Thymic cellularity and percentages of DN, DP, CD4 SP, and CD8 SP thymocytes in miR-185 Tg-6 mice (n=70). Each shape (black circle, red square, and blue triangle) represents an individual Tg-6 mouse. Colored shapes were used to track the cellularity and corresponding subset percentages of the Tg-6 mice. MiR-185 Tg-6 mice that had the highest DN percentages (blue triangles) had also the lowest percentages of DP and SP thymocytes, resulting in the lowest thymus cellularity.

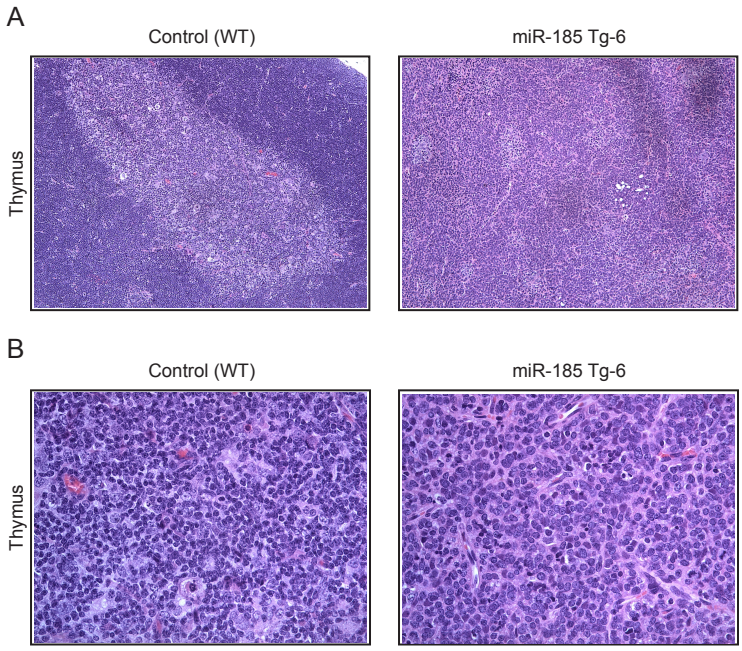

Figure 5.3. MiR-185 transgenic mice with thymic hypoplasia. (**A**-**B**) H&E staining of thymic tissues from the control and miR-185 Tg-6 mice with 10X (**A**) and 40X (**B**) original magnification.

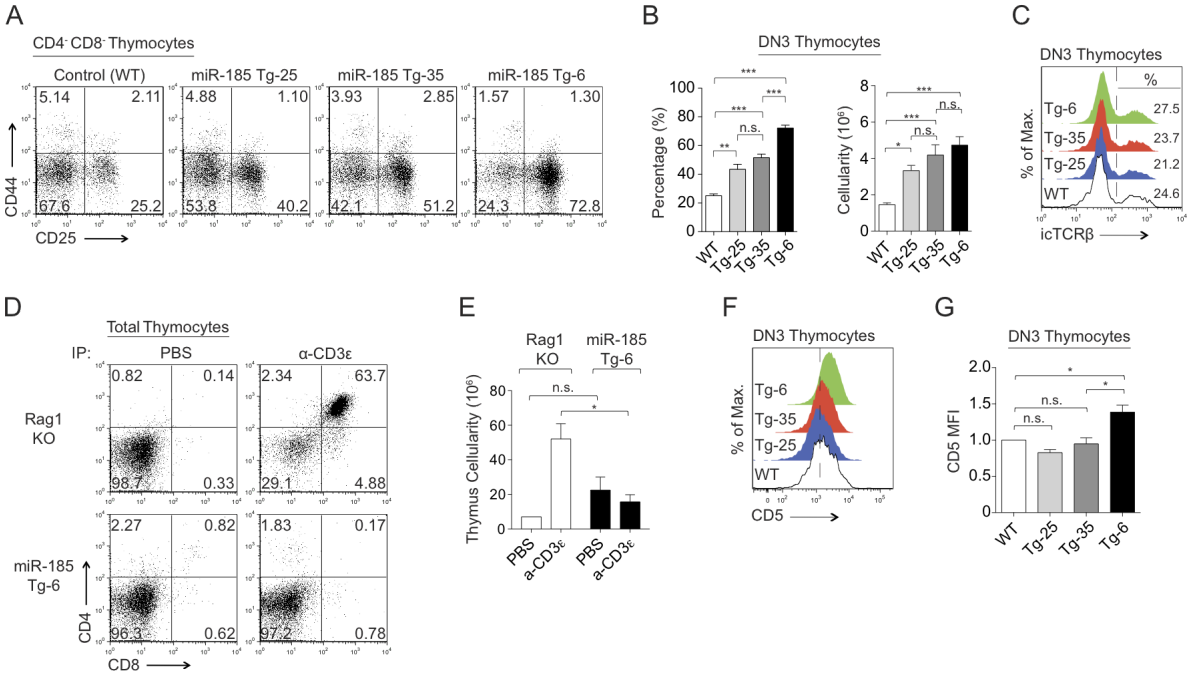

Figure 5.4. Increasing levels of miR-185 attenuate T cell development at TCR-β selection checkpoint. (**A**) Surface expression of CD25 and CD44 gated on $CD4^-CD8^-$ ($B220^-$, $NK1.1^-$, $TCR\gamma\delta^-$, $CD11b^-$, and $CD11c^-$) thymocytes of the control and miR-185 Tg mice. (**B**) Average percentages and absolute cell numbers of DN3 ($CD25^+CD44^-$) thymocytes are shown as the mean +/- SEM using at least 6 mice per group (n.s. = non-significant, $*p < 0.05$, $**p < 0.01$, $***p < 0.001$; One-way ANOVA followed by Tukey's post-hoc test). (**C**) Histograms show expression levels of intracellular TCRβ (icTCRβ) in DN3 thymocytes. The average percentages were shown for the miR-185 Tg and control mice (n=2 mice per group). (**D**) Total thymocytes from PBS or anti-CD3ε treated $Rag1^{-/-}$ and miR-185 Tg-6 mice were stained for CD4 and CD8, and analyzed by FACS at 5 days post-IP (intraperitoneal) injection. (**E**) Total thymus cellularity of anti-CD3ε and PBS injected $Rag1^{-/-}$ and miR-185 Tg-6 mice (n=3 mice per group; n.s. = non-significant, $*p < 0.05$, $**p < 0.01$, $***p < 0.001$; Two-way ANOVA followed by Bonferroni's post-hoc test). (**F**) Representative histogram shows surface expression levels of CD5 in DN3 thymocytes. Dashed line indicates the mean fluorescence of CD5 expression in the control mouse. (**G**) Relative MFI (Mean Fluorescence Intensity) levels of CD5 in DN3 thymocytes from the control and miR-185 Tg-mice. Each bar is the mean +/- SEM of 2 independent experiments (n.s. = non-significant, $*p < 0.05$, $**p < 0.01$, $***p < 0.001$; One-way ANOVA, followed by Tukey's post-hoc test).

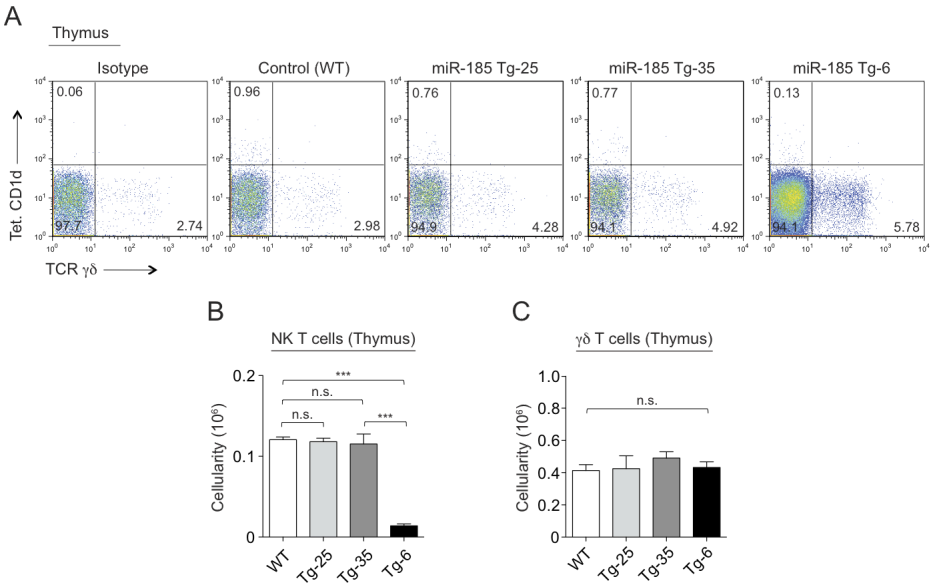

Figure 5.5. NK T and γδ T cells in miR-185 transgenic thymus. (**A**) Representative FACS profiles of NK T (Peptide-loaded CD1d tetramer^{+}) and γδ T cells gating on CD4^{-}CD8^{-}B220^{-} CD11b^{-}CD11c^{-} population in the thymus of control and miR-185 Tg mice. Peptide-unloaded CD1d tetramer was used as an isotype control in the wild type thymocytes. (**B-C**) Bar graphs represent the mean +/- SEM cell numbers of NK T cells (**B**) and γδ T cells (**C**) in the thymus of the control and miR-185 Tg mice using at least 3 mice per group (n.s. = non-significant, $*p < 0.05$, $**p < 0.01$, $***p < 0.001$; One-way ANOVA, followed by Tukey's post-hoc test).

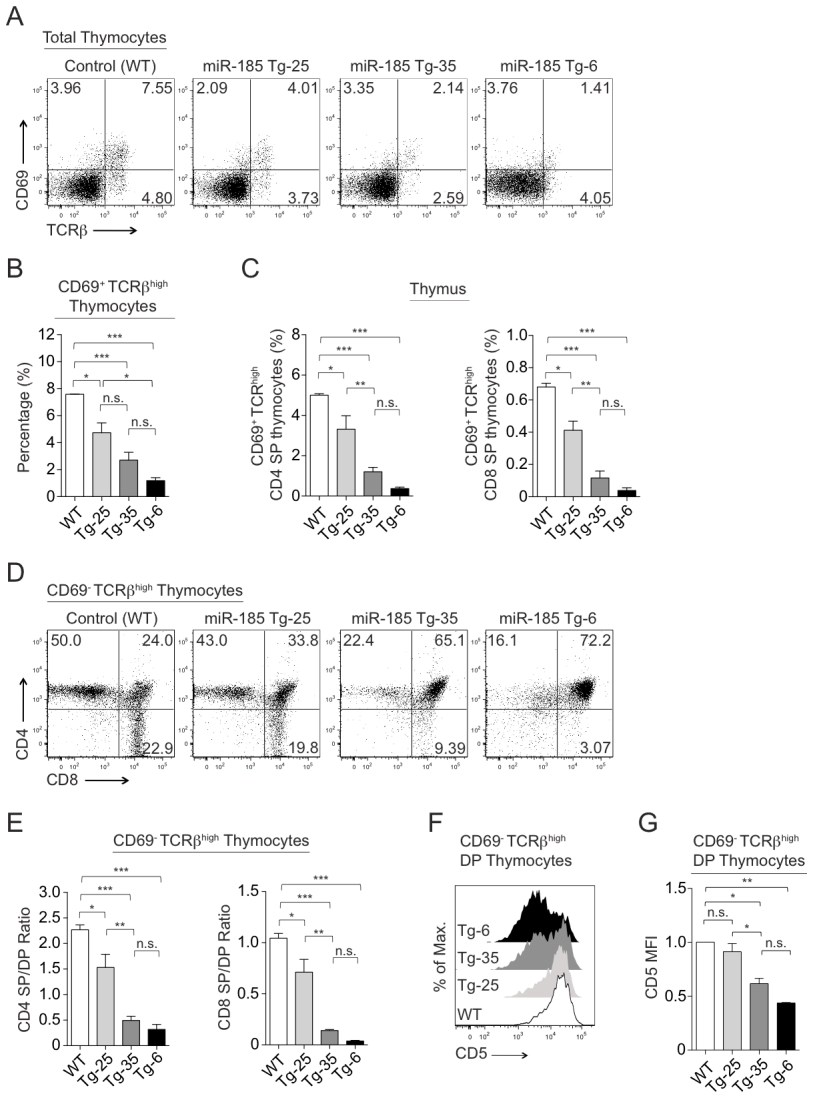

Figure 5.6. Transgenic expression of miR-185 attenuates T cell development at TCR-positive selection checkpoint. (**A**) Flow cytometric analysis of CD69 and TCRβ expression on total thymocytes from the control and miR-185 Tg mice. (**B**) Average percentages of $CD69^{+}TCR\beta^{high}$ total thymocytes. (**C**) Average percentages of $CD69^{+}TCR\beta^{high}$ CD4 SP (left) and $CD69^{+}TCR\beta^{high}$ CD8 SP (right) thymocytes. (**D**) Plots represent CD4 by CD8 profiles of $CD69^{-}TCR\beta^{high}$ thymocytes. (**E**) Cellularity ratios of the $CD69^{-}TCR\beta^{high}$ CD4 SP (left) and the $CD69^{-}TCR\beta^{high}$ CD8 SP (right) to the $CD69^{-}TCR\beta^{high}$ DP thymocytes were established for the results shown in (D). (**F**) Histogram shows CD5 expression on $CD69^{-}TCR\beta^{high}$ DP thymocytes from the WT (white), Tg-25 (light gray), Tg-35 (dark gray), and Tg-6 (black) mice. (**G**) Relative MFI levels of CD5 in $CD69^{-}TCR\beta^{high}$ DP thymocytes. (**A-G**) Data are of 3 independent experiments. Each bar shows the mean +/- SEM (n.s. = non-significant, $*p < 0.05$, $**p < 0.01$, $***p < 0.001$; One-way ANOVA, followed by Tukey's post-hoc test).

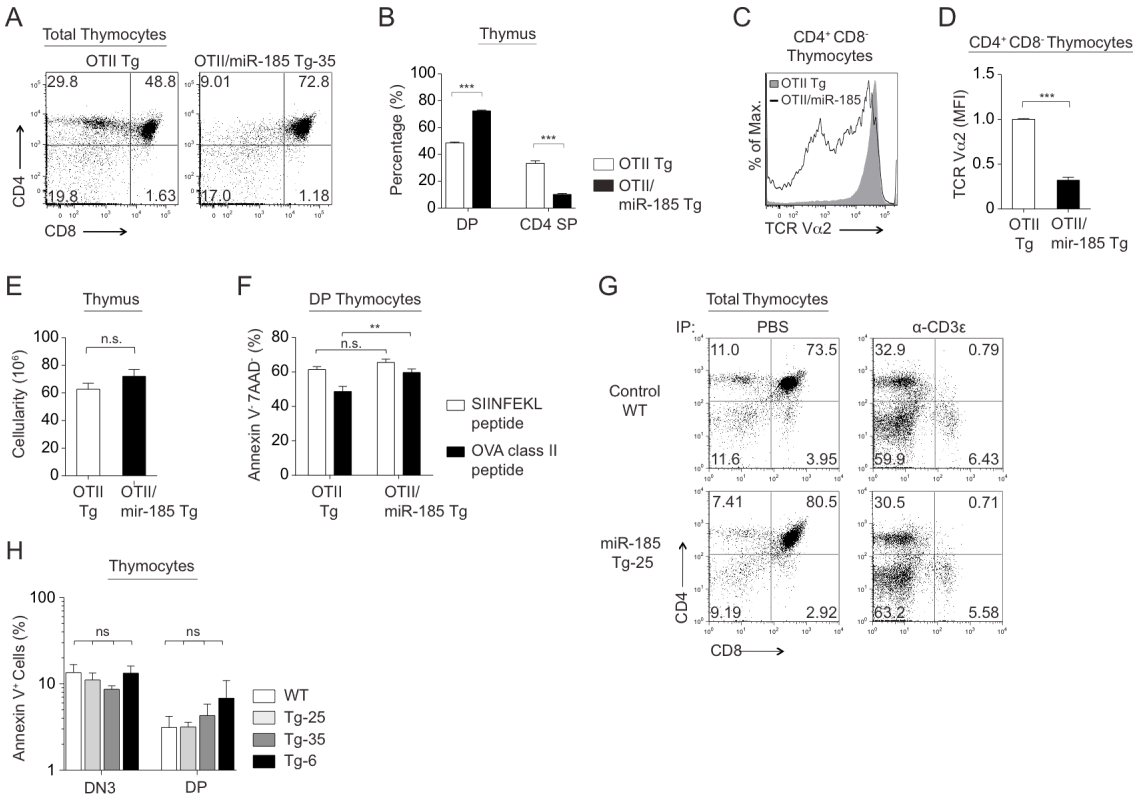

Figure 5.7. Impaired positive selection in OTII/miR-185 transgenic mice. (**A**) FACS analysis of CD4 and CD8 expression on total thymocytes from OTII Tg and OTII/miR-185 Tg-35 mice. (**B**) Average percentages of DP and CD4 SP thymocytes are shown. (**C**) Surface expression of TCR Vα2 gated on $CD4^+CD8^-$ thymocytes from OTII Tg (dark gray) and OTII/miR-185 Tg-35 mice (black line). (**D**) Relative MFI (Mean Fluorescence Intensity) levels of TCR Vα2 on $CD4^+CD8^-$ thymocytes. (**A-D**) Data are of at least 6 mice per group. Bar graphs represent the mean +/- SEM values (*$p < 0.05$, **$p < 0.01$, ***$p < 0.001$; Two-tailed unpaired Student's *t*-test). (**E**) Total thymus cellularity of OTII Tg and OTII/miR-185 Tg mice was represented as the mean +/- SEM of at least 6 mice per group (n.s. = non-significant, Two-tailed unpaired Student's *t*-test). (**F**) Percentage of live (Annexin V^- $7AAD^-$) DP thymocytes upon *in vitro* treatment of OTII Tg and OTII/miR-185 Tg thymocytes with SIINFEKL peptide as a negative control and OVA class II peptide. Each bar is the mean +/- SEM of 3 mice per group (n.s. = non-significant, *$p < 0.05$, **$p < 0.01$, ***$p < 0.001$; Two-way ANOVA followed by Bonferroni's post-hoc test). (**G**) Thymocytes from PBS or anti-CD3ε (200 mg/ml) treated the control and miR-185 Tg-25 mice were stained for CD4 and CD8, and analyzed by FACS, after 3 days post-IP injection. Data are representative of 3 mice per group. (**H**) Graph shows the mean +/- SEM percentages of Annexin V^+ DN3 and of DP thymocytes from Control (white), Tg-25 (light Gray), Tg-35 (dark Gray), and Tg-6 (black) mice (n=3 mice per group) (n.s. = non-significant, *$p < 0.05$, **$p < 0.01$, ***$p < 0.001$; One-way ANOVA, followed by Tukey's post-hoc test).

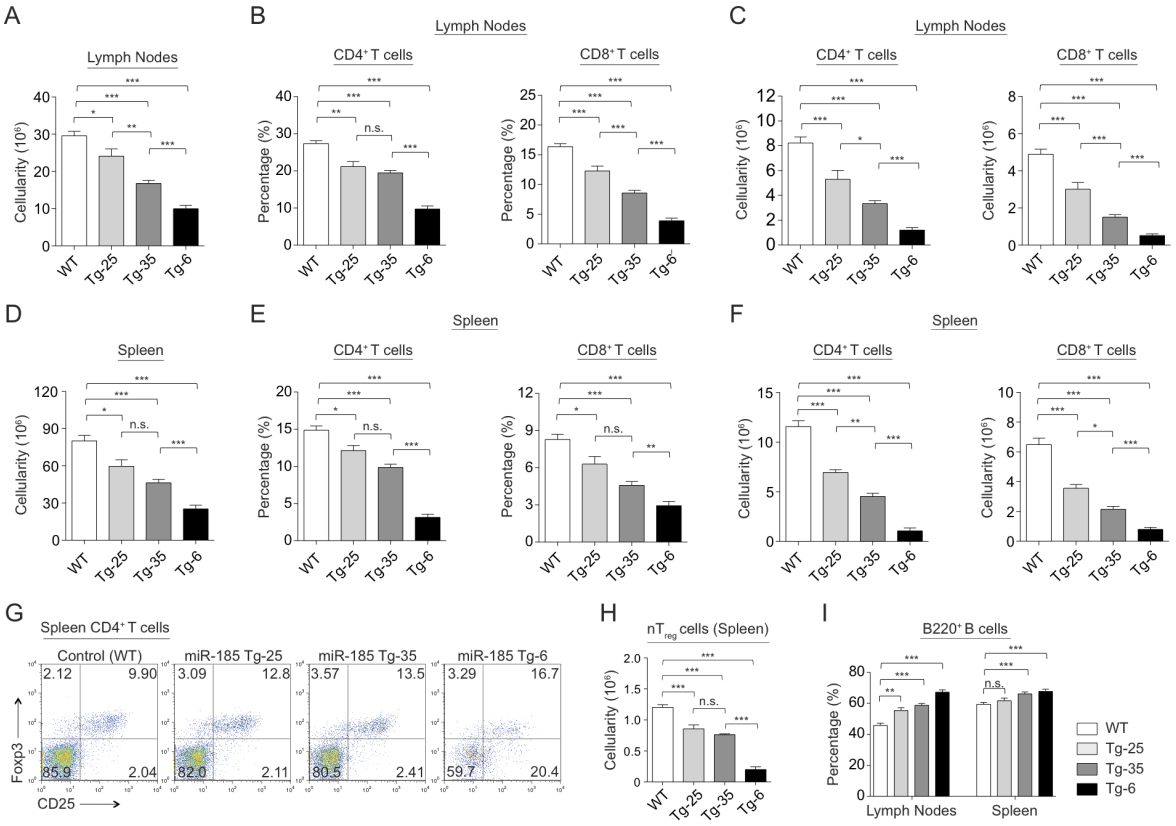

Figure 5.8. Elevated levels of miR-185 cause a peripheral T cell lymphopenia. (**A**) Total cellularity of the lymph nodes in the wild type (WT) and miR-185 Tg mice. (**B-C**) Average percentages (**B**) and absolute numbers (**C**) of $CD4^+$ and $CD8^+$ T cells in the lymph nodes. (**A-C**) Data are of the mean +/- SEM from WT (n=40), Tg-25 (n=16), Tg-35 (n=46), and Tg-6 (n=59) mice (*$p < 0.05$, **$p < 0.01$, ***$p < 0.001$; One-way ANOVA followed by Tukey's post-hoc test). (**D**) Total cellularity of the spleen in the WT and miR-185 Tg mice. (**E-F**) Average percentages (**E**) and absolute numbers (**F**) of $CD4^+$ and $CD8^+$ T cells in the spleen. (**D-F**) Data are of the mean +/- SEM from WT (n=24), Tg-25 (n=12), Tg-35 (n=30), and Tg-6 (n=36) mice (n.s. = non-significant, *$p < 0.05$, **$p < 0.01$, ***$p < 0.001$; One-way ANOVA, followed by Tukey's post-hoc test). (**G**) Representative FACS plots show percentages of natural regulatory T cells ($Foxp3^+$ $CD25^+$ $CD4^+$) in the spleen of the WT and miR-185 Tg mice. (**H**) Absolute numbers of natural regulatory T (nT_{reg}) cells in the spleen. Data are of the mean +/- SEM from at least 3 mice per group (n.s. = non-significant, *$p < 0.05$, **$p < 0.01$, ***$p < 0.001$; One-way ANOVA followed by Tukey's post-hoc test). (**I**) Graph shows the mean +/- SEM percentages of $B220^+$ B cells in the lymph nodes and spleen of the WT and miR-185 Tg mice using at least 10 mice per group (n.s. = non-significant, *$p < 0.05$, **$p < 0.01$, ***$p < 0.001$; One-way ANOVA, followed by Tukey's post-hoc test).

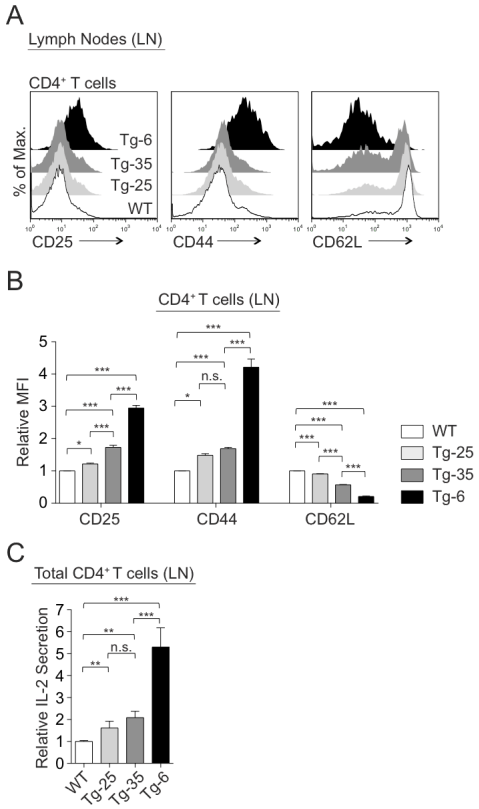

Figure 5.9. MiR-185 transgenic peripheral T cells exhibit a hyper-activated phenotype. (**A**) Surface expression of CD25, CD44, and CD62L on gated $CD4^+$ T lymphocytes in the lymph nodes of WT (white), Tg-25 (light gray), Tg-35 (dark gray), and Tg-6 (black) mice. (**B**) Graph shows the relative MFI levels +/- SEM of CD25, CD44, and CD62L markers on $CD4^+$ T cells in the lymph nodes of WT (white), Tg-25 (light gray), Tg-35 (dark gray), and Tg-6 (black) mice using at least 5 mice per group (n.s. = non-significant, $*p < 0.05$, $**p < 0.01$, $***p < 0.001$; One-way ANOVA, followed by Tukey's post-hoc test). (**C**) Graph represents relative IL-2 secretion from anti-CD3ε/CD28 stimulated total $CD4^+$ T cells in miR-185 Tg lines and the control (WT), set to 1. Each bar is the mean +/- SEM of at least 5 independent experiments (n.s. = non-significant, $*p < 0.05$, $**p < 0.01$, $***p < 0.001$; Two-tailed unpaired Student's *t*-test).

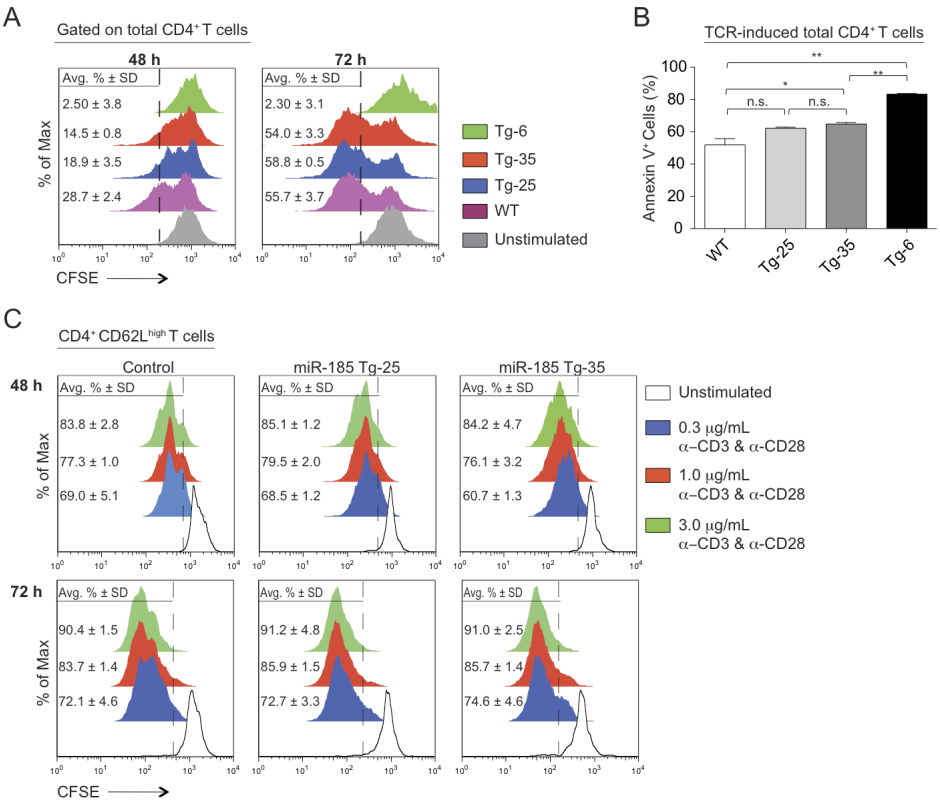

Figure 5.10. Peripheral T cells from miR-185 transgenic mice display normal proliferative responses. (**A**) Histograms show proliferation of bulk lymphocytes gated on total $CD4^+$ T cells from the control and miR-185 Tg mice, labeled with CFSE (1 mM), and stimulated with anti-CD3ε/CD28 (3 mg/ml) for 48 and 72 hrs (h). Dashed line indicates the gate. Average percentages +/- SD were provided (Gray, unstimulated; Purple, Wild type; Blue, Tg-25; Red, Tg-35; Green, Tg-6). (**B**) Average +/- SEM percentages of Annexin V^+ total $CD4^+$ peripheral T cells isolated from miR-185 Tg mice versus the control upon TCR-stimulation with anti-CD3ε/CD28 (3 mg/ml) for 48 hrs (h) *in vitro* (n.s. = non-significant, *$p < 0.05$, **$p < 0.01$, ***$p < 0.001$; Two-tailed unpaired Student's *t*-test). (**C**) Histograms show proliferation of naive $CD4^+CD62L^{high}$ T cells from the control (WT) and miR-185 Tg mice, as measured with CFSE (300 nM) staining followed by stimulations with anti-CD3ε/CD28 for 48 and 72 hrs at indicated concentrations: White, unstimulated; Blue, 0.3 mg/ml; Red, 1 mg/ml; Green, 3 mg/ml. Dashed line indicates the gate. Average percentages +/- SD were provided. Insufficient numbers of naive T cells from the miR-185 Tg-6 line precluded an assessment of their proliferative capacity. (**A-C**) Data are of 2 independent experiments, performed in duplicate for each group.

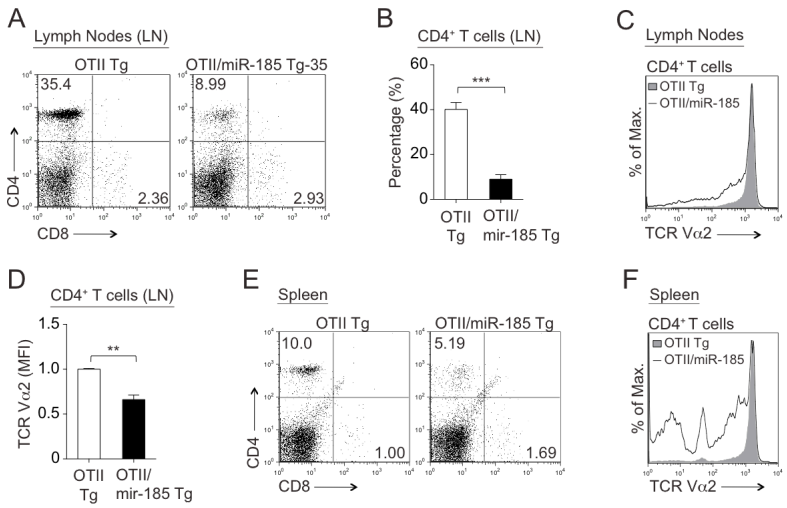

Figure 5.11. Reduced number of peripheral T cells in OTII/miR-185 transgenic mice. (**A**) Lymphocytes from the lymph nodes of OTII Tg and OTII/miR-185 Tg mice were stained for CD4 and CD8, and analyzed by FACS. (**B**) Average percentages of $CD4^+CD8^-$ T cells in the lymph nodes. (**C**) Surface expression of TCR Vα2 gated on $CD4^+CD8^-$ T cells from the lymph nodes of OTII Tg (dark gray) and OTII/miR-185 Tg mice (black line). (**D**) Relative MFI levels of TCR Vα2 on $CD4^+CD8^-$ lymphocytes. (**A-D**) Data are of at least 6 mice per group. Bar graphs represent the mean +/- SEM values (*$p < 0.05$, **$p < 0.01$, ***$p < 0.001$; Two-tailed unpaired Student's *t*-test). (**E**) Splenocytes from OTII Tg and OTII/miR-185 Tg mice were stained for CD4 and CD8, and analyzed by FACS. (**F**) Histogram shows surface expression of TCR Vα2 on splenic $CD4^+$ $CD8^-$ T cells of OTII Tg (dark gray) and OTII/miR-185 Tg-35 mice (black line). Data are representative of at least 2 mice per group.

Table 5.1. The top 25 down-regulated genes with predicted miR-185 binding sites on their 3' UTR and/or coding sequences in miR-185 transgenic DN3 thymocytes.

Gene Symbol	Fold	Description
Mzb1	-4.84	Marginal zone B and B1-cell specific protein
Hk2	-4.19	Hexokinase II
Hoxa7	-3.81	Homeo box A7
Tpst1	-3.79	Protein-tyrosine sulfotransferase 1
Mcm10	-3.26	Minichromosome maintenance deficient 10
Camk4	-3.24	Calcium/calmodulin-dependent protein kinase IV
Stab1	-3.20	Stabilin 1
E130012A19Rik	-3.10	RIKEN cDNA E130012A19 gene
2310044H10Rik	-3.06	RIKEN cDNA 2310044H10 gene, MIRTA22
Abcf2	-2.94	ATP-binding cassette, sub-family F (GCN20), member 2
Gja1	-2.75	Gap junction membrane channel protein alpha 1
Gga2	-2.73	Golgi associated, gamma adaptin ear containing, ARF binding protein 2
Nsf	-2.59	N-ethylmaleimide sensitive fusion protein
Ccdc53	-2.52	Coiled-coil domain containing 53
Mns1	-2.41	Meiosis-specific nuclear structural protein 1
Ncl	-2.40	Nucleolin
Hmga1	-2.38	High mobility group AT-hook 1
Shmt1	-2.36	Serine hydroxymethyltransferase 1
Mcm5	-2.26	Minichromosome maintenance deficient 5
Igf2bp3	-2.22	Insulin-like growth factor 2 mRNA binding protein 3
Nfatc3	-2.21	Nuclear factor of activated T cells, cytoplasmic, calcineurin dependent 3
Rrm1	-2.19	Ribonucleotide reductase M1
Suz12	-2.18	Suppressor of zeste 12 homolog (Drosophila)
Igf1r	-2.14	Insulin-like growth factor I receptor
Rcl1	-2.13	RNA terminal phosphate cyclase-like 1

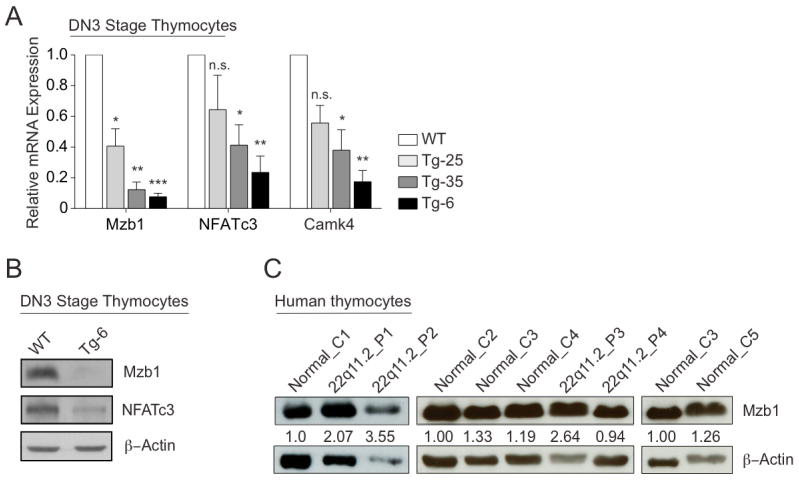

Figure 5.12. MiR-185 targets a number of genes in developing thymocytes. (**A**) Relative mRNA levels of Mzb1, NFATc3, and Camk4 in DN3 thymocytes, normalized to the endogenous Gapdh levels, were determined by real-time quantitative PCR. WT values were set to 1. Data shown are of the mean +/- SEM of at least 3 independent experiments performed in triplicates. Bars are representative of WT (white), Tg-25 (light gray), Tg-35 (dark gray), and Tg-6 (black) mice. (n.s. = non-significant, *$p < 0.05$, **$p < 0.01$, ***$p < 0.001$; versus the threshold set as 1; One sample Student's *t*-test) (**B**) Immunoblot analysis of Mzb1 and NFATc3 expression in miR-185 Tg-6 DN3 thymocytes compared to the wild type control. β-actin was used as the endogenous control. (**C**) Mzb1 protein expression levels in human thymocytes obtained from 5 normal individuals (Normal_C1-C5) and 4 patients with 22q11.2 deletion syndrome (22q11.2_P1-P4). β-actin was used as the endogenous control. The relative amounts of Mzb1 protein were determined by normalizing to the β-actin, indicated with numbers for each lane. Band intensities of Mzb1 and β-actin were measured using the ImageJ software. The Mzb1/β-actin ratio was calculated by dividing the band intensity of Mzb1 to that of the β- actin for each sample. Relative Mzb1 levels were then determined for each experiment indicated as a group. This was done by normalizing the Mzb1/β-actin ratio for each sample relative to the first control sample. The first control sample was set as 1 in each 3 independent experiments.

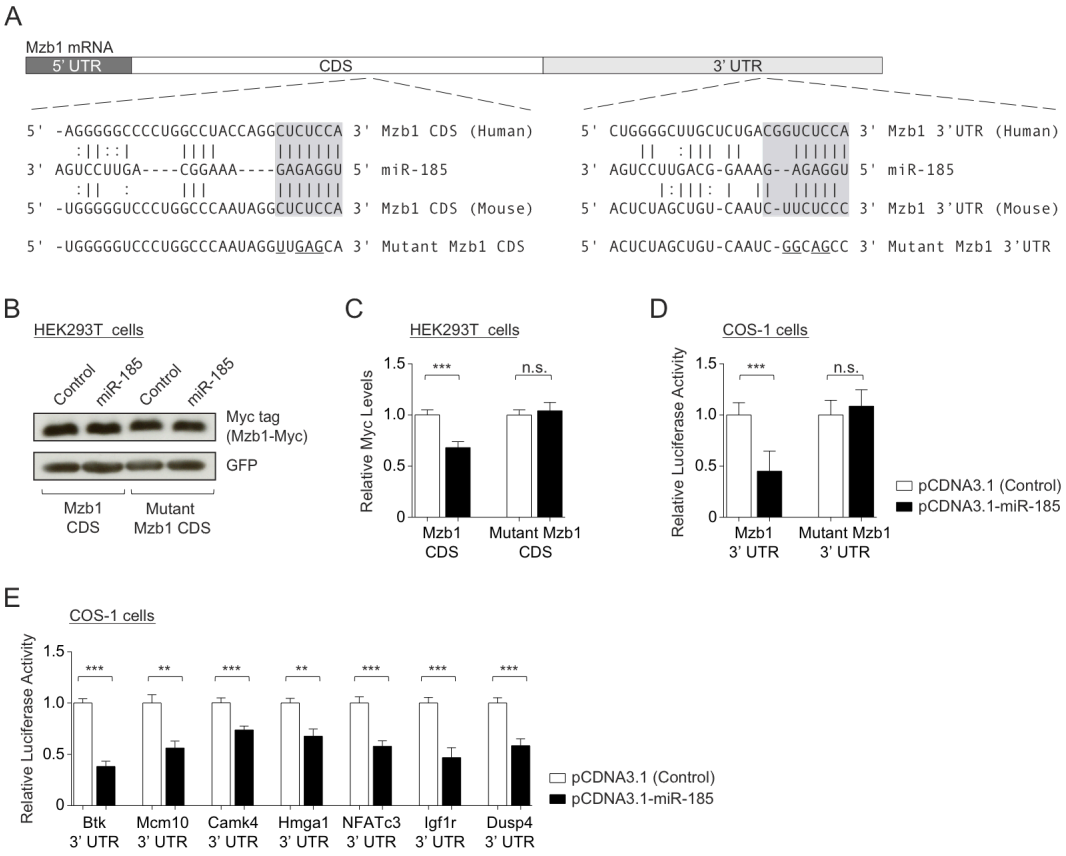

Figure 5.13. MiR-185 directly targets Mzb1 mRNA. (**A**) The Mzb1 CDS and 3' UTR each contain one putative miR-185 binding site. Diagram shows conserved miR-185 base pairing with human and murine Mzb1 mRNA. Mutated Mzb1 sequences were underlined. (**B**) Expression levels of Myc tag in HEK293T cells transfected with the plasmid containing either wild type Mzb1- or mutant Mzb1-Myc fusion, along with the empty vector (white) or pCDNA3.1/miR-185 (black). A GFP-expressing plasmid was used as the transfection control. (**C**) Relative expression levels of Mzb1-Myc were calculated by normalizing to GFP levels for each lane. Each bar represents the mean +/- SEM of 4 independent experiments performed in at least duplicates (n.s. = non-significant, $*p < 0.05$, $**p < 0.01$, $***p < 0.001$; Two-tailed unpaired Student's *t*-test). (**D-E**) Relative luciferase activity normalized to beta-galactosidase of COS-1 cells transfected with the luciferase plasmids containing the indicated 3' UTRs (Mzb1, Mutant Mzb1, Btk, Mcm10, Camk4, Hmga1, NFATc3, Igf1r, and Dusp4), along with either the empty vector (white) or pCDNA3.1-miR-185 (black). Btk 3' UTR, a previously validated target of miR-185, was used as a positive control in (E). Data shown are the mean +/- SEM of 4 independent experiments, each performed in triplicate or quadruplicates (n.s. = non-significant, $*p < 0.05$, $**p < 0.01$, $***p < 0.001$; Two-tailed unpaired Student's *t*-test).

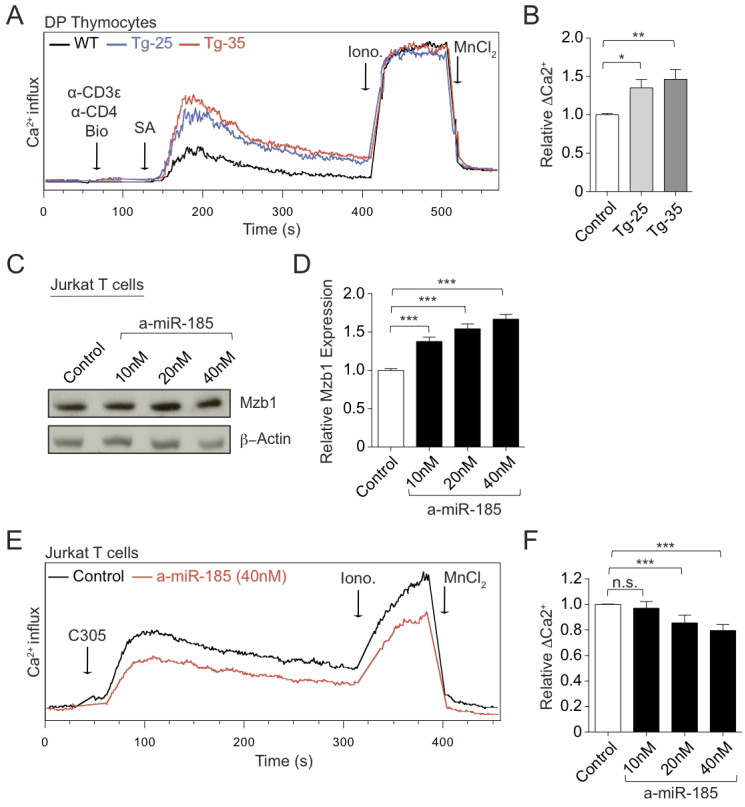

Figure 5.14. MiR-185 affects TCR-stimulated intracellular calcium responses. (**A**) Intracellular calcium flux was analyzed by flow cytometry in DP thymocytes from the WT (black line), Tg-25 (blue line), and Tg-35 (red line) mice. DP thymocytes were gated by size. Black arrows indicate the time points for each treatment. Fluo-3 AM loaded thymocytes were treated with biotinylated anti-CD3ε and anti-CD4, followed by Streptavidin (SA), Ionomycin (Iono.), and $MnCl_2$. (**B**) Relative changes in TCR-triggered peak Ca^{2+}-influx over background. Data are of the mean +/- SEM of 6 independent experiments (*$p < 0.05$, **$p < 0.01$, ***$p < 0.001$; Two-tailed unpaired Student's *t*-test). (**C**) Representative immunoblot shows Mzb1 expression in Jurkat T cells transfected with miR-185 inhibitor (a-miR-185), compared to the control (miR negative control inhibitor). β-actin was used as the endogenous control. (**D**) The relative amounts of Mzb1 protein were determined by normalizing to the β-actin. Data are of the mean +/- SEM of 5 independent experiments, performed in at least duplicates (*$p < 0.05$, **$p < 0.01$, ***$p < 0.001$; Two-tailed unpaired Student's *t*-test). (**E**) Intracellular calcium responses were analyzed by flow cytometry over time in Jurkat T cells following transfection with a-miR-185 (red line) and the control inhibitor (black line). Fluo-3 AM loaded Jurkat T cells were treated with the mAb C305.2 (anti-TCRβ), Ionomycin (Iono.), and $MnCl_2$. Black arrows indicate the time points for each treatment. (**F**) Relative changes in TCR-triggered peak Ca^{2+}-influx over background. Data are of the mean +/- SEM of 4 independent experiments (n.s. = non-significant, *$p < 0.05$, **$p < 0.01$, ***$p < 0.001$; Two-tailed unpaired Student's *t*-test).

CHAPTER SIX

DISCUSSION

Stress-responsive microRNAs in the thymus

Thymus is the most stress-sensitive lymphoid tissue, undergoing a rapid involution defined by severe reductions in size, cellularity, and functionality. Given that thymus has a vital role in maintaining an effective immune system, why this organ is extremely vulnerable to various physiological and pathological stresses has been a subject to debate for a long time [197,198,199]. One of the reasons may be that the body aims to offset economical usage of energy under stress conditions by suspending thymopoiesis, a high-energy demanding process [59,199]. It is also thought that attenuation of thymic output could prevent rise of regulatory T cells during microbial infections or effector T cells against fetus in the case of pregnancy [172,197,198]. Nevertheless, our current knowledge of mechanisms behind the stress-induced thymic atrophy is still limited, and this necessitates a better understanding due to high incidence of morbidity and often mortality in elderly with stress-weakened immune system.

Systemic glucocorticoids (GCs) are the main contributors to the massive loss of DP thymocytes upon stress stimuli. Several studies have investigated GC-mediated cell death, but mostly by *in vitro* assays, thus lacking an *in vivo* relevance [36,176]. MiRs are crucial players in mediating various cellular processes in response to GCs [176]. An initial study utilizing *in vitro* cultured primary rat thymocytes demonstrated that mature miRs are down-

regulated within hours of GC exposure, primarily due to reductions in Dicer [131]. Indeed, miRs could exhibit dynamic *in vivo* expression changes during thymic atrophy and recovery phases. Accordingly, we performed the first miR profiling of murine thymus tissues at later time points, during which the most dramatic changes in cellularity are evident following LPS and/or Dex injections. MiR profiling revealed 7 up- and 11 down-regulated thymic miRs in response to stress. Several down-regulated miRs (miR-181a, miR-15a, and miR-26b) had increased levels of expression at earlier time points upon stress-induction, suggesting that their dysregulation might be independent of the severity of thymic atrophy. In addition, these miRs, such as miR-17-92 family, exhibited differential stress-induced changes in their expression at distinct stages of thymopoiesis. This could help to explain why each thymocyte subset has a different degree of sensitivity to stress-induced GCs. Moreover, majority of thymic miRs had an altered expression profile in other tissues following stress. This suggests a general stress-mediated mechanism responsible for the regulation of these miRs in the body. Strikingly, miR-150, miR-181d, miR-128, and miR-205 were only stress-responsive in the thymus. Further characterization of these 4 miRs will be interesting to reveal whether they contribute to the extreme stress-sensitivity of thymus.

Most stress-responsive miRs in the thymus have previously been implicated in regulating apoptosis and cell survival. In particular, miR-17-92 family members are known to target pro-apoptotic genes, such as Bim, in immature thymocytes [87,131]. Reduced miR-17-92 expression could partly contribute to the increased cell death in DP thymocytes upon GC exposure. Nevertheless, changes in a single miR or its target might not be sufficient to uncover stress-induced thymic atrophy. First of all, miR functions are not only dependent on

cellular concentrations of miRs, but also dependent on the abundance of target mRNAs, which can also be substantially affected by stress conditions [168,175]. Thus, stress-responsive thymic miRs likely have novel and/or additional gene targets in thymocytes apart from their validated targets in other cell types. Thymic miRs that remained unchanged upon stress could also play roles in the regulation of thymic involution due to stress-induced alterations in their mRNA targets. Second, stress can lead to derepression of target mRNAs by altering the activity of miR-RISC complex. This is achieved through occupation of miR target sites by other RNA-binding proteins under stress conditions [168]. Finally, multiple miRs can have common gene targets and/or diverse gene targets in the same signaling pathway. This might indicate combinatorial effects of stress-responsive miRs during thymic atrophy.

To my knowledge, the work herein represented the first time identification of differentially regulated miRs in murine thymus upon LPS and/or Dex injections. Further characterization of individual miRs with transgenic and gene-targeting approaches will improve our current understanding of molecular mechanisms involved in stress-induced thymic atrophy. MiRs are emerging as promising therapeutic agents and/or targets for the treatment of several human diseases. Thus, discovery of stress-responsive thymic miRs has a tremendous clinical value with the potential to intervene in immune regulation and tolerance under normal and pathological conditions.

Elevated stress sensitivity in miR-181d transgenic thymocytes

MiR-181 family members exhibit dynamic expression patterns during thymopoiesis under normal and stress conditions. In particular, miR-181d undergoes a 15-fold down-regulation in response to stress-induction, whereas miR-181a and miR-181b are reduced around 2- and 6-fold, respectively. Of note, miR-181c remains at negligible levels in the thymus. Together, these data indicate that distinct transcriptional and post-transcriptional mechanisms are involved in differential regulation of miR-181 family members. One mechanism could be through stress-mediated changes in stability of these miRs, resulting in variable abundance of each miR during thymic atrophy. Further studies deciphering the molecular basis of differential expression of miR-181 family members will be beneficial to better understand their roles in thymopoiesis.

Previous reports demonstrated that miR-181 family members could have both shared and distinct gene targets [94,95,132,177]. Normal thymopoiesis noted both in miR-181a/b and miR-181c/d knockout mice demonstrated an evidence of functional redundancy between these miRs [99,100]. On the other hand, miR-181a/b deficiency blocked NK T cell development in mice, while loss of miR-181c/d had no apparent effects on these cells [100]. This further indicated that relative abundance of miR-181 family members defines their compensatory or unique functions in a particular cell type. Hence, miR-181d, the most dramatically altered stress-responsive miR, might have a distinct role during thymic involution.

In order to study the impact of miR-181d on thymopoiesis under normal and stress conditions, we utilized both gain- and loss-of-function approaches. T cell-specific transgenic expression of miR-181d impaired thymopoiesis with a significant decrease in DP

thymocytes. This reduction became more drastic upon LPS and/or Dex injections. However, mutating miR-181d sequence did not have any apparent effect on T cell development, consistent with the recent reports on miR-181c/d knockout mice. This is again indicative of overlapping functions between miR-181 family members, with sharing the same seed sequence. Moreover, bioinformatic analysis of differentially regulated genes among miR-181d transgenic and knockin thymocytes revealed that miR-181d regulates similar biological pathways and processes previously implicated for the other family members. These pathways include TCR signaling, PI3K/Akt signaling, and apoptotic pathways. Characterization of these key pathways will improve understanding of miR-modulated intrathymic mechanisms in the context of thymic atrophy.

MiR-181 family members are known to regulate cell survival by targeting anti-apoptotic genes, such as Bcl2 and Mcl1 [177]. Transgenic expression of miR-181d might further decrease expression of these genes, rendering DP thymocytes extremely sensitive to GC-induced apoptosis. In addition, GCs are also thought to reduce TCR signaling capacity, leading to death by neglect in DP thymocytes [35]. Thus, altered TCR signaling strength by elevated levels of miR-181d could account for reduced number of DP thymocytes in miR-181d transgenic mice under normal and stress conditions. Accordingly, down-regulation of miR-181 family members upon stress might be beneficial for recovering from thymic atrophy.

PI3K- and PPAR-signaling pathways are significantly enriched within dysregulated genes in the miR-181d transgenic thymocytes, suggesting an impact of miR-181d on cellular metabolic processes. Stress can lead to a metabolic reprogramming in immature thymocytes

by reducing miR-181d levels. This could explain massive loss of DP thymocytes during thymic atrophy via shutting down the high-energy consumption processes, such as T cell repertoire selection.

Together with the identification of stress-responsive miRs in the thymus, my work further demonstrates the involvement of miRs in modulating thymic atrophy. In particular, transgenic expression of miR-181d augments stress-sensitivity of DP thymocytes, whereas targeting the miR-181d exclusively does not suffice to rescue thymocyte depletion following stress. At first glance, this suggests cooperative functions of miR-181 family members, but other stress-responsive miRs could also influence thymic atrophy in a combinatorial manner. Overall, these findings will support miR-based therapeutic interventions in GC-resistant hematological malignancies.

Transgenic expression of miR-185 attenuates T cell development

MiR-185, another stress responsive thymic miR, is located within the human 22q11.2 gene locus. This region undergoes a hemizygous deletion in patients with the 22q11.2 deletion/DiGeorge syndrome; a primary immunodeficiency disease associated with thymus and parathyroid gland abnormalities, heart defects, psychiatric disorders, and/or mild facial dysmorphology [110]. These variable clinical presentations in the patients are partly explained by the extent of monoallelic deletion on chromosome 22 at position 22q11.2 [110]. Although this critical region has been mapped, the genetic elements whose deficiency causes poor thymocyte development remain unknown.

We utilized a gain-of-function approach to determine the impact of miR-185 on T cell development. This caused a partial block at the DN3 stage of thymopoiesis. In addition, elevated miR-185 levels attenuated positive selection of DP thymocytes, which in turn resulted in a peripheral T cell lymphopenia with remaining cells exhibiting a hyper-activated phenotype. These developmental impairments likely result from the combinatorial effects of at least 3 miR-185 targets (Mzb1, NFATc3, and Camk4). Numerous additional putative targets of miR-185 were uncovered. Many are involved in regulating cell growth and differentiation, and the combined reduction of these genes might contribute to the attenuated thymopoiesis identified in miR-185 transgenic mice [200,201,202,203,204].

In the case of stress-induced thymic atrophy, miR-185 undergoes a dramatic reduction in DP thymocytes. Such down-regulation of miR-185 might be necessary for the survival of DP thymocytes, since its over-expression attenuates proper selection and further differentiation of these cells.

It is known that patients with 22q11.2 deletion syndrome have an increased prevalence of autoimmune disorders and B cell defects attributed to the T cell lymphopenia. Since miR-185 is expressed at 42% normal levels in the patients [109], slightly elevated levels of multiple gene targets of miR-185 would be anticipated. MiR-185 is downregulated in marginal zone B cells, consistent with the higher levels of Btk and Mzb1 in those cells. A further reduction in miR-185 could increase Btk and Mzb1 levels, effectively increasing the development of self-reactive B cells and fast autoantibody secretion, respectively [117,186]. These changes could account for the augmented autoantibody production noted in some of the 22q11.2 deletion syndrome patients with a miR-185 haploinsufficiency. A subset of

these patients have low T cell numbers and impaired T cell functions, all of which emanate from the thymic hypoplasia [113,114]. Increased Mzb1 levels in thymocytes and peripheral $CD4^+$ T cells in such patients could reduce cell expansion and altered T helper cell commitment, as previously reported [186].

Mouse models of 22q11.2 deletion syndrome confirm that miR-185 is haploinsufficient [115,116]. These mice have neurological abnormalities resulting from enhanced calcium regulated neurotransmitter release, which is linked to elevations in a distinct miR-185 target, the calcium regulator, SERCA2 [115]. Since SERCA2 is expressed at very low levels in thymocytes, it may not be the principal target of miR-185 in immature thymocytes. Another miR-185 target identified in our screen is 2310044H10Rik, a Golgi-associated neuronal inhibitor. Derepression of this gene due to reduced miR-185 levels in mouse models of 22q11.2 deletion syndrome leads to structural alterations in hippocampal neurons [116]. These are of relevance to human 22q11.2 deletion syndrome patients, as many of these patients have neurological complications, such as schizophrenia in adults.

Overall, these findings implicate miR-185 as an important regulator of T cell development through its targeting of genes with validated roles in the immune system. Although miR-185 is not expected to uncover the basis of all 22q11.2/DiGeorge syndrome complications, further characterization of other miR-185 targets will be valuable in identifying the contribution of its haploinsufficiency to various clinical phenotypes noted in this syndrome.

Additional comments

Besides the identification of stress-responsive miRs in murine thymus, it is of significance to uncover differentially regulated mRNAs in distinct stages of thymopoiesis following PBS and LPS or Dex injections. This will help to determine genetic targets of stress-responsive miRs and elucidate miR-mediated molecular mechanisms in the context of stress-induced thymic atrophy.

The use of murine models to study human diseases, particularly inflammatory diseases, has been a matter of debate. A recent study has shown that genomic responses in humans upon acute inflammatory stress stimuli exhibited a weak correlation with the corresponding mouse models [205]. Thus, characterization of stress-responsive RNA species in human thymocytes and thymic epithelial cells will have an enormous clinical potential to treat individuals undergoing thymic involution.

It is still poorly understood whether each member of a miR family sharing the same seed sequence has common and/or unique functions. This is evident with miR-181ab and miR-181cd knockout mice, both exhibiting normal thymopoiesis. However, complete knockout of all miR-181 family members results in embryonic lethality. Indeed, T cell-specific elimination of all miR-181 family members will reveal the necessity of these miRs during T cell development and functions. Molecular targets of a single miR in T cells can display variability depending on the relative abundance of the miR and its target mRNAs during distinct stages of development. Thus, miR-181d transgenic and knockin mice might exhibit altered peripheral T cell differentiation and responses. For example, miR-181d is highly expressed in induced regulatory T cells. Identification of the role of miR-181d in these cells will provide new insights into the regulation of immune tolerance.

Given the validated targets of miR-185 in the neurons and lymphocytes with relevance to human 22q11.2 deletion/DiGeorge syndrome, functional characterization of this miR in other cell types, such as cardiac, epithelial, and innate immune cells, is appealing. Utilizing a miR-185 knockout mouse model will be of great use for this purpose, and will reveal its role in complex biological systems.

REFERENCES

1. Swain SL (1983) T cell subsets and the recognition of MHC class. Immunol Rev 74: 129-142.

2. Schmitt TM, Zuniga-Pflucker JC (2005) Thymus-derived signals regulate early T-cell development. Crit Rev Immunol 25: 141-159.

3. Boehm T, Bleul CC (2006) Thymus-homing precursors and the thymic microenvironment. Trends Immunol 27: 477-484.

4. Petrie HT, Zuniga-Pflucker JC (2007) Zoned out: functional mapping of stromal signaling microenvironments in the thymus. Annu Rev Immunol 25: 649-679.

5. Godfrey DI, Kennedy J, Suda T, Zlotnik A (1993) A developmental pathway involving four phenotypically and functionally distinct subsets of CD3-CD4-CD8- triple-negative adult mouse thymocytes defined by CD44 and CD25 expression. J Immunol 150: 4244-4252.

6. Rothenberg EV, Moore JE, Yui MA (2008) Launching the T-cell-lineage developmental programme. Nat Rev Immunol 8: 9-21.

7. Livak F, Tourigny M, Schatz DG, Petrie HT (1999) Characterization of TCR gene rearrangements during adult murine T cell development. J Immunol 162: 2575-2580.

8. Mombaerts P, Iacomini J, Johnson RS, Herrup K, Tonegawa S, et al. (1992) RAG-1-deficient mice have no mature B and T lymphocytes. Cell 68: 869-877.

9. Shinkai Y, Koyasu S, Nakayama K, Murphy KM, Loh DY, et al. (1993) Restoration of T cell development in RAG-2-deficient mice by functional TCR transgenes. Science 259: 822-825.

10. van Oers NS, von Boehmer H, Weiss A (1995) The pre-T cell receptor (TCR) complex is functionally coupled to the TCR-zeta subunit. J Exp Med 182: 1585-1590.

11. Saint-Ruf C, Ungewiss K, Groettrup M, Bruno L, Fehling HJ, et al. (1994) Analysis and expression of a cloned pre-T cell receptor gene. Science 266: 1208-1212.

12. Ciofani M, Knowles GC, Wiest DL, von Boehmer H, Zuniga-Pflucker JC (2006) Stage-specific and differential notch dependency at the alphabeta and gammadelta T lineage bifurcation. Immunity 25: 105-116.

13. Balciunaite G, Ceredig R, Rolink AG (2005) The earliest subpopulation of mouse thymocytes contains potent T, significant macrophage, and natural killer cell but no B-lymphocyte potential. Blood 105: 1930-1936.

14. Robey E, Fowlkes BJ (1994) Selective events in T cell development. Annu Rev Immunol 12: 675-705.

15. Guo J, Hawwari A, Li H, Sun Z, Mahanta SK, et al. (2002) Regulation of the TCRalpha repertoire by the survival window of CD4(+)CD8(+) thymocytes. Nat Immunol 3: 469-476.

16. Hernandez-Munain C, Sleckman BP, Krangel MS (1999) A developmental switch from TCR delta enhancer to TCR alpha enhancer function during thymocyte maturation. Immunity 10: 723-733.

17. von Boehmer H, Teh HS, Kisielow P (1989) The thymus selects the useful, neglects the useless and destroys the harmful. Immunol Today 10: 57-61.

18. Starr TK, Jameson SC, Hogquist KA (2003) Positive and negative selection of T cells. Annu Rev Immunol 21: 139-176.

19. Kisielow P, von Boehmer H (1995) Development and selection of T cells: facts and puzzles. Adv Immunol 58: 87-209.

20. Germain RN (2002) T-cell development and the CD4-CD8 lineage decision. Nat Rev Immunol 2: 309-322.

21. Singer A, Adoro S, Park JH (2008) Lineage fate and intense debate: myths, models and mechanisms of CD4- versus CD8-lineage choice. Nat Rev Immunol 8: 788-801.

22. Anderson MS, Venanzi ES, Klein L, Chen Z, Berzins SP, et al. (2002) Projection of an immunological self shadow within the thymus by the aire protein. Science 298: 1395-1401.

23. Gruver AL, Sempowski GD (2008) Cytokines, leptin, and stress-induced thymic atrophy. J Leukoc Biol 84: 915-923.

24. Milentijevic D, Rubel IF, Liew AS, Helfet DL, Torzilli PA (2005) An in vivo rabbit model for cartilage trauma: a preliminary study of the influence of impact stress magnitude on chondrocyte death and matrix damage. J Orthop Trauma 19: 466-473.

25. Chao MW, Gibbs P, Wirth A, Quong G, Guiney MJ, et al. (2005) Radiotherapy in the management of solitary extramedullary plasmacytoma. Intern Med J 35: 211-215.

26. Hauri-Hohl MM, Zuklys S, Keller MP, Jeker LT, Barthlott T, et al. (2008) TGF-beta signaling in thymic epithelial cells regulates thymic involution and postirradiation reconstitution. Blood 112: 626-634.

27. Muller-Hermelink HK, Sale GE, Borisch B, Storb R (1987) Pathology of the thymus after allogeneic bone marrow transplantation in man. A histologic immunohistochemical study of 36 patients. Am J Pathol 129: 242-256.

28. O'Brien PC, Roos DE, Pratt G, Liew KH, Barton MB, et al. (2006) Combined-modality therapy for primary central nervous system lymphoma: long-term data from a Phase II multicenter study (Trans-Tasman Radiation Oncology Group). Int J Radiat Oncol Biol Phys 64: 408-413.

29. Murgita RA, Wigzell H (1981) Regulation of immune functions in the fetus and newborn. Prog Allergy 29: 54-133.

30. Rocklin RE, Kitzmiller JL, Kaye MD (1979) Immunobiology of the maternal-fetal relationship. Annu Rev Med 30: 375-404.

31. Chandra RK (1979) Nutritional deficiency and susceptibility to infection. Bull World Health Organ 57: 167-177.

32. Chandra RK (1992) Protein-energy malnutrition and immunological responses. J Nutr 122: 597-600.

33. Luz C, Dornelles F, Preissler T, Collaziol D, da Cruz IM, et al. (2003) Impact of psychological and endocrine factors on cytokine production of healthy elderly people. Mech Ageing Dev 124: 887-895.

34. Heuser I, Deuschle M, Luppa P, Schweiger U, Standhardt H, et al. (1998) Increased diurnal plasma concentrations of dehydroepiandrosterone in depressed patients. J Clin Endocrinol Metab 83: 3130-3133.

35. Ashwell JD, Lu FW, Vacchio MS (2000) Glucocorticoids in T cell development and function*. Annu Rev Immunol 18: 309-345.

36. Herold MJ, McPherson KG, Reichardt HM (2006) Glucocorticoids in T cell apoptosis and function. Cell Mol Life Sci 63: 60-72.

37. Jenkins BD, Pullen CB, Darimont BD (2001) Novel glucocorticoid receptor coactivator effector mechanisms. Trends Endocrinol Metab 12: 122-126.

38. Luisi BF, Xu WX, Otwinowski Z, Freedman LP, Yamamoto KR, et al. (1991) Crystallographic analysis of the interaction of the glucocorticoid receptor with DNA. Nature 352: 497-505.

39. Baumann S, Dostert A, Novac N, Bauer A, Schmid W, et al. (2005) Glucocorticoids inhibit activation-induced cell death (AICD) via direct DNA-dependent repression of the CD95 ligand gene by a glucocorticoid receptor dimer. Blood 106: 617-625.

40. Brewer JA, Khor B, Vogt SK, Muglia LM, Fujiwara H, et al. (2003) T-cell glucocorticoid receptor is required to suppress COX-2-mediated lethal immune activation. Nat Med 9: 1318-1322.

41. Forsthoefel AM, Thompson EA (1987) Glucocorticoid regulation of transcription of the c-myc cellular protooncogene in P1798 cells. Mol Endocrinol 1: 899-907.

42. Wang Z, Malone MH, He H, McColl KS, Distelhorst CW (2003) Microarray analysis uncovers the induction of the proapoptotic BH3-only protein Bim in multiple models of glucocorticoid-induced apoptosis. J Biol Chem 278: 23861-23867.

43. Abrams MT, Robertson NM, Yoon K, Wickstrom E (2004) Inhibition of glucocorticoid-induced apoptosis by targeting the major splice variants of BIM mRNA with small interfering RNA and short hairpin RNA. J Biol Chem 279: 55809-55817.

44. Bouillet P, Metcalf D, Huang DC, Tarlinton DM, Kay TW, et al. (1999) Proapoptotic Bcl-2 relative Bim required for certain apoptotic responses, leukocyte homeostasis, and to preclude autoimmunity. Science 286: 1735-1738.

45. Bouillet P, Purton JF, Godfrey DI, Zhang LC, Coultas L, et al. (2002) BH3-only Bcl-2 family member Bim is required for apoptosis of autoreactive thymocytes. Nature 415: 922-926.

46. Erlacher M, Labi V, Manzl C, Bock G, Tzankov A, et al. (2006) Puma cooperates with Bim, the rate-limiting BH3-only protein in cell death during lymphocyte development, in apoptosis induction. J Exp Med 203: 2939-2951.

47. Rudolph B, Hueber AO, Evan GI (2000) Reversible activation of c-Myc in thymocytes enhances positive selection and induces proliferation and apoptosis in vitro. Oncogene 19: 1891-1900.

48. Broussard-Diehl C, Bauer SR, Scheuermann RH (1996) A role for c-myc in the regulation of thymocyte differentiation and possibly positive selection. J Immunol 156: 3141-3150.

49. Veis DJ, Sorenson CM, Shutter JR, Korsmeyer SJ (1993) Bcl-2-deficient mice demonstrate fulminant lymphoid apoptosis, polycystic kidneys, and hypopigmented hair. Cell 75: 229-240.

50. Savino W (2006) The thymus is a common target organ in infectious diseases. PLoS Pathog 2: e62.

51. Medzhitov R (2007) Recognition of microorganisms and activation of the immune response. Nature 449: 819-826.

52. Medzhitov R (2008) Origin and physiological roles of inflammation. Nature 454: 428-435.

53. Saluk-Juszczak J, Wachowicz B (2005) [The proinflammatory activity of lipopolysaccharide]. Postepy Biochem 51: 280-287.

54. Deftos ML, He YW, Ojala EW, Bevan MJ (1998) Correlating notch signaling with thymocyte maturation. Immunity 9: 777-786.

55. Radtke F, Fasnacht N, Macdonald HR (2010) Notch signaling in the immune system. Immunity 32: 14-27.

56. Choi YI, Jeon SH, Jang J, Han S, Kim JK, et al. (2001) Notch1 confers a resistance to glucocorticoid-induced apoptosis on developing thymocytes by down-regulating SRG3 expression. Proc Natl Acad Sci U S A 98: 10267-10272.

57. Anz D, Thaler R, Stephan N, Waibler Z, Trauscheid MJ, et al. (2009) Activation of melanoma differentiation-associated gene 5 causes rapid involution of the thymus. J Immunol 182: 6044-6050.

58. Papadopoulou AS, Dooley J, Linterman MA, Pierson W, Ucar O, et al. (2012) The thymic epithelial microRNA network elevates the threshold for infection-associated thymic involution via miR-29a mediated suppression of the IFN-alpha receptor. Nat Immunol 13: 181-187.

59. Ventevogel MS, Sempowski GD (2013) Thymic rejuvenation and aging. Curr Opin Immunol.

60. Dixit VD (2010) Thymic fatness and approaches to enhance thymopoietic fitness in aging. Curr Opin Immunol 22: 521-528.

61. Kim YK, Kim VN (2007) Processing of intronic microRNAs. EMBO J 26: 775-783.

62. Rodriguez A, Griffiths-Jones S, Ashurst JL, Bradley A (2004) Identification of mammalian microRNA host genes and transcription units. Genome Res 14: 1902-1910.

63. Ansel KM (2013) RNA regulation of the immune system. Immunol Rev 253: 5-11.

64. Lee Y, Jeon K, Lee JT, Kim S, Kim VN (2002) MicroRNA maturation: stepwise processing and subcellular localization. EMBO J 21: 4663-4670.

65. Tili E, Michaille JJ, Costinean S, Croce CM (2008) MicroRNAs, the immune system and rheumatic disease. Nat Clin Pract Rheumatol 4: 534-541.

66. Landthaler M, Yalcin A, Tuschl T (2004) The human DiGeorge syndrome critical region gene 8 and Its D. melanogaster homolog are required for miRNA biogenesis. Curr Biol 14: 2162-2167.

67. Lee Y, Ahn C, Han J, Choi H, Kim J, et al. (2003) The nuclear RNase III Drosha initiates microRNA processing. Nature 425: 415-419.

68. Yi R, Qin Y, Macara IG, Cullen BR (2003) Exportin-5 mediates the nuclear export of pre-microRNAs and short hairpin RNAs. Genes Dev 17: 3011-3016.

69. Ketting RF, Fischer SE, Bernstein E, Sijen T, Hannon GJ, et al. (2001) Dicer functions in RNA interference and in synthesis of small RNA involved in developmental timing in C. elegans. Genes Dev 15: 2654-2659.

70. Lund E, Guttinger S, Calado A, Dahlberg JE, Kutay U (2004) Nuclear export of microRNA precursors. Science 303: 95-98.

71. Lewis BP, Burge CB, Bartel DP (2005) Conserved seed pairing, often flanked by adenosines, indicates that thousands of human genes are microRNA targets. Cell 120: 15-20.

72. Sandberg R, Neilson JR, Sarma A, Sharp PA, Burge CB (2008) Proliferating cells express mRNAs with shortened 3' untranslated regions and fewer microRNA target sites. Science 320: 1643-1647.

73. Lytle JR, Yario TA, Steitz JA (2007) Target mRNAs are repressed as efficiently by microRNA-binding sites in the 5' UTR as in the 3' UTR. Proc Natl Acad Sci U S A 104: 9667-9672.

74. Orom UA, Nielsen FC, Lund AH (2008) MicroRNA-10a binds the 5'UTR of ribosomal protein mRNAs and enhances their translation. Mol Cell 30: 460-471.

75. Ajay SS, Athey BD, Lee I (2010) Unified translation repression mechanism for microRNAs and upstream AUGs. BMC Genomics 11: 155.

76. Tay Y, Zhang J, Thomson AM, Lim B, Rigoutsos I (2008) MicroRNAs to Nanog, Oct4 and Sox2 coding regions modulate embryonic stem cell differentiation. Nature 455: 1124-1128.

77. Bartel DP (2004) MicroRNAs: genomics, biogenesis, mechanism, and function. Cell 116: 281-297.

78. Kloosterman WP, Plasterk RH (2006) The diverse functions of microRNAs in animal development and disease. Dev Cell 11: 441-450.

79. Kozomara A, Griffiths-Jones S (2011) miRBase: integrating microRNA annotation and deep-sequencing data. Nucleic Acids Res 39: D152-157.

80. Cobb BS, Nesterova TB, Thompson E, Hertweck A, O'Connor E, et al. (2005) T cell lineage choice and differentiation in the absence of the RNase III enzyme Dicer. J Exp Med 201: 1367-1373.

81. Koralov SB, Muljo SA, Galler GR, Krek A, Chakraborty T, et al. (2008) Dicer ablation affects antibody diversity and cell survival in the B lymphocyte lineage. Cell 132: 860-874.

82. Park CY, Choi YS, McManus MT (2010) Analysis of microRNA knockouts in mice. Hum Mol Genet 19: R169-175.

83. Rodriguez A, Vigorito E, Clare S, Warren MV, Couttet P, et al. (2007) Requirement of bic/microRNA-155 for normal immune function. Science 316: 608-611.

84. Thai TH, Calado DP, Casola S, Ansel KM, Xiao C, et al. (2007) Regulation of the germinal center response by microRNA-155. Science 316: 604-608.

85. Vigorito E, Perks KL, Abreu-Goodger C, Bunting S, Xiang Z, et al. (2007) microRNA-155 regulates the generation of immunoglobulin class-switched plasma cells. Immunity 27: 847-859.

86. Ventura A, Young AG, Winslow MM, Lintault L, Meissner A, et al. (2008) Targeted deletion reveals essential and overlapping functions of the miR-17 through 92 family of miRNA clusters. Cell 132: 875-886.

87. Xiao C, Srinivasan L, Calado DP, Patterson HC, Zhang B, et al. (2008) Lymphoproliferative disease and autoimmunity in mice with increased miR-17-92 expression in lymphocytes. Nat Immunol 9: 405-414.

88. Bezman NA, Chakraborty T, Bender T, Lanier LL (2011) miR-150 regulates the development of NK and iNKT cells. J Exp Med 208: 2717-2731.

89. Xiao C, Calado DP, Galler G, Thai TH, Patterson HC, et al. (2007) MiR-150 controls B cell differentiation by targeting the transcription factor c-Myb. Cell 131: 146-159.

90. Zheng Q, Zhou L, Mi QS (2012) MicroRNA miR-150 is involved in Valpha14 invariant NKT cell development and function. J Immunol 188: 2118-2126.

91. Kirigin FF, Lindstedt K, Sellars M, Ciofani M, Low SL, et al. (2012) Dynamic MicroRNA Gene Transcription and Processing during T Cell Development. J Immunol 188: 3257-3267.

92. Kuchen S, Resch W, Yamane A, Kuo N, Li Z, et al. (2010) Regulation of microRNA expression and abundance during lymphopoiesis. Immunity 32: 828-839.

93. Neilson JR, Zheng GX, Burge CB, Sharp PA (2007) Dynamic regulation of miRNA expression in ordered stages of cellular development. Genes Dev 21: 578-589.

94. Ji J, Yamashita T, Budhu A, Forgues M, Jia HL, et al. (2009) Identification of microRNA-181 by genome-wide screening as a critical player in EpCAM-positive hepatic cancer stem cells. Hepatology 50: 472-480.

95. Liu G, Min H, Yue S, Chen CZ (2008) Pre-miRNA loop nucleotides control the distinct activities of mir-181a-1 and mir-181c in early T cell development. PLoS One 3: e3592.

96. Ebert PJ, Jiang S, Xie J, Li QJ, Davis MM (2009) An endogenous positively selecting peptide enhances mature T cell responses and becomes an autoantigen in the absence of microRNA miR-181a. Nat Immunol 10: 1162-1169.

97. Li QJ, Chau J, Ebert PJ, Sylvester G, Min H, et al. (2007) miR-181a is an intrinsic modulator of T cell sensitivity and selection. Cell 129: 147-161.

98. Cichocki F, Felices M, McCullar V, Presnell SR, Al-Attar A, et al. (2011) Cutting edge: microRNA-181 promotes human NK cell development by regulating Notch signaling. J Immunol 187: 6171-6175.

99. Fragoso R, Mao T, Wang S, Schaffert S, Gong X, et al. (2012) Modulating the strength and threshold of NOTCH oncogenic signals by mir-181a-1/b-1. PLoS Genet 8: e1002855.

100. Henao-Mejia J, Williams A, Goff LA, Staron M, Licona-Limon P, et al. (2013) The MicroRNA miR-181 Is a Critical Cellular Metabolic Rheostat Essential for NKT

Cell Ontogenesis and Lymphocyte Development and Homeostasis. Immunity 38: 984-997.

101. Zietara N, Lyszkiewicz M, Witzlau K, Naumann R, Hurwitz R, et al. (2013) Critical role for miR-181a/b-1 in agonist selection of invariant natural killer T cells. Proc Natl Acad Sci U S A 110: 7407-7412.

102. Jeker LT, Bluestone JA (2013) MicroRNA regulation of T-cell differentiation and function. Immunol Rev 253: 65-81.

103. Dooley J, Linterman MA, Liston A (2013) MicroRNA regulation of T-cell development. Immunol Rev 253: 53-64.

104. Calin GA, Sevignani C, Dumitru CD, Hyslop T, Noch E, et al. (2004) Human microRNA genes are frequently located at fragile sites and genomic regions involved in cancers. Proc Natl Acad Sci U S A 101: 2999-3004.

105. Zhang B, Pan X, Anderson TA (2006) MicroRNA: a new player in stem cells. J Cell Physiol 209: 266-269.

106. Bhattacharya A, Ziebarth JD, Cui Y (2012) Systematic analysis of microRNA targeting impacted by small insertions and deletions in human genome. PLoS One 7: e46176.

107. de Pontual L, Yao E, Callier P, Faivre L, Drouin V, et al. (2011) Germline deletion of the miR-17 approximately 92 cluster causes skeletal and growth defects in humans. Nat Genet 43: 1026-1030.

108. Mencia A, Modamio-Hoybjor S, Redshaw N, Morin M, Mayo-Merino F, et al. (2009) Mutations in the seed region of human miR-96 are responsible for nonsyndromic progressive hearing loss. Nat Genet 41: 609-613.

109. de la Morena MT, Eitson JL, Dozmorov IM, Belkaya S, Hoover AR, et al. (2013) Signature MicroRNA expression patterns identified in humans with 22q11.2 deletion/DiGeorge syndrome. Clin Immunol 147: 11-22.

110. Kobrynski LJ, Sullivan KE (2007) Velocardiofacial syndrome, DiGeorge syndrome: the chromosome 22q11.2 deletion syndromes. Lancet 370: 1443-1452.

111. Sullivan KE (2007) DiGeorge syndrome/velocardiofacial syndrome: the chromosome 22q11.2 deletion syndrome. Adv Exp Med Biol 601: 37-49.

112. Karayiorgou M, Simon TJ, Gogos JA (2010) 22q11.2 microdeletions: linking DNA structural variation to brain dysfunction and schizophrenia. Nat Rev Neurosci 11: 402-416.

113. Kanaya Y, Ohga S, Ikeda K, Furuno K, Ohno T, et al. (2006) Maturational alterations of peripheral T cell subsets and cytokine gene expression in 22q11.2 deletion syndrome. Clin Exp Immunol 144: 85-93.

114. Piliero LM, Sanford AN, McDonald-McGinn DM, Zackai EH, Sullivan KE (2004) T-cell homeostasis in humans with thymic hypoplasia due to chromosome 22q11.2 deletion syndrome. Blood 103: 1020-1025.

115. Earls LR, Fricke RG, Yu J, Berry RB, Baldwin LT, et al. (2012) Age-Dependent MicroRNA Control of Synaptic Plasticity in 22q11 Deletion Syndrome and Schizophrenia. J Neurosci 32: 14132-14144.

116. Xu B, Hsu PK, Stark KL, Karayiorgou M, Gogos JA (2013) Derepression of a Neuronal Inhibitor due to miRNA Dysregulation in a Schizophrenia-Related Microdeletion. Cell 152: 262-275.

117. Belver L, de Yebenes VG, Ramiro AR (2010) MicroRNAs prevent the generation of autoreactive antibodies. Immunity 33: 713-722.

118. Lindsay MA (2008) microRNAs and the immune response. Trends Immunol 29: 343-351.

119. Lodish HF, Zhou B, Liu G, Chen CZ (2008) Micromanagement of the immune system by microRNAs. Nat Rev Immunol 8: 120-130.

120. O'Connell RM, Taganov KD, Boldin MP, Cheng G, Baltimore D (2007) MicroRNA-155 is induced during the macrophage inflammatory response. Proc Natl Acad Sci U S A 104: 1604-1609.

121. van Rooij E, Sutherland LB, Liu N, Williams AH, McAnally J, et al. (2006) A signature pattern of stress-responsive microRNAs that can evoke cardiac hypertrophy and heart failure. Proc Natl Acad Sci U S A 103: 18255-18260.

122. van Rooij E, Sutherland LB, Qi X, Richardson JA, Hill J, et al. (2007) Control of stress-dependent cardiac growth and gene expression by a microRNA. Science 316: 575-579.

123. Bonauer A, Carmona G, Iwasaki M, Mione M, Koyanagi M, et al. (2009) MicroRNA-92a controls angiogenesis and functional recovery of ischemic tissues in mice. Science 324: 1710-1713.

124. van Rooij E, Sutherland LB, Thatcher JE, DiMaio JM, Naseem RH, et al. (2008) Dysregulation of microRNAs after myocardial infarction reveals a role of miR-29 in cardiac fibrosis. Proc Natl Acad Sci U S A 105: 13027-13032.

125. O'Connell RM, Chaudhuri AA, Rao DS, Baltimore D (2009) Inositol phosphatase SHIP1 is a primary target of miR-155. Proc Natl Acad Sci U S A 106: 7113-7118.

126. Taganov KD, Boldin MP, Chang KJ, Baltimore D (2006) NF-kappaB-dependent induction of microRNA miR-146, an inhibitor targeted to signaling proteins of innate immune responses. Proc Natl Acad Sci U S A 103: 12481-12486.

127. Tili E, Michaille JJ, Cimino A, Costinean S, Dumitru CD, et al. (2007) Modulation of miR-155 and miR-125b levels following lipopolysaccharide/TNF-alpha stimulation and their possible roles in regulating the response to endotoxin shock. J Immunol 179: 5082-5089.

128. Iliopoulos D, Hirsch HA, Struhl K (2009) An epigenetic switch involving NF-kappaB, Lin28, Let-7 MicroRNA, and IL6 links inflammation to cell transformation. Cell 139: 693-706.

129. Billard MJ, Gruver AL, Sempowski GD (2011) Acute endotoxin-induced thymic atrophy is characterized by intrathymic inflammatory and wound healing responses. PLoS One 6: e17940.

130. Kong FK, Chen CL, Cooper MD (2002) Reversible disruption of thymic function by steroid treatment. J Immunol 168: 6500-6505.

131. Smith LK, Shah RR, Cidlowski JA (2010) Glucocorticoids modulate microRNA expression and processing during lymphocyte apoptosis. J Biol Chem 285: 36698-36708.

132. Belkaya S, Silge RL, Hoover AR, Medeiros JJ, Eitson JL, et al. (2011) Dynamic modulation of thymic microRNAs in response to stress. PLoS One 6: e27580.

133. van Oers NS, Tohlen B, Malissen B, Moomaw CR, Afendis S, et al. (2000) The 21- and 23-kD forms of TCR zeta are generated by specific ITAM phosphorylations. Nat Immunol 1: 322-328.

134. Zhumabekov T, Corbella P, Tolaini M, Kioussis D (1995) Improved version of a human CD2 minigene based vector for T cell-specific expression in transgenic mice. J Immunol Methods 185: 133-140.

135. Becker AM, Blevins JS, Tomson FL, Eitson JL, Medeiros JJ, et al. (2010) Invariant NKT cell development requires a full complement of functional CD3 zeta immunoreceptor tyrosine-based activation motifs. J Immunol 184: 6822-6832.

136. Pall GS, Codony-Servat C, Byrne J, Ritchie L, Hamilton A (2007) Carbodiimide-mediated cross-linking of RNA to nylon membranes improves the detection of siRNA, miRNA and piRNA by northern blot. Nucleic Acids Res 35: e60.

137. Dozmorov MG, Guthridge JM, Hurst RE, Dozmorov IM (2010) A comprehensive and universal method for assessing the performance of differential gene expression analyses. PLoS One 5.

138. Wang J, Duncan D, Shi Z, Zhang B (2013) WEB-based GEne SeT AnaLysis Toolkit (WebGestalt): update 2013. Nucleic Acids Res 41: W77-83.

139. Zhang B, Kirov S, Snoddy J (2005) WebGestalt: an integrated system for exploring gene sets in various biological contexts. Nucleic Acids Res 33: W741-748.

140. Douek DC, McFarland RD, Keiser PH, Gage EA, Massey JM, et al. (1998) Changes in thymic function with age and during the treatment of HIV infection. Nature 396: 690-695.

141. Winoto A, Littman DR (2002) Nuclear hormone receptors in T lymphocytes. Cell 109 Suppl: S57-66.

142. Hotchkiss RS, Swanson PE, Freeman BD, Tinsley KW, Cobb JP, et al. (1999) Apoptotic cell death in patients with sepsis, shock, and multiple organ dysfunction. Crit Care Med 27: 1230-1251.

143. Haynes BF, Markert ML, Sempowski GD, Patel DD, Hale LP (2000) The role of the thymus in immune reconstitution in aging, bone marrow transplantation, and HIV-1 infection. Annu Rev Immunol 18: 529-560.

144. Wang SD, Huang KJ, Lin YS, Lei HY (1994) Sepsis-induced apoptosis of the thymocytes in mice. J Immunol 152: 5014-5021.

145. Howard JK, Lord GM, Matarese G, Vendetti S, Ghatei MA, et al. (1999) Leptin protects mice from starvation-induced lymphoid atrophy and increases thymic cellularity in ob/ob mice. J Clin Invest 104: 1051-1059.

146. Ageev AK, Sidorin VS, Rogachev MV, Timofeev IV (1986) [Morphologic characteristics of the changes in the thymus and spleen in alcoholism]. Arkh Patol 48: 33-39.

147. Webster JI, Tonelli L, Sternberg EM (2002) Neuroendocrine regulation of immunity. Annu Rev Immunol 20: 125-163.

148. Vacchio MS, Papadopoulos V, Ashwell JD (1994) Steroid production in the thymus: implications for thymocyte selection. J Exp Med 179: 1835-1846.

149. Hick RW, Gruver AL, Ventevogel MS, Haynes BF, Sempowski GD (2006) Leptin selectively augments thymopoiesis in leptin deficiency and lipopolysaccharide-induced thymic atrophy. J Immunol 177: 169-176.

150. Bronstein-Sitton N, Cohen-Daniel L, Vaknin I, Ezernitchi AV, Leshem B, et al. (2003) Sustained exposure to bacterial antigen induces interferon-gamma-dependent T cell receptor zeta down-regulation and impaired T cell function. Nat Immunol 4: 957-964.

151. Sempowski GD, Hale LP, Sundy JS, Massey JM, Koup RA, et al. (2000) Leukemia inhibitory factor, oncostatin M, IL-6, and stem cell factor mRNA expression in human thymus increases with age and is associated with thymic atrophy. J Immunol 164: 2180-2187.

152. Sempowski GD, Rhein ME, Scearce RM, Haynes BF (2002) Leukemia inhibitory factor is a mediator of Escherichia coli lipopolysaccharide-induced acute thymic atrophy. Eur J Immunol 32: 3066-3070.

153. Shimon I, Yan X, Ray DW, Melmed S (1997) Cytokine-dependent gp130 receptor subunit regulates human fetal pituitary adrenocorticotropin hormone and growth hormone secretion. J Clin Invest 100: 357-363.

154. Jameson JM, Cruz J, Costanzo A, Terajima M, Ennis FA (2010) A role for the mevalonate pathway in the induction of subtype cross-reactive immunity to influenza A virus by human gammadelta T lymphocytes. Cell Immunol 264: 71-77.

155. Chatham WW, Kimberly RP (2001) Treatment of lupus with corticosteroids. Lupus 10: 140-147.

156. Hoffman HM, Simon A (2009) Recurrent febrile syndromes: what a rheumatologist needs to know. Nat Rev Rheumatol 5: 249-256.

157. Pieters R, Schrappe M, De Lorenzo P, Hann I, De Rossi G, et al. (2007) A treatment protocol for infants younger than 1 year with acute lymphoblastic leukaemia (Interfant-99): an observational study and a multicentre randomised trial. Lancet 370: 240-250.

158. Lowenberg M, Verhaar AP, van den Brink GR, Hommes DW (2007) Glucocorticoid signaling: a nongenomic mechanism for T-cell immunosuppression. Trends Mol Med 13: 158-163.

159. Wyllie AH (1980) Glucocorticoid-induced thymocyte apoptosis is associated with endogenous endonuclease activation. Nature 284: 555-556.

160. Grosshans H, Filipowicz W (2008) Molecular biology: the expanding world of small RNAs. Nature 451: 414-416.

161. Chong MM, Rasmussen JP, Rudensky AY, Littman DR (2008) The RNAseIII enzyme Drosha is critical in T cells for preventing lethal inflammatory disease. J Exp Med 205: 2005-2017.

162. Liston A, Lu LF, O'Carroll D, Tarakhovsky A, Rudensky AY (2008) Dicer-dependent microRNA pathway safeguards regulatory T cell function. J Exp Med 205: 1993-2004.

163. Zhou X, Jeker LT, Fife BT, Zhu S, Anderson MS, et al. (2008) Selective miRNA disruption in T reg cells leads to uncontrolled autoimmunity. J Exp Med 205: 1983-1991.

164. Curtale G, Citarella F, Carissimi C, Goldoni M, Carucci N, et al. (2010) An emerging player in the adaptive immune response: microRNA-146a is a modulator of IL-2 expression and activation-induced cell death in T lymphocytes. Blood 115: 265-273.

165. Lu LF, Boldin MP, Chaudhry A, Lin LL, Taganov KD, et al. (2010) Function of miR-146a in controlling Treg cell-mediated regulation of Th1 responses. Cell 142: 914-929.

166. O'Connell RM, Kahn D, Gibson WS, Round JL, Scholz RL, et al. (2010) MicroRNA-155 promotes autoimmune inflammation by enhancing inflammatory T cell development. Immunity 33: 607-619.

167. van Rooij E (2011) The art of microRNA research. Circ Res 108: 219-234.

168. Leung AK, Sharp PA (2010) MicroRNA functions in stress responses. Mol Cell 40: 205-215.

169. Mendell JT (2008) miRiad roles for the miR-17-92 cluster in development and disease. Cell 133: 217-222.

170. Zhou B, Wang S, Mayr C, Bartel DP, Lodish HF (2007) miR-150, a microRNA expressed in mature B and T cells, blocks early B cell development when expressed prematurely. Proc Natl Acad Sci U S A 104: 7080-7085.

171. Cortez MA, Bueso-Ramos C, Ferdin J, Lopez-Berestein G, Sood AK, et al. (2011) MicroRNAs in body fluids--the mix of hormones and biomarkers. Nat Rev Clin Oncol 8: 467-477.

172. Dooley J, Liston A (2012) Molecular control over thymic involution: from cytokines and microRNA to aging and adipose tissue. Eur J Immunol 42: 1073-1079.

173. Frankfurt O, Rosen ST (2004) Mechanisms of glucocorticoid-induced apoptosis in hematologic malignancies: updates. Curr Opin Oncol 16: 553-563.

174. Heinonen KM, Vanegas JR, Brochu S, Shan J, Vainio SJ, et al. (2011) Wnt4 regulates thymic cellularity through the expansion of thymic epithelial cells and early thymic progenitors. Blood 118: 5163-5173.

175. Mendell JT, Olson EN (2012) MicroRNAs in stress signaling and human disease. Cell 148: 1172-1187.

176. Sionov RV (2013) MicroRNAs and Glucocorticoid-Induced Apoptosis in Lymphoid Malignancies. ISRN Hematol 2013: 348212.

177. Ouyang YB, Lu Y, Yue S, Giffard RG (2012) miR-181 targets multiple Bcl-2 family members and influences apoptosis and mitochondrial function in astrocytes. Mitochondrion 12: 213-219.

178. Liang J, Slingerland JM (2003) Multiple roles of the PI3K/PKB (Akt) pathway in cell cycle progression. Cell Cycle 2: 339-345.

179. Liu ZP, Wang Z, Yanagisawa H, Olson EN (2005) Phenotypic modulation of smooth muscle cells through interaction of Foxo4 and myocardin. Dev Cell 9: 261-270.

180. Van Der Heide LP, Hoekman MF, Smidt MP (2004) The ins and outs of FoxO shuttling: mechanisms of FoxO translocation and transcriptional regulation. Biochem J 380: 297-309.

181. Wolfer A, Bakker T, Wilson A, Nicolas M, Ioannidis V, et al. (2001) Inactivation of Notch 1 in immature thymocytes does not perturb CD4 or CD8T cell development. Nat Immunol 2: 235-241.

182. Trotta R, Chen L, Costinean S, Josyula S, Mundy-Bosse BL, et al. (2013) Overexpression of miR-155 causes expansion, arrest in terminal differentiation and functional activation of mouse natural killer cells. Blood 121: 3126-3134.

183. Ensenauer RE, Adeyinka A, Flynn HC, Michels VV, Lindor NM, et al. (2003) Microduplication 22q11.2, an emerging syndrome: clinical, cytogenetic, and molecular analysis of thirteen patients. Am J Hum Genet 73: 1027-1040.

184. Yobb TM, Somerville MJ, Willatt L, Firth HV, Harrison K, et al. (2005) Microduplication and triplication of 22q11.2: a highly variable syndrome. Am J Hum Genet 76: 865-876.

185. Dweep H, Sticht C, Pandey P, Gretz N (2011) miRWalk--database: prediction of possible miRNA binding sites by "walking" the genes of three genomes. J Biomed Inform 44: 839-847.

186. Flach H, Rosenbaum M, Duchniewicz M, Kim S, Zhang SL, et al. (2010) Mzb1 protein regulates calcium homeostasis, antibody secretion, and integrin activation in innate-like B cells. Immunity 33: 723-735.

187. Shimizu Y, Meunier L, Hendershot LM (2009) pERp1 is significantly up-regulated during plasma cell differentiation and contributes to the oxidative folding of immunoglobulin. Proc Natl Acad Sci U S A 106: 17013-17018.

188. van Anken E, Pena F, Hafkemeijer N, Christis C, Romijn EP, et al. (2009) Efficient IgM assembly and secretion require the plasma cell induced endoplasmic reticulum protein pERp1. Proc Natl Acad Sci U S A 106: 17019-17024.

189. Hoffman BG, Williams KL, Tien AH, Lu V, de Algara TR, et al. (2006) Identification of novel genes and transcription factors involved in spleen, thymus and immunological development and function. Genes Immun 7: 101-112.

190. Oukka M, Ho IC, de la Brousse FC, Hoey T, Grusby MJ, et al. (1998) The transcription factor NFAT4 is involved in the generation and survival of T cells. Immunity 9: 295-304.

191. Raman V, Blaeser F, Ho N, Engle DL, Williams CB, et al. (2001) Requirement for Ca2+/calmodulin-dependent kinase type IV/Gr in setting the thymocyte selection threshold. J Immunol 167: 6270-6278.

192. Zemble R, Luning Prak E, McDonald K, McDonald-McGinn D, Zackai E, et al. (2010) Secondary immunologic consequences in chromosome 22q11.2 deletion syndrome (DiGeorge syndrome/velocardiofacial syndrome). Clin Immunol 136: 409-418.

193. Salmena L, Poliseno L, Tay Y, Kats L, Pandolfi PP (2011) A ceRNA hypothesis: the Rosetta Stone of a hidden RNA language? Cell 146: 353-358.

194. Imam JS, Buddavarapu K, Lee-Chang JS, Ganapathy S, Camosy C, et al. (2010) MicroRNA-185 suppresses tumor growth and progression by targeting the Six1 oncogene in human cancers. Oncogene 29: 4971-4979.

195. Liu M, Lang N, Chen X, Tang Q, Liu S, et al. (2011) miR-185 targets RhoA and Cdc42 expression and inhibits the proliferation potential of human colorectal cells. Cancer Lett 301: 151-160.

196. Takahashi Y, Forrest AR, Maeno E, Hashimoto T, Daub CO, et al. (2009) MiR-107 and MiR-185 can induce cell cycle arrest in human non small cell lung cancer cell lines. PLoS One 4: e6677.

197. Aronson M (1991) Hypothesis: involution of the thymus with aging--programmed and beneficial. Thymus 18: 7-13.

198. Dowling MR, Hodgkin PD (2009) Why does the thymus involute? A selection-based hypothesis. Trends Immunol 30: 295-300.

199. Shanley DP, Aw D, Manley NR, Palmer DB (2009) An evolutionary perspective on the mechanisms of immunosenescence. Trends Immunol 30: 374-381.

200. Afanasyeva EA, Mestdagh P, Kumps C, Vandesompele J, Ehemann V, et al. (2011) MicroRNA miR-885-5p targets CDK2 and MCM5, activates p53 and inhibits proliferation and survival. Cell Death Differ 18: 974-984.

201. Chehtane M, Khaled AR (2010) Interleukin-7 mediates glucose utilization in lymphocytes through transcriptional regulation of the hexokinase II gene. Am J Physiol Cell Physiol 298: C1560-1571.

202. Kuczma M, Lee JR, Kraj P (2011) Connexin 43 signaling enhances the generation of Foxp3+ regulatory T cells. J Immunol 187: 248-257.

203. Oviedo-Orta E, Perreau M, Evans WH, Potolicchio I (2010) Control of the proliferation of activated CD4+ T cells by connexins. J Leukoc Biol 88: 79-86.

204. So CW, Karsunky H, Wong P, Weissman IL, Cleary ML (2004) Leukemic transformation of hematopoietic progenitors by MLL-GAS7 in the absence of Hoxa7 or Hoxa9. Blood 103: 3192-3199.

205. Seok J, Warren HS, Cuenca AG, Mindrinos MN, Baker HV, et al. (2013) Genomic responses in mouse models poorly mimic human inflammatory diseases. Proc Natl Acad Sci U S A 110: 3507-3512.